

# **Drug-excipient-shell interactions using thermoplastic starch-based capsules for oral lipid-based drug delivery**

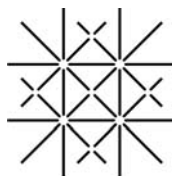
**Inauguraldissertation**

zur  
Erlangung der Würde eines Doktors der Philosophie  
vorgelegt der  
Philosophisch-Naturwissenschaftlichen Fakultät  
der Universität Basel

von

ZDRAVKA MISIC

aus Sisak, Kroatien



UNI  
BASEL

Basel, 2014

Genehmigt von der Philosophisch - Naturwissenschaftlichen Fakultät  
auf Antrag von

Herrn Prof. Dr. Georgios Imanidis (Fakultätsverantwortlicher)

Herrn Prof. Dr. Martin Kuentz (Korreferent)

Herrn Prof. Dr. Bruno Gander (Korreferent)

Basel, den 25. März 2014

Prof. Dr. Jörg Schibler

Dekan

**To my parents Ljuba and Stevo Tadić,  
my sister Tatjana, and my husband Miran**

# Abstract

Worldwide, gelatin has been used in the rotary die process as a shell-forming material of soft capsules due to its unique physicochemical properties. The development of soft gelatin capsules (SGCs) is, however, challenging because of their highly dynamic nature. Migrations of components between the shell and the fill, as well as between the shell and the external environment, are very common. These migrations might occur during manufacture, drying and on storage. A major challenge is the large amount of water (up to 35% w/w) that the capsule shell contains immediately after encapsulation. During drying the water migrates from the shell into the environment and the fill until equilibrium moisture content is reached. The water migration pattern greatly depends on the nature of the fill formulation. For lipophilic oily formulations there is no water uptake from the shell. However, a considerably hydrophilic fill might take up a high amount of water (up to 20% w/w). Some water migrates back into the shell with further drying, resulting in capsules containing up to ~ 8% w/w of water in the fill. This water creates a risk of drug precipitation in the fill mass, since the drug solubility in the formulation can be greatly reduced.

To overcome the disadvantages of gelatin, a great effort has been directed into finding new materials as a substitute for gelatin in soft capsules. The present thesis comprises two studies that focus on a novel thermoplastic shell material for soft capsules. A particular aim was to gain a better mechanistic understanding of drug-excipient-shell interactions using SGCs and different starch-based thermoplastic capsules. Since thermoplastic capsules allow a filling at rather high temperatures, formulations that are even solid at room temperature can be encapsulated. Therefore, a third study used such solid lipid-based formulations with the aim to investigate drug-excipient-shell interactions on different biopharmaceutical levels *in vitro*.

Recently, a novel starch-based polyvinyl alcohol thermoplastic capsule (S-PVA-C) has been introduced by researchers at Swiss Caps AG, member of the Aenova group (Kirchberg, Switzerland). In the first study, we provided a thorough physical characterization of the new shell material. Additionally, we aimed to determine whether this capsule material is associated with less water exchange between the fill and the capsule shell compared to gelatin, thus preventing precipitation of a poorly water-soluble drug in the fill mass. Both SGCs and S-PVA-Cs were filled with a hydrophilic lipid-based system of fenofibrate and different water migration patterns were observed. SGCs exhibited considerable water migration from the soft gelatin shell to the fill during drying resulting in drug crystallization. In contrast, S-PVA-Cs displayed no substantial water exchange or drug crystallization upon storage. Therefore, S-PVA-Cs provided a more robust drug product following encapsulation of a rather hydrophilic lipid-based formulation compared to SGCs. Furthermore, the thermoplastic capsule material exhibited larger surface roughness and higher resistance to mechanical deformation compared to gelatin. These physical properties may be beneficial for capsule coating and for reducing the duration of the manufacturing process.

The second study is focused on the biorelevant drug release from the novel S-PVA-Cs, SGCs, and VegaGels<sup>®</sup>. We studied the effect of the shell material by considering microstructural formulation changes during hydration. It was found that S-PVA-Cs opened only partially in biorelevant media compared to completely opened SGCs and VegaGels<sup>®</sup>. This different opening mechanism caused sustained drug release from S-PVA-Cs for formulation that demonstrated high viscosity upon hydration. Such a rheological effect on drug release was barely noted for SGCs or VegaGels<sup>®</sup>. Additionally, small angle x-ray scattering (SAXS) showed differences in the hydrated microstructure (using a Teubner-Strey model for microemulsions). Our results suggested that even though S-PVA-Cs are highly attractive for encapsulation of rather hydrophilic formulations, some care is needed regarding an immediate release form.

In the third study we developed a solid lipid-based system that requires elevated filling temperatures for encapsulation. We aimed at better mechanistic understanding of the effects of drug-excipient interactions at different biopharmaceutical levels (*i.e.* anhydrous formulation, upon dispersion in simple buffer media and, in particular, regarding precipitation kinetics). Loratadine and carvedilol were chosen as model basic drugs. Drug-OA molecular complexes were formed upon addition of oleic acid (OA) in the formulation, which led to a marked increase in drug solubility. Precipitation kinetics of drug formulations was monitored in phosphate buffer (pH = 6.5) in real-time using focused beam reflectance measurements. The results clearly demonstrated that OA influenced the extent of drug precipitation as well as its kinetics. More importantly, solid-state analysis showed an amorphous precipitate demonstrating that OA acted also as a precipitation modifier. The role of OA as a precipitation inhibitor, and more importantly as a precipitation modifier, can be used in a novel formulation approach. *In situ* forming amorphous system obtained from OA-containing formulation may be valuable from a biopharmaceutical perspective for the delivery of poorly soluble basic drugs.

In summary, the present thesis introduced novel starch-based thermoplastic capsules (S-PVA-Cs) and demonstrated their advantage over SGCs with respect to hydrophilic lipid-based formulations. Release studies in biorelevant media revealed differences in how formulations hydrated and interacted with the shell material. Drug-excipient-shell interactions were observed in various capsule types (SGCs, S-PVA-Cs, and VegaGels<sup>®</sup>) at different levels of biopharmaceutical *in vitro* testing. A better mechanistic understanding was attained that may guide future development of soft capsule products.

# Contents

<b>Abstract</b> .....	<b>i</b>
<b>Contents</b> .....	<b>iv</b>
<b>1 Introduction</b> .....	<b>1</b>
1.1. Background.....	1
1.2. Objectives .....	4
<b>2 Theoretical section</b> .....	<b>6</b>
2.1. Soft gelatin capsules .....	6
2.1.1. Composition of soft gelatin capsule shell .....	6
2.1.2. Advantages of soft gelatin capsules .....	9
2.1.3. Challenges and limitations of soft gelatin capsules .....	10
2.2. Alternative materials for soft capsules .....	14
2.3. Manufacturing methods .....	18
2.3.1. Globex method .....	18
2.3.2. Rotary die method.....	20
2.3.3. Production of non-gelatin soft capsules.....	22
2.4. Comparison of soft gelatin capsules versus non-gelatin soft capsules .....	24
2.5. Oral lipid-based formulations for poorly water-soluble drugs.....	25
2.6. Self-microemulsifying drug delivery systems (SMEDDS) .....	29
2.6.1. Excipients in SMEDDS .....	30

---

2.6.2. <i>In vitro</i> testing of SMEDDS.....	33
2.7. Drug precipitation.....	34
2.8. Focused beam reflectance measurement (FBRM) .....	37
2.9. Drug supersaturation.....	38
2.9.1. Drug supersaturation triggered by oral administration of LBF .....	38
2.9.2. Supersaturatable (S-SEDDS) and supersaturated (super-SNEDDS) drug delivery systems.....	40
<b>3 Novel starch-based PVA thermoplastic capsules for hydrophilic lipid-based formulations.....</b>	<b>43</b>
Summary.....	43
3.1. Introduction .....	44
3.2. Materials and methods.....	47
3.2.1. Materials .....	47
3.2.2. Methods .....	47
3.2.2.1. Production and physical characterization of the S-PVA and soft gelatin films.....	47
3.2.2.1.1. Surface texture measurements .....	48
3.2.2.1.2. Residual water content.....	49
3.2.2.1.3. X-ray diffraction (XRD) .....	50
3.2.2.1.4. Differential scanning calorimetry (DSC).....	50
3.2.2.2. Solubility studies and excipients phase behaviour .....	51
3.2.2.2.1. Solubility studies of fenofibrate in excipients and mixtures with water.....	51
3.2.2.2.2. Preparation of the SMEDDS and particle size measurements.....	52
3.2.2.3. Characterization of the S-PVA-Cs and a comparison with SGCs .....	53
3.2.2.3.1. Production of the S-PVA-Cs and SGCs .....	53



---

3.2.2.3.2. Drying kinetics-water activity measurement.....	54
3.2.2.3.3. Determination of the dissolved drug concentration in the capsule formulation .....	54
3.2.2.3.4. Texture analysis .....	55
3.2.2.3.5. <i>In vitro</i> disintegration and drug release testing.....	55
3.2.2.4. HPLC method .....	56
3.2.2.5. Data analysis .....	56
3.3. Results.....	56
3.3.1. Physical characterization of the S-PVA and gelatin films.....	56
3.3.1.1. Surface texture measurements .....	56
3.3.1.2. Residual water content .....	58
3.3.1.3. X-ray diffraction (XRD).....	58
3.3.1.4. Thermal analysis by DSC .....	59
3.3.2. Solubility studies and excipients phase behaviour.....	60
3.3.3. Characterization of the S-PVA-Cs and a comparison with SGCs.....	64
3.3.3.1. Drying kinetics-water activity measurement .....	64
3.3.3.2. Determination of the dissolved drug concentration in the capsule formulation....	65
3.3.3.3. Texture analysis.....	68
3.3.3.4. <i>In vitro</i> disintegration and drug release testing .....	69
3.4. Discussion .....	70
3.5. Conclusion.....	73
<b>4 Understanding biorelevant drug release from a novel thermoplastic capsule by considering microstructural formulation changes during hydration.....</b>	<b>75</b>
Summary.....	75

---

4.1. Introduction .....	76
4.2. Materials and methods .....	78
4.2.1. Materials .....	78
4.2.2. Methods .....	80
4.2.2.1. Preparation and hydration of the formulations.....	80
4.2.2.2. Preparation of drug-containing formulations (solubility studies).....	80
4.2.2.3. Characterisation.....	81
4.2.2.3.1. Particle size measurements.....	81
4.2.2.3.2. Rheological studies .....	81
4.2.2.3.3. Small angle x-ray scattering (SAXS) studies .....	82
4.2.2.3.4. Biorelevant drug release studies .....	83
4.2.2.3.5. Texture analysis of dosage form disintegration .....	83
4.2.2.4. HPLC method .....	84
4.3. Results.....	85
4.3.1. Characterization .....	85
4.3.1.1. Particle size measurements .....	85
4.3.1.2. Rheological studies.....	86
4.3.1.3. Small angle x-ray scattering (SAXS).....	87
4.3.1.4. Analysis of capsule disintegration and drug release .....	90
4.4. Discussion .....	94
4.4.1. Effect of the shell material .....	95
4.4.2. Effect of microstructural formulation change .....	96
4.5. Conclusions .....	99

---

<b>5 Understanding interactions of oleic acid with basic drugs in solid lipids on different biopharmaceutical levels.....</b>	<b>101</b>
Summary.....	101
5.1. Introduction .....	102
5.2. Materials and methods .....	105
5.2.1. Materials .....	105
5.2.2. Methods .....	105
5.2.2.1. Preparation of solid systems .....	105
5.2.2.2. Characterization of solid systems.....	106
5.2.2.2.1. X-ray diffraction (XRD) .....	106
5.2.2.2.2. Differential scanning calorimetry (DSC).....	106
5.2.2.2.3. Particle size measurements following aqueous dispersion of solid systems	106
5.2.2.3. Spectroscopic and rheological characterization of drug-excipient molecular interactions .....	107
5.2.2.3.1. UV spectroscopy .....	107
5.2.2.3.2. Mechanical chip-based rheology .....	107
5.2.2.3.3. FTIR .....	108
5.2.2.4. Testing of the anhydrous drug-loaded solid systems .....	108
5.2.2.4.1. Van't Hoff solubility study .....	108
5.2.2.4.2. Drug loading of solid systems .....	109
5.2.2.5. Zeta potential measurements of dispersed drug-loaded solid systems.....	110
5.2.2.6. Drug precipitation testing upon dispersion and release from capsules .....	110
5.2.2.6.1. Drug precipitation upon aqueous dispersion .....	110
5.2.2.6.2. Drug release testing.....	111

---

5.2.2.7. HPLC method .....	112
5.2.2.8 Data analysis .....	112
5.3. Results.....	112
5.3.1. Characterization of solid drug-free systems.....	112
5.3.1.1. X-ray diffraction (XRD).....	113
5.3.1.2. Differential scanning calorimetry (DSC) .....	113
5.3.1.3. Particle size measurements following aqueous dispersion of solid systems .....	114
5.3.2. Characterization of solid drug-loaded systems.....	115
5.3.2.1. Drug-exciptent interaction in oily mixtures.....	115
5.3.2.2. Solubility study .....	117
5.3.3. Zeta potential measurements of dispersed drug-loaded systems .....	121
5.3.4. Drug precipitation testing upon dispersion and release from capsules .....	122
5.3.4.1. Drug precipitation upon aqueous dispersion.....	122
5.3.4.2. Drug release testing .....	130
5.4. Discussion .....	131
5.5. Conclusions .....	138
<b>6 Final remarks and outlook .....</b>	<b>140</b>
<b>Bibliography .....</b>	<b>143</b>
<b>List of Abbreviations.....</b>	<b>160</b>
<b>List of Symbols .....</b>	<b>164</b>
<b>List of Figures.....</b>	<b>166</b>
<b>List of Tables.....</b>	<b>169</b>
<b>Curriculum Vitae .....</b>	<b>170</b>

## **Chapter 1**

# **Introduction**

### **1.1. Background**

Soft gelatin capsules (SGCs) are established pharmaceutical dosage forms that have been in use for over 160 years (1). Besides masking odours and unpleasant tastes, SGCs offer many other advantages over other oral dosage forms, including an improved swallowability, optional drug protection against hydrolysis or oxidation, and an ability to readily dissolve in gastric fluids (2). SGCs are suitable for administration of poorly water-soluble drugs in dissolved form, which is one of several strategies by which lipid-based formulations can enhance oral bioavailability. Several other benefits of SGCs derive from the fact that the encapsulation process requires that the drug is in solution or at least suspended in a liquid fill (3, 4). Drug in solution or suspension, typically leads to a much higher degree of reproducibility compared to tablets and hard gelatin capsules filled with powder or granules, since a positive displacement pump is employed for the filling process. Moreover, a higher content uniformity of low-dose drugs is usually achieved compared to powder blends of other conventional oral dosage forms.

However, gelatin has also several drawbacks. For example, the animal source of gelatin can be an issue for patients living under religious (Jews, Muslims, Buddhists, and Hindus)

or dietary restrictions (vegetarians and vegans) (5). Also, unmodified gelatin is susceptible to cross-linking, which can be an issue for *in vitro* drug release. Migration of drug and other formulation components (*e.g.* hydrophilic co-solvents) into the capsule shell presents another potential drawback of SGCs (6-12). Additionally, water exchange between the shell and the formulation can also be critical. Typically, the gelatin shell contains a large amount of water (up to 35% w/w) immediately after encapsulation. Depending on the nature of a fill mass, this water may migrate from the capsule shell into the fill and decrease drug solubility leading to precipitation in the fill mass (2, 13).

To overcome the disadvantages of gelatin, there has been a great interest in the last decade in finding substitutes for soft capsules. However, only a few non-gelatin soft capsule prototypes and methods of encapsulation have been patented so far. All materials were based on plant-derived hydrocolloids (*e.g.* carrageenan, modified starch), except for one that mainly comprised a synthetic polymer (polyvinyl alcohol) (14-16). For the manufacture of such nongelatin capsules, processes like casting or extrusion are coupled with the standard rotary die process (17, 18). However, it appears that options for manufacturing capsules from carrageenan or starch-based materials are limited due to the technical difficulties. Carrageenan, like other hydrocolloids, requires a large fraction of water for full hydration, which in turn reduces the strength of the film. Therefore, a method for extracting a portion of water from the film-forming composition was recommended (19). To avoid these water-related issues, already in 2002 polyvinyl alcohol (PVA) has been proposed for the encapsulation process (16). Although PVA is less hygroscopic than hydrocolloids or gelatin, it lacks the gelling properties. Therefore, it was suggested to use preformed rolls of almost water-free films that can be fed into the rotary die encapsulation.

The research of novel shell materials has brought to light the difficulties of replacing gelatin. In particular, the production step remains a technical challenge for alternative materials. Furthermore, it remains uncertain whether such alternative soft capsules have

any pharmaceutical advantages other than their non-animal origin. This stresses the need for more pharmaceutical research in the area of identifying new shell materials.

Research activities conducted in Swiss Caps AG (Kirchberg, Switzerland) resulted recently in a novel starch-based thermoplastic material that was obtained from a two-step extrusion process. The new shell material combines the thermoplastic properties of starch with the characteristics of PVA. In our first study, we aimed at exploring whether this material would be specifically suited for encapsulation of hydrophilic lipid-based formulations (LBFs).

*In vitro* drug release tests to evaluate drug and formulation behaviour under simulated physiological conditions are essential for efficient drug development. To better simulate the environment of gastro-intestinal (GI) tract, many biorelevant dissolution media have been developed and tested over the last decade (20, 21). Such biorelevant media, containing bile salts and phospholipids, are especially interesting for LBFs, since these natural surfactants can affect drug solubilization as well as reduce interfacial oil/water tension, which would affect formulation dispersion. Until recently, biorelevant drug release from soft capsules was not often investigated. As the shell material might have an impact on the drug release profile, there is a need for research in this direction. Moreover, the interaction of the shell material and the hydrated formulation should be studied, in order to gain better mechanistic understanding of the fate of the encapsulated formulation upon oral administration.

Apart from studying formulation-shell interactions, also drug-excipient interactions (at the level of the anhydrous formulation and upon dispersion) are important from a biopharmaceutical perspective. Better understanding of drug-excipient interactions and their impact on formulation properties and the fate of formulation in GI lumen is crucial for a more rational selection of systems in pharmaceutical formulation development.

## 1.2. Objectives

The present thesis is subdivided into four chapters that focus on innovations in soft capsule technology and a better mechanistic understanding of drug-excipient-shell interactions using SGCs and various starch-based thermoplastic capsules.

In the theoretical section (Chapter 2) an overview of alternative shell materials, their manufacturing methods, and comparison to SGCs is provided. In addition, drug precipitation and supersaturation following dispersion and digestion of LBF are described.

In Chapter 3 the aim was to physically characterize the novel starch-based PVA thermoplastic shell material (S-PVA) and to explore its pharmaceutical characteristics for soft capsule technology. Especially, the potential of the novel starch-based PVA thermoplastic capsules (S-PVA-Cs) for encapsulation of hydrophilic LBFs was evaluated. Moreover, we aimed to determine whether S-PVA-Cs exhibit less water exchange between the fill and the capsule shell compared to SGCs, thus preventing precipitation of a poorly water-soluble drug in the fill mass.

Chapter 4 is focused on the biorelevant drug release from the novel S-PVA-Cs, SGCs, and VegaGels<sup>®</sup>. Particular attention was directed to microstructural formulation changes during hydration. These formulation hydration changes were to be studied by means of small angle x-ray scattering (SAXS) and microchip-based rheology. Furthermore, we investigated the correlation of the opening mechanism of capsules with the formulation hydration and its impact on the drug release profiles.

In Chapter 5 the solid-lipid based system that contains oleic acid and requires elevated filling temperatures for encapsulation was developed. The aim was to elucidate interactions of oleic acid with basic drugs in solid lipids on different levels of biopharmaceutical *in vitro* testing. A particular interest was in the influence of drug-oleic



acid interactions on drug precipitation kinetics and on the solid-state properties of the precipitates following dispersion.

---

## **Chapter 2**

# **Theoretical section**

### **2.1. Soft gelatin capsules**

Soft gelatin capsules (SGCs) are single-unit solid dosage forms consisting of a soft gelatin shell and usually a liquid or a semi-solid filling. They are one-piece hermetically sealed capsules, which can be administered via various routes, although the oral route is the most common one. In the following paragraphs composition of the shell material, as well as advantages and challenges of SGCs will be discussed.

#### **2.1.1. Composition of soft gelatin capsule shell**

A soft gelatin capsule shell usually consists of gelatin, plasticizer(s), and water. It may also contain other minor additives such as preservatives, colouring and opacifying agents, flavourings and sweeteners, gastro-resistant substances, or even active compounds.

Gelatin is basically protein derived from the native protein collagen which is present in animal skin, bone, and hide. It has unique physicochemical properties (*e.g.* solubility, solution viscosity, thermally reversible gelation properties) making it particularly suitable

for the pharmaceutical capsule industry. Produced gelatin films are strong, clear, flexible, and easily soluble in gastric juices. The major sources of collagen for the production of gelatin are porcine skin, cattle hides, and bones (22). The manufacturing procedure comprises cleaning of raw material, pretreatment, extraction of gelatin, filtration, concentration/evaporation, sterilization, and drying. The raw material can be pretreated with either dilute acid (acid pretreatment) or alkali, depending on the origin of the collagen. A short acid pretreatment is typically used for the less covalently cross-linked collagens found in young animals, while a more intense alkali pretreatment is normally applied for more covalently cross-linked collagens from older animals. Gelatin derived from acid-treated and alkali-treated precursors are known as type A and type B, respectively (23). As mentioned earlier, gelatin has a unique ability to form a thermally reversible gel. Gel strength depends upon the gelatin concentration, pH, temperature, and maturing time. The Bloom value is the most important industrial criterion for grading a batch of commercial gelatin. It defines the gel strength as the force required for a 12.7 mm diameter flat-bottomed cylindrical plunger to depress the surface of a 6.67% w/w gelatin gel (matured at 10° C for 16-18h) to a depth of 4 mm (22). Pharmacopoeial specifications for gelatin (24) generally present minimum requirements (pH, conductivity, gel strength), while capsule manufacturers require more detailed specifications including some performance-related parameters. Apart from gelatin type and gel strength, industrial specifications usually include viscosity at 60° C and 6.67% w/w concentration in water, viscosity breakdown (the impact of temperature and time on the degradation of gelatin), melting point, setting point, setting time, particle size, and molecular weight distribution. An ideal soft capsule gelatin should have a gel strength of 150-200 Bloom, a viscosity of 2.8-4.5 mPas, a well-controlled degree of viscosity breakdown, a well-defined particle size, and a broad molecular weight distribution (25). Table 2.1 lists the main gelatin types and grades used for soft capsule production. Recently, gelatins derived from poultry and fish have been introduced as alternatives to gelatin of bovine and porcine origin. While poultry gelatin has comparable physicochemical properties to those of pigskin gelatin, and therefore could be used as a substitute for conventional gelatin, fish gelatin lacks the

gelling and setting attributes needed for soft capsule production. The overall technological issues, limited availability, and high costs are the main reasons that these alternative gelatin sources have not yet become commercially available.

**Table 2.1:** Physicochemical properties of pharmaceutical-grade soft capsule gelatins (LB-limed bone, LH-limed hide, AB-acid bone, PS-pigskin). Adapted from reference (25).

<b>Gelatin</b>	<b>Origin of raw material</b>	<b>Type</b>	<b>Bloom (g) (10° C; 6.67% w/w)</b>	<b>Viscosity (mPas) (60° C; 6.67% w/w)</b>
160 LB	Bovine/porcine bone	B	155-185	3.4-4.2
160 LH	Bovine hide	B	150-170	3.5-4.2
160 LB/LB	Blend of bovine/porcine bone and bovine hide	B	150-170	3.5-4.2
200 AB	Bovine bone	A	180-210	2.7-3.2
200 PS	Pigskin	A	190-210	2.5-3.1
160 PS/LB/LH	Blend of pigskin, bovine/porcine bone and bovine hide	A/B	145-175	2.7-3.3

As mentioned beforehand, the soft gelatin shell typically contains gelatin, plasticizer(s), and water. The weight ratio of water to dry gelatin (W/G) can vary from 0.7 to 1.3, depending on the viscosity of the gelatin. After encapsulation and drying, most of the water is removed, leading to final capsules with a moisture content of 4-10%. The weight ratio of dry plasticizer and dry gelatin (P/G) determines the shell strength and usually

varies between 0.3 and 1. Plasticizers have a highly important role in shell formulation. Thus, plasticizers ensure that the capsules retain their elasticity during the drying process and subsequent storage, *i.e.* that brittleness is avoided. Commonly used plasticizers for soft gelatin capsules are polyalcohols (*e.g.* glycerol, some grades of non-crystallising aqueous sorbitol, and sorbitan/sorbitol solutions). The selection and concentration of the plasticizer together with the residual moisture and the thickness of the shell (250-500  $\mu\text{m}$ ) determine the hardness and mechanical stability of the capsule. Glycerol is the most frequently used plasticizer, due to its high plasticizer efficacy, sufficient compatibility and its lacking interference with the formation of a stable three-dimensional gelatin network (25).

### **2.1.2. Advantages of soft gelatin capsules**

The first invention of gelatin capsules dates from the early 19<sup>th</sup> century, as a result of the need to mask the obnoxious taste of many drugs popular at that time (1). Besides masking odours and unpleasant tastes, SGCs offer many other advantages over other oral dosage forms, including an improved swallowability, optional drug protection against hydrolysis or oxidation, and an ability to readily dissolve in gastric fluids (2). Recently, significant advances have been made in the development of liquid and semi-solid formulations for SGCs. Studies have focused on increasing drug bioavailability and decreasing plasma variability by improving solubility and promoting drug absorption (26-29). The SGC encapsulation process has the pharmaceutical advantage, that the drug is solubilized or at least suspended in a liquid fill. A positive displacement pump is employed for the filling process and therefore a much higher degree of reproducibility is obtained compared to tablets and hard gelatin capsules filled with powder or granules. Moreover, a higher content uniformity of low-dose drugs is usually achieved compared to powder blends of other conventional oral dosage forms (3).

### 2.1.3. Challenges and limitations of soft gelatin capsules

Worldwide, many consumers of pharmaceutical products readily accept SGCs due to their favourable characteristics for an oral dosage form. However, SGCs have also some drawbacks. One of them is the animal source of gelatin that can be an issue for patients living under religious (Jews, Muslims, Buddhists, and Hindus) or dietary restrictions (vegetarians and vegans). In addition, the appearance of transmitting animal diseases, especially bovine spongiform encephalopathy (BSE; commonly known as mad cow disease) raised many concerns among both manufacturers and consumers. The BSE crisis hit the gelatin industry worldwide, although the scientific community reported early on that the gelatin manufacturing process delivered a safe product, even if infected animal materials were used (5).

Nowadays, gelatin manufacturers have established certified Quality Management Systems according to the worldwide standard ISO 9001 in order to ensure that their products comply with all required physical, chemical, microbiological, and technical production and quality standards (30). Additionally, manufacturers of pharmaceutical gelatin have to follow strict guidelines published by many national and international regulation authorities (*e.g.* Food and Drug Administration, FDA, “Guidance for Industry”, and European CPMP’s regulation “Note for Guidance” EMEA/410/01 Rev.3) (31, 32).

One of the key challenges in the development of SGCs is preventing or minimizing the chemical and physical interactions between the capsule shell and the formulation fill (compatibility issues). One well-known chemical interaction is the cross-linking of gelatin in presence of aldehydes. Cross-linking is chemical covalent bonding between different polypeptide chains, which may results in partially insoluble gelatin protein. This phenomenon can affect *in vitro* drug release by forming swollen, rubbery water-insoluble membranes that are known as pellicles and that may act as a barrier to drug release.

However, *in vivo* disintegration of cross-linked capsules is rapid, which led scientists to develop a two-tier *in vitro* dissolution test using enzymes (*e.g.* pepsin) (33). Some approaches to minimizing the cross-linking of gelatin include use of excipients with a low aldehyde content, incorporation of succinic acid into the gelatin shell, and/or the addition of antioxidants to the formulation. Antioxidants are often necessary, because auto-oxidative degradation of some excipients (*e.g.* polyethylene glycol) may generate aldehydes (34). Another chemical interaction that might occur is esterification or transesterification of drugs with polyols. To prevent this unwanted interaction, Gullapalli *et al.* (35) suggested a glycerol-free shell formulation and the addition of polyvinyl pyrrolidone to the fill.

A soft gelatin capsule is a very dynamic system, as presented in Figure 2.1. Migrations of constituents between the shell and the fill, as well as the shell and the external environment, are very common. These migrations might occur during manufacture, drying and on storage, and they present substantial challenges for development of stable SGCs.

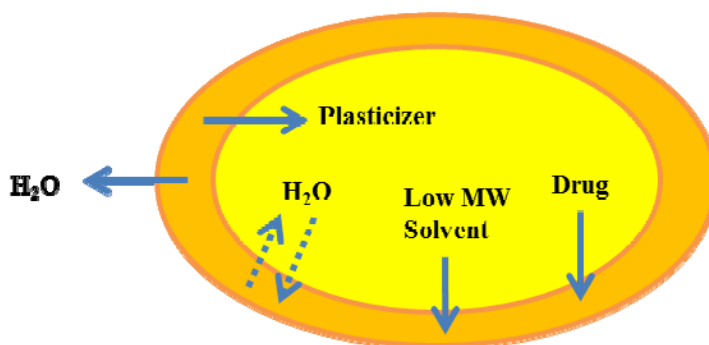


**Figure 2.1:** Schematic representation of fill/shell dynamics during drying process and storage. Arrows indicate possible migrations and MW holds for molecular weight.

Immediately after encapsulation, the capsule shell contains high water content ( $\geq 30\%$  w/w). During a two-step drying process (*primary and secondary drying*) water migrates from the shell into the environment and the fill until equilibrium moisture content is reached (usually 10-15% w/w). As reported by Gullapalli *et al.* (2), the water migration pattern greatly depends on the nature of the fill formulation. While for lipophilic oily formulations there is no water uptake from the shell, a rather hydrophilic fill might pick up a higher amount of water (up to 20% w/w) during primary drying. During secondary drying, some water migrates back into the shell, resulting in capsules containing up to 8% w/w of water in the fill. This water creates a risk of drug precipitation in the fill mass, as shown by Serajuddin *et al.* (13). They demonstrated that even a small increase in water content in polyethylene glycol 400 (PEG 400) can greatly reduce the drug solubility. After the drying process, the packaging and storage of produced SGCs might also be problematic due to the moisture and temperature sensitivity of the gelatin material and, therefore, special care should be taken in very hot and humid regions.

The gelatin capsule shell is compatible with a broad range of liquid and semi-solid lipophilic excipients, solubilizing agents, surfactants, and absorption enhancers. However, the encapsulation of hydrophilic components is very critical, as they usually migrate easily into the shell. Namely, hydrophilic excipients such as low-molecular weight PEG, ethanol, and propylene glycol can readily diffuse into the capsule shell and act as plasticizers. Recently, Cao *et al.* (10) studied the effects of different kinds of plasticizers on the mechanical properties of gelatin films. They concluded that PEG of lower molecular weights (MW) exhibited better plasticizing effects when compared to PEG of higher MW. Also, mannitol and sorbitol proved to be good plasticizers. In addition, it was shown that malic acid (short-chain fatty acid) diffused into gelatin film and improved the flexibility of tested film. Plasticizers in the shell also tend to migrate into a hydrophilic fill. Therefore, to avoid compatibility issues, the amount of hydrophilic excipients should be kept to a minimum level. Besides reducing their amount, other approaches for the successful encapsulation of hydrophilic fill mass have also been suggested. For example,



Brox *et al.* (36) proposed to partially replace glycerol with sorbitol in the capsule shell, and to add glycerol and sorbitol into the fill material.

Volatile excipients (*e.g.* ethyl alcohol, commonly used as a co-solvent for poorly water-soluble components) can easily diffuse through gelatin shells and potentially cause the precipitation of a dissolved drug (11, 12). In such cases, solvent-tight packaging material (aluminium blister) is commonly used to prevent volatilization.

Migration of drug into the capsule shell presents another potential drawback of SGCs. The extent of drug migration greatly depends on its aqueous solubility and partition coefficient between water and non-polar solvent, as demonstrated by Armstrong *et al.* (6, 7). They also showed that there was no correlation between the extent of drug migration and the drug solubility in the fill formulation (isopropyl myristate). Later, Gebre-Mariam *et al.* (8, 9) studied the effect of gelatin grade and concentration on drug migration through gelatin films. It was found that the diffusion of the analysed compound (4-hydroxybenzoic acid) was independent of the type of gelatin used. They concluded that the microviscosity of the prepared gelatin films, rather than the bulk viscosity, was the critical factor governing drug diffusion.

In summary, even though SGC provide an attractive dosage form, there are certainly some challenges and limitations of gelatin as a shell-forming material. Therefore, there was a great interest in the last decade to either modify existing gelatin shell compositions or to elucidate novel shell materials. In 2001, Gennadios (37) proposed to partially replace gelatin with gum acacia (up to 20% w/w). This novel capsule shell composition offered obvious economic benefits, as gum acacia is much cheaper than gelatin. In addition, shorter drying, opening and disintegration times were presented as some functional improvements of the developed shell composition. Also recently, the patent by Zoppetti *et al.* (38) was granted for novel soft gelatin capsules containing a cyclodextrin in the capsule shell. This delivery system was developed particularly for the encapsulation of poorly water-soluble drugs (PWSD). Upon disintegration of such a capsule, an active

compound would form a complex with a cyclodextrin, which would improve the drug solubility. In the next paragraph is provided an overview for potential gelatin substitutes in soft capsule technology.

## **2.2. Alternative materials for soft capsules**

The search for the ideal replacement of gelatin in soft capsule technology has resulted so far in only a few potential alternative materials. This could be due to the fact that as well as overcoming the above-mentioned drawbacks of gelatin, capsule shell polymers would need regulatory approval and adequate methods of production (either coupled with the standard rotary die soft capsule process, or by using different machinery).

To date, most patented soft capsule prototypes have been based on plant-derived hydrocolloids (14, 15), with one exception that contained a synthetic polymer (16). With respect to plant-derived hydrocolloids, two types of carrageenan (iota and kappa), and modified starch of different origin (pea, corn, potato, tapioca) were used in different combinations. For example, the mixture of iota carrageenan with modified starch (hydroxypropyl potato starch) was described in the patent US 6,340,473 (15). Conventional plasticizers (*e.g.* glycerol and sorbitol) and water were added, and the mixture was casted to form mechanically strong, elastic films. A similar film-forming composition comprising iota and kappa carrageenan with modified corn starch was patented by Fonkwe *et al.* (39). Recently, Popescu *et al.* (40) studied various blends of carrageenan with modified starch from different sources (pea, corn, potato). They concluded that the origin of the starch had an impact on the rheological and mechanical properties of the prepared films, which could be due to the different amylose content. Pea starch was shown to be a promising non-gelatin material for soft capsules, as the produced capsules were clear and shiny with good mechanical strength and elasticity.

However, the procedure for the production of hydrocolloid-containing films is rather demanding. Namely, hydrocolloids require a large amount of water for their full hydration. If the produced films are not sufficiently dried, the retained water reduces the film strength. Therefore, a very useful method for extracting a portion of water from the films was proposed by Archibald *et al.* (19). They used an extruder/dryer that included a series of individually controllable heating zones along its length. As the film-forming composition was heated and agitated in the extruder/dryer, the excess water was extracted through several water extraction ports. However, the extrusion process for the production of starch-based shell material with low water content was already introduced earlier by Broker *et al.* (14).

Another interesting approach to overcome these water-related issues was suggested by Brown *et al.* (16). They used synthetic polymers, such as polyvinyl alcohol (PVA). As PVA lacks the gelling properties of hydrocolloids or gelatin, these authors suggested using preformed rolls of almost water-free films that could be fed into the rotary die encapsulation. Also recently, Reich *et al.* (41) evaluated polymer films made of Kollicoat Protect<sup>®</sup> (coating polymer mixture comprising PVA-PEG graft copolymers and PVA; BASF) using a small-scale casting drum. This casting device simulated the conditions of the rotary die machine and proved to be a useful laboratory tool for screening non-gelatin film-forming polymers. Kollicoat Protect<sup>®</sup> formed homogenous polymer films of well-defined thickness, whose mechanical properties were dependent on water content. As a follow-up to this research, Meyer-Böhm *et al.* (42) studied various combinations of modified starch types (tapioca, corn, pea) and Kollicoat Protect<sup>®</sup>. They demonstrated that modified pea starch improved flexibility of the produced films compared to the starchless films.

Research activities conducted in Swiss Caps AG (Kirchberg, Switzerland) resulted recently in a novel starch-based thermoplastic material that was obtained from a two-step extrusion process. The new shell material combines the thermoplastic properties of starch with the characteristics of PVA. In our first study we aimed to physically characterize the

novel starch-based PVA thermoplastic shell material (S-PVA) and to explore its pharmaceutical advantages over gelatin for soft capsule technology.

Today, several types of plant-based soft capsules are commercially available. Table 2.2 outlines the most common non-gelatin soft capsules on the market. Basically, both qualitative and quantitative compositions of the presented capsule prototypes are similar. The main difference is the water content in the finished product, due to the different manufacturing processes.

**Table 2.2:** Overview of selected commercial non-gelatin soft capsules.

	<b>Composition</b>	<b>Method of production</b>	<b>Manufacturer</b>	<b>Patent</b>
<b>Vegicaps<sup>®</sup></b>	Modified starch/iota carrageenan blend, plasticizer, water 52.5% :37.5% :10% (w/w)	Melt-on-demand, casting and rotary die method	Catalent	US 6,884,060 US 6,340,473 US 6,582,727
<b>VegaGels<sup>®</sup></b>	Potato starch, glycerol, sorbitol, carrageenan, and water 66% : 18% : 10% : 1% : 5% (w/w)	Extrusion and rotary die method	Swiss Caps AG, member of AENOVA group	US 6,790,495
<b>SeaGel<sup>®</sup></b>	Kappa or iota carrageenan, starch, optionally a plasticizer, water	Extrusion/casting and rotary die method	FMC Biopolymer	US 7,807,194

Until now, all plant-based soft capsules were intended only for healthcare and nutritional consumers. They are most commonly used for the encapsulation of simple lipophilic oils (vitamins A, E, vegetable oils), multivitamins and some herbals (Table 2.3).

**Table 2.3:** List of selected commercially available lipophilic oils encapsulated in non-gelatin soft capsules, in Europe, in 2013.

Trade name	Active ingredients/Dose	Distributor
Opti 3 Omega-3 EPA & DHA	EPA (200 mg), DHA (400 mg), D <sub>3</sub> (5 µg)	ESB Developments <sup>1</sup>
Surbex Natopherol <sup>®</sup>	d-α tocopherol	Abbott <sup>2</sup>
Garlic pearls	Pure concentrated garlic oil	
Omega 3,6,9	Organic Flaxseed Oil (1000 mg)	
VitaEPA	Omega-3 Fatty Acids (300 mg), EPA (180 mg), DHA (120 mg) and Natural Vitamin E (2 IU)	VitaHealth <sup>2</sup>
Primolin gold	Evening primrose oil (1000 mg), vitamin E	
UltraClean Algal DHA and Omega	Schizochytrium sp. (microalgae) and Hippophae rhamnoides (sea buckthorn), DHA (300 mg)	BioCeuticals <sup>2</sup>
Actilife Omega-3	DHA (250 mg),	Migros <sup>3</sup>
Omega 3 Linseed oil 1000	α Linolenic acid (500mg), Folic acid (600 µg), Vitamin B6 (4.2 mg), Vitamin B 12 (7.5µg)	DM Drogeriemarkt <sup>3</sup>
Marinalis, marine lipids	Tuna fish oil (500 mg), DHA (120 mg), EPA (30 mg)	Sofinol <sup>3</sup>

<sup>1</sup>SeaGel<sup>®</sup> FMC technology; <sup>2</sup>Vegicaps<sup>®</sup> capsule; <sup>3</sup>VegaGels<sup>®</sup> capsule; EPA-Eicosapentaenoic acid; DHA-Docosahexaenoic acid; IU-international units

## **2.3. Manufacturing methods**

In the early 19<sup>th</sup> century soft gelatin capsules were produced one at a time in individual moulds. As technology advanced, the individual moulds were replaced by multiple moulding units, which led to the development of plates containing die pockets (*plate process*) (3). As this method requires several operators and the equipment cannot be purchased any more, it is almost obsolete today. Up till now, several other methods (*e.g.* Norton, Accogel) have been invented, but are nowadays rarely employed. The commercially important equipment and processes in soft capsule technology that are used contemporarily will be described in the following paragraphs.

### **2.3.1. Globex method**

Seamless, spherical soft gelatin capsules can be produced by the Globex method (Figure 2.2). The lipophilic fill and the gelatin shell formulations are stored separately and kept at elevated temperatures (> 60° C) (43).

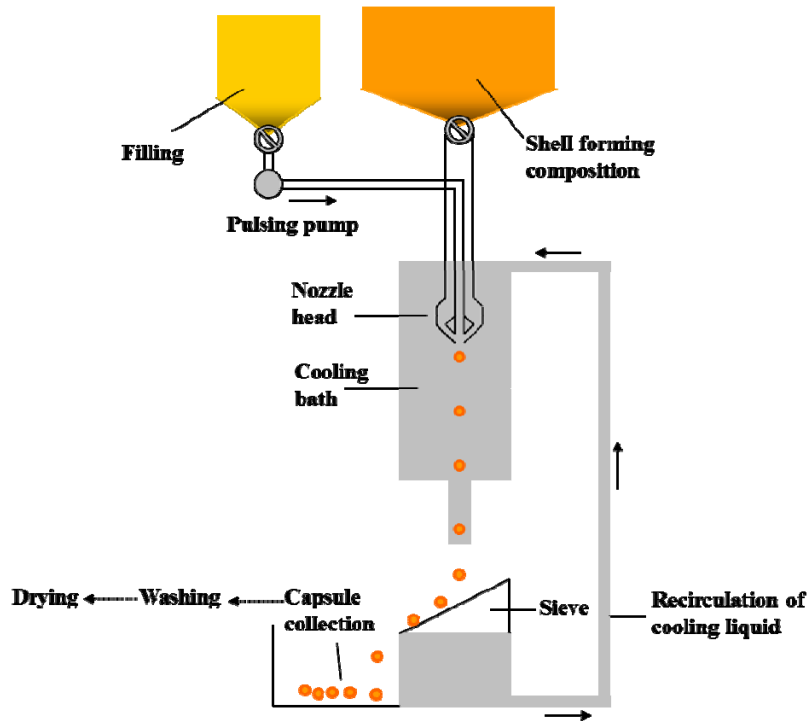


**Figure 2.2:** Process outline of the Globex method. Adapted from reference (44).

They are both simultaneously pumped through a concentric double tube, with the fill in the inner one. The liquids are discharged into a cooling bath (*e.g.* liquid paraffin at 4° C) as droplets consisting of a liquid fill with a molten gelatin outer film. The droplets assume spherical shape, as the shell material possesses a higher surface tension compared to the surface tension of the fill. Upon cooling, gelatin congeals thereby forming a flexible and firm capsule shell. The produced capsules are collected, washed and dried. The main disadvantage of this method is the necessity of optimizing the surface tension between the fill and the shell material (44).

### 2.3.2. Rotary die method

The rotary die method was invented in 1933 by Robert Pauli Scherer. To date, it has become the standard manufacturing procedure for encapsulation of liquids and semi-solids in soft gelatin capsules. The illustration of the production process is shown in Figure 2.3.

For the rotary die method, the fill and the shell material are prepared in separate containers. The shell formulation is made by initially mixing water and plasticizer(s) with gelatin in a suitable vessel at room temperature (RT). The mixture is then melted completely at high temperatures ( $\sim 90\text{-}95^\circ\text{C}$ ) under vacuum with slow mixing, until a clear gel is obtained. The molten mass is transferred to heated tanks and kept at  $57\text{-}60^\circ\text{C}$ . From the tanks, the gelatin solution is fed into two spreader boxes placed above cooled rotating drums ( $13\text{-}14^\circ\text{C}$ ). The spreader boxes control the flow of the shell-forming material onto rotating casting drums. The thickness of the formed gelatin ribbons can be varied depending on the capsule application (from  $600\text{-}1000\ \mu\text{m}$ ), but usually it is about  $800\ \mu\text{m}$ . The formed ribbons are lubricated by feeding them over guide rolls through a mineral oil bath. Subsequently, they are guided over counter-rotating rolls that contain the shape forming dies. The die cavities on the left-hand roll form the left half of the capsule; the die cavities on the right-hand roll form the right half of the capsule. As the die rolls rotate, die cavities on the two rolls match and the two passing gelatin ribbons can be sealed and cut along the edge of the dies. As a result, the lower parts of the capsules are sealed. The filling material flows by gravity from a filling tank into a positive displacement pump. The pump accurately injects the fill through the wedge and into the partially sealed gelatin ribbons between the die rolls. As the die rolls continue to rotate, the filled capsules are completely sealed and cut out. The produced capsules have to be washed to remove the mineral oil lubricant (44).

After encapsulation, the capsules are subjected to a two-step drying process (*primary and secondary drying*). During primary drying, capsules are transferred into rotating drums at



20-30° C until about 50-60% of the water content in the shell is removed. For secondary drying, capsules are placed in tunnel dryers at a relative humidity of 10-30% and 20-25° C until the equilibrium is reached. This might take from several hours to several days depending on the gelatin formulation used. The shell of the dried capsules at equilibrium normally contains 6-10% water, which is determined during quality control testing. Additional analysis, such as seam thickness and rupture tests, are also employed on the finished capsules. Afterwards, the capsules might be sent for ink printing (for identification purposes), enteric-coating (for modified-release dosage forms) or directly to packaging into blisters (3, 44).

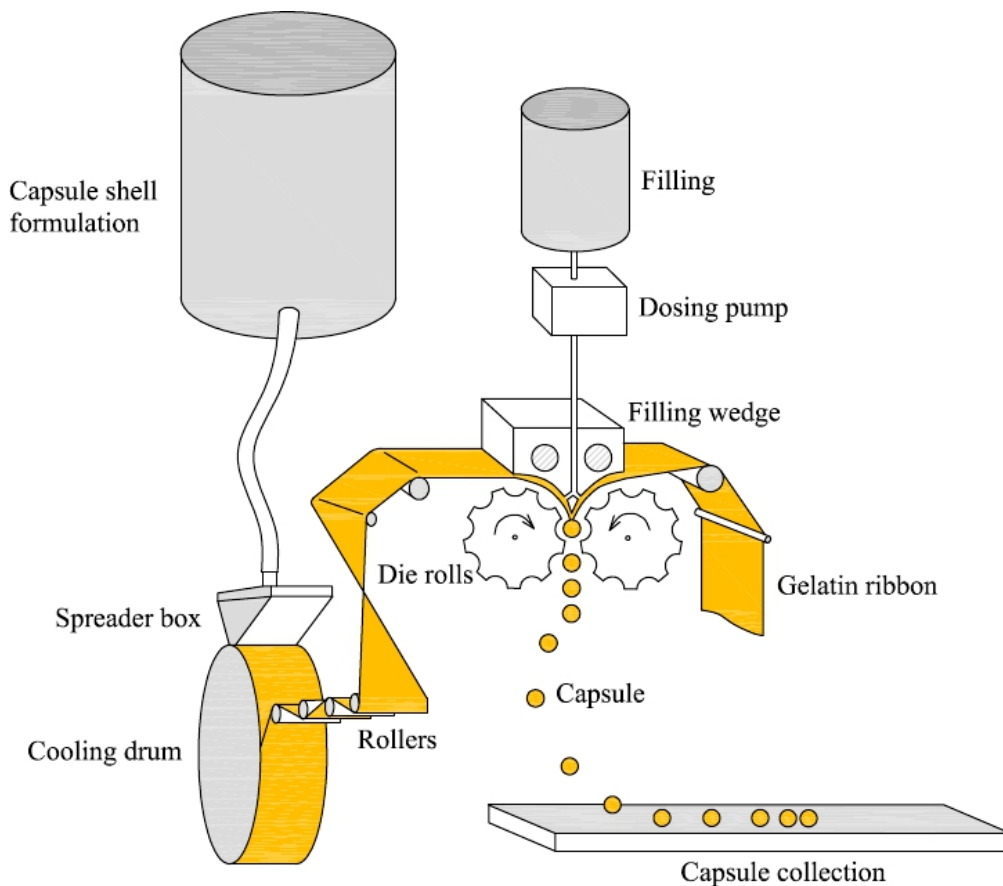


**Figure 2.3:** Illustration of the rotary die method. Adapted from reference (44).

The rotary die method has several advantages over the Globex method. For example, there are no restrictions regarding the fill (other than compatibility with the shell). It also enables the production of capsules of different shapes, sizes, or even colours. Additionally, the manufacturing rates are faster so that up to 100 000 capsules per hour can be produced. However, the costs are higher due to the large amount of shell waste, and machinery maintenance. Another disadvantage of the rotary die method is the risk of leakage through imperfect seams, which is avoided by the Globex method as the produced capsules are seamless. In line with these different technological aspects, the rotary die method is the most commonly used process today for the production of soft gelatin capsules.

### **2.3.3. Production of non-gelatin soft capsules**

As shown in Table 2.2, the shell formulations of non-gelatin soft capsules are usually starch-based. Accordingly, the machinery for the production of shell ribbons was adjusted to the existing rotary die method. For example, Vegicaps<sup>®</sup> are produced using melt-on-demand and casting technology coupled with the rotary die method (17). For this technology, the film-forming material is prepared in bulk (allowed to solidify), and is transferred to tanks. Only the required amount of solid shell formulation from the tanks is melted in the melt-on-demand device and transported under pressure to the casting drum. The casted ribbons are further guided over rolls to rotating dies and the fill is encapsulated.

The manufacturing process of SeaGel<sup>®</sup> capsules was patented recently by FMC Biopolymer (18). Firstly, all components of the shell-forming material are heated, hydrated, mixed, solubilized and de-aerated in a suitable double jacketed vessel at 90-95°

C. In the next step, the molten mass can be formed into a film either by casting the mixture onto a cooling drums or by passing the mixture through an extruder. The formed films are used for encapsulation using the conventional rotary die process.

In contrast to Vegicaps<sup>®</sup> and SeaGel<sup>®</sup> capsules, the shell material of VegaGels<sup>®</sup> is produced in a two-step extrusion process, as presented in Figure 2.4. In the first step, the shell formulation is mixed by means of a double-screw extruder at 130-140° C under high pressure of 115-120 bar to form granules. Formed granules can be stored in plastic tanks or mixed with colourants and used immediately for the second extrusion process. For this subsequent extrusion, a single-screw extruder is employed at about 100-135° C. The obtained extrudate is pressed through a slit die at 115° C to form a shell ribbon used further on in the rotary die method. This manufacturing process was also used for the encapsulation of the novel starch-based PVA thermoplastic capsules (S-PVA-Cs) that are described in detail in Chapter 3.

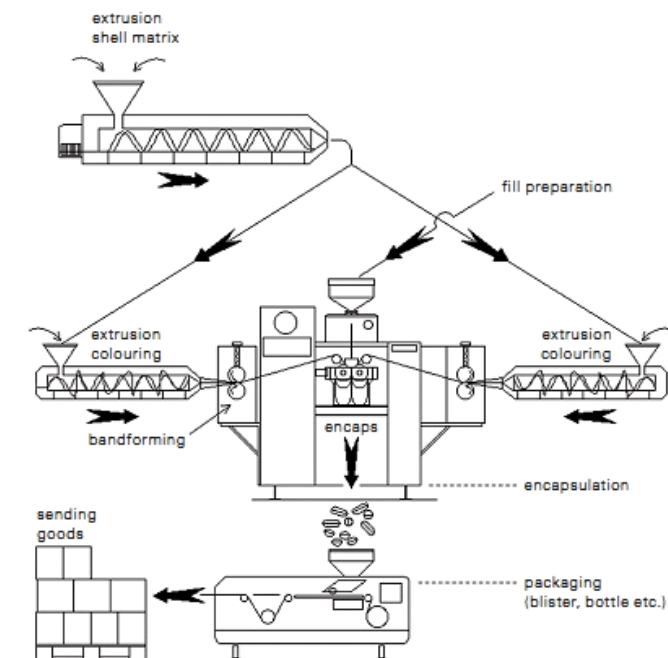


**Figure 2.4:** Schematic outline of the manufacturing process of VegaGels<sup>®</sup>. Reprinted from reference (14) with permission from Swiss Caps AG.

## 2.4. Comparison of soft gelatin capsules versus non-gelatin soft capsules

The different shell capsule technologies can be compared by means of the shell material, processing characteristics as well as by considering biopharmaceutical aspects. Table 2.4 provides such an overview of most relevant features of soft capsule technologies.

**Table 2.4:** Soft gelatin capsules versus non-gelatin soft capsules.

	Soft gelatin capsules	Non-gelatin soft capsules
Shell composition	Animal origin Gelatin, plasticizer, water, etc.	Plant-based Modified starch (potato), carrageenan (or PVA), plasticizer, water etc.
Fill composition	Type I-IV according to LFCS	Type I-IV according to LFCS Potential improvement for type IIIB-IV
Fill pH	Slightly acidic to slightly basic	Slightly acidic to highly alkaline
Manufacturing process	Rotary die method	Melt-on-demand/casting/extrusion coupled with the rotary die method
Fill temperature	Maximum: 35-40° C (primarily liquids)	Maximum: 65-75° C (for S-PVA-C: 100-140° C) (viscous liquids, semi-solids; high melting point formulations)
Large scale manufacture and available marketed products	Good technical feasibility with many market products (Pharmaceuticals and Health & Nutritional)	Technical feasibility demonstrated with products on the market (OTC and Health & Nutritional; No pharmaceuticals)
Shell compatibility with fill excipients	Mostly lipophilic Limitations: hydrophilic excipients; low MW and short/medium-chain lengths	Wide range: from lipophilic to hydrophilic Potentially less limitations

	<b>Soft gelatin capsules</b>	<b>Non-gelatin soft capsules</b>
Drug migration	Probable in the case of small acidic compounds	Not expected
Water migration	Very dynamic system (potential limitation for hydrophilic formulations)	Slight water migration
Shell disintegration	Fast	Fast (for S-PVA-C: short lag-time)
Dissolution	Potential cross-linking	No cross-linking

LFCS - lipid formulation classification system; S-PVA-C - starch-based PVA capsule; OTC – over the counter

## 2.5. Oral lipid-based formulations for poorly water-soluble drugs

Poorly water-soluble drugs (PWSD) are typical outcomes of high throughput screening in drug discovery programmes. According to their permeability, these drugs can be categorized by the Biopharmaceutics Classification System (BCS) as class II (high permeable) or class IV (low permeable) compounds (Figure 2.5) (45). Additionally, this classification system includes highly soluble drugs and also differentiates them according to permeability (class I and class III). From a pharmaceutical perspective, poorly-soluble compounds (class II and IV) are especially challenging, but various formulation strategies can help in reducing biopharmaceutical issues. Particularly, in case of class II compounds, several formulation approaches exist to cope with a limiting solubility or a critical drug dissolution rate (46).

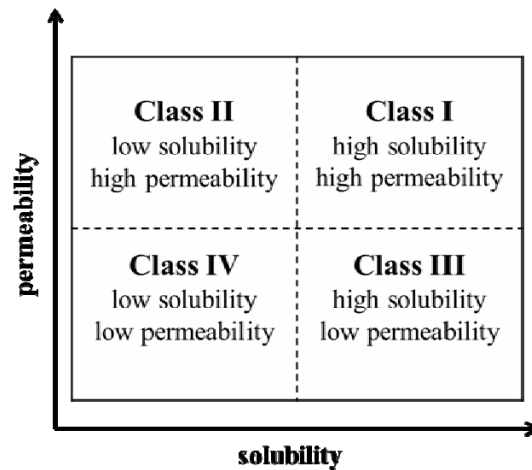


**Figure 2.5:** Biopharmaceutics Classification System according to Amidon *et al.* (45).

Nowadays, oral lipid-based formulations (LBFs) have become one of the most interesting formulation strategies for PWS. Their main advantage is that the drug remains in solution during its transit period in the lumen of the gastrointestinal tract (GIT). Although drug solubilization is the primary mechanism by which LBFs improve drug absorption, they may also protect the drug from chemical and enzymatic degradation in the GIT, as well as promote lymphatic drug transport (Figure 2.6).

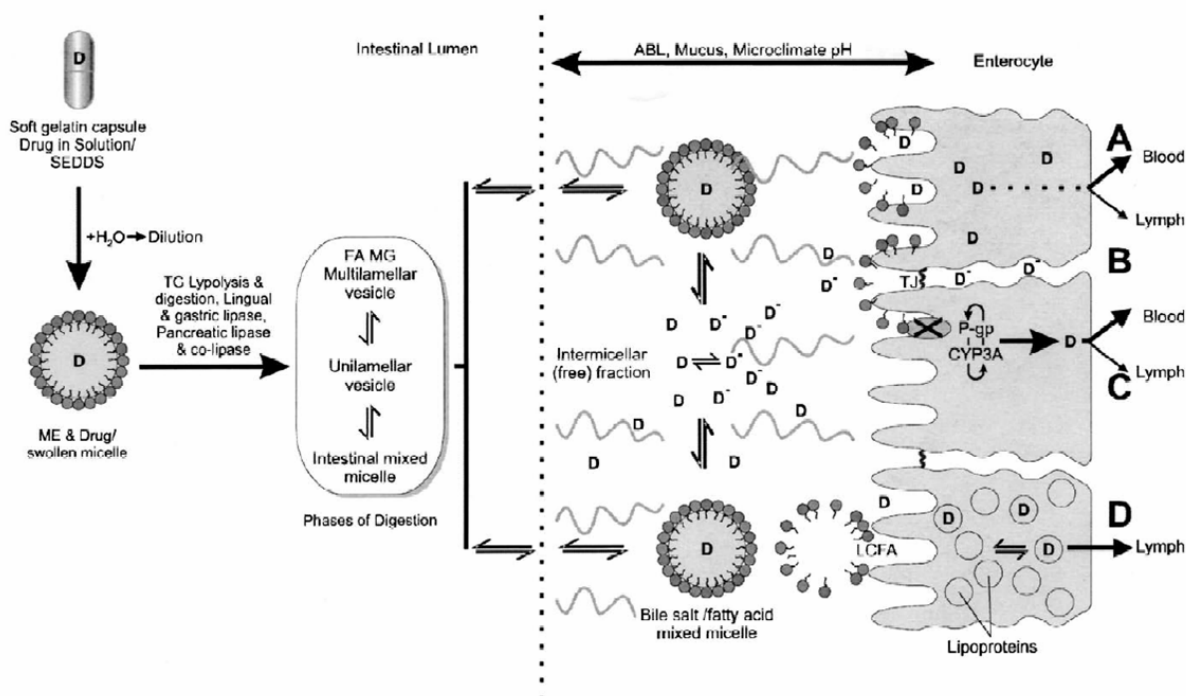


**Figure 2.6:** Schematic diagram of intestinal drug transport from LBF via the portal and the mesenteric lymphatic routes. (A) Increased membrane fluidity facilitating transcellular absorption, (B) opening of tight junctions to allow paracellular transport, (C) inhibition of P-gp and/or CYP450 to increase intracellular concentration and residence time, and (D) stimulation of lipoprotein/chylomicron production. ABL-aqueous boundary layer; D-drug;  $D^-$ -ionized drug; FA MG-fatty acid monoglyceride; LCFA-long-chain fatty acid; ME-microemulsion; SEDDS-self-emulsifying drug delivery system; TG-triglyceride; TJ-tight junction. Reprinted from reference (47) with permission from Elsevier.

LBFs range from simple oils to complex mixtures comprising oils, lipophilic and hydrophilic surfactants, and hydrophilic co-solvents (48). In 2000, Pouton proposed the

Lipid Formulation Classification System (LFCS) to categorize LBFs into classes based on the polarity of excipient blends (Table 2.5) (49). Type I formulations are simple, non-toxic solutions of the drug in oils (*e.g.* triglycerides, mixtures of mono- and diglycerides). They generate coarse oil droplets upon dispersion and would have to be digested to free fatty acids and 2-monoglycerides to further promote drug absorption. Due to their lipophilicity they are particularly appropriate for drug compounds with rather high lipophilicity, *e.g.*,  $\log P > 4$ . Type II formulations are combinations of oils and lipophilic surfactants (*e.g.* lecithin, Labrafil<sup>®</sup> M1944CS) and they are employed when higher drug solubility in a formulation is needed. These formulations spontaneously self-emulsify upon gentle agitation. Fine emulsions (0.25-2  $\mu\text{m}$ ) are generated and they are usually digested thereby enhancing drug absorption. Type III formulations contain oils, hydrophilic surfactants (*e.g.* Gelucire<sup>®</sup> 44/14, Cremophor<sup>®</sup> RH 40), and co-solvents (*e.g.* PEG, propylene glycol), which may further facilitate the self-emulsification process in the GIT. Depending on the oil content in type III formulations, we can differentiate type IIIA formulations (up to 80% w/w oil) and type IIIB formulations (< 20% w/w oil). While type IIIB formulations form smaller particles (<50 nm) compared to type IIIA formulations (100-250 nm), they also present a greater risk of drug precipitation upon aqueous dispersion due to a loss of solvent capacity. In 2006, Pouton introduced an updated version of the LFCS that contained an additional category (type IV formulations) (50). These formulations are oil-free and represent the most hydrophilic lipid-based formulations comprised only of hydrophilic surfactants and co-solvents. Type IV formulations commonly offer increased drug payloads and produce micellar structures when introduced in aqueous media. It has been suggested that this in turn led to rapid drug release and increased drug absorption (51). However, adding more hydrophilic excipients may also foster drug precipitation upon formulation dispersion, therefore some care is needed when using this type of lipid-based system.



**Table 2.5:** Composition of lipid-based formulations (% w/w) according to LFCS (50).

Excipient	Type I	Type II	Type IIIA	Type IIIB	Type IV
Oils	100	40-80	40-80	<20	-
Lipophilic surfactants (HLB<12)	-	20-60	-	-	0-20
Hydrophilic surfactants (HLB>12)	-	-	20-40	20-50	30-80
Co-solvents	-	-	0-40	20-50	0-50

HLB - hydrophilic-lipophilic balance

In this thesis particular interest was directed towards the encapsulation of hydrophilic lipid-based formulations, such as self-microemulsifying drug delivery systems (SMEDDS), since they present a special challenge in terms of capsule compatibility. Therefore the following paragraph describes these systems in more detail.

## 2.6. Self-microemulsifying drug delivery systems (SMEDDS)

Self-microemulsifying drug delivery systems (SMEDDS) are defined as thermodynamically stable isotropic mixtures of oil, surfactant/co-surfactant, and a solubilized drug. These formulations rapidly and spontaneously form transparent o/w microemulsions (droplet size <50 nm) in contact with aqueous media (52). Upon oral administration, SMEDDS are easily dispersed in the gastrointestinal fluids, as the motility of the stomach and small intestine endows the gentle agitation needed for emulsification (53). Recently, the name SMEDDS has been challenged because obtained colloidal dispersions may not necessarily be true microemulsions but nano-emulsions instead (54). The latter system is only kinetically stable and is not a thermodynamically stable system

like microemulsions. The definition of microemulsions as thermodynamically stable systems was proposed already in 1981 by Danielsson and Lindman (55). Some authors preferred to use the name self-nanoemulsifying system (SNEDDS) but this does not help as long as the true nature of the colloidal dispersion has not been identified, which most scientific reports do not clarify. A very recent article proposed a guideline for differentiating the different types of nano-dispersion (56). However, such experimental differentiation is primarily of academic interest because it is most likely of lesser importance from a biopharmaceutical perspective.

### **2.6.1. Excipients in SMEDDS**

The primary aim in the selection of adequate excipients for self-emulsifying formulations is finding an excipient or combination of excipients that will enable the solubilization of the entire drug dose (57). A major concern represents the chemical and physical stability of the drug in the formulation, which both have to be monitored during formulation development. Another important criterion in excipient selection is the toxicity and safety that are evaluated by regulatory authorities. “Generally recognised as safe” (GRAS) excipients are excipients tested by the United States Food and Drug Administration (FDA) and they are considered as non-toxic to humans and animals (58). The FDA also recommends the accepted amounts of excipients in the Inactive Ingredient Database (IID), where they publish qualitative and quantitative compositions of approved drug products on the US market (59).

Medium-chain triglycerides (MCT; *e.g.* Miglyol<sup>®</sup> 812 N, coconut oil) and long-chain triglycerides (LCT; *e.g.* olive oil, peanut oil) are the most commonly used oils for the formulation of SMEDDS (60). To empower rapid and facile dispersion in the GIT, SMEDDS require the incorporation of large amounts of surfactants (up to 50% w/w) that possess relatively high HLB (hydrophilic-lipophilic balance) values. Since surfactants often have potential toxic effects, particularly when they are used at high amounts, it is

important to consider the oral tolerability these excipients. Therefore, non-ionic surfactants are usually favoured over their ionic counterparts, as they have been reported to have minimal toxicity. Also, surfactants of natural origin (*e.g.* lecithin or Peceol<sup>®</sup>) are generally less toxic compared to synthetic surfactants (*e.g.* Tween 80<sup>®</sup>). Such natural surfactants may, however not always exhibit the same performance of self-emulsification as compared to synthetic amphiphile. In addition, surfactants can facilitate drug absorption via reversibly changing of the intestinal permeability (61). Formulations comprising of oils and hydrophilic surfactants might not have sufficient solubilizing capacity for some drugs. In such cases, the addition of hydrophilic co-solvents (*e.g.* ethanol, propylene glycol, glycerol, PEG) is needed (50). However, since these excipients normally change their solubilizing properties following dispersion in GI fluids, the risk of drug precipitation raises (62). Therefore, hydrophilic co-solvents should be added carefully.

Ternary phase diagrams typically help to find optimum concentrations or suitable concentration ranges of the excipients in the final formulation. Each point in the phase diagram corresponds to a certain combination of oil, surfactant, and co-surfactant. Usually, all combinations of different amounts of excipients are evaluated for their self-emulsification properties by mixing with aqueous media (*e.g.* water, buffers or biorelevant media) in biopharmaceutically relevant ratios (*e.g.* 1:200 v/v). The resulting dispersions are checked visually and analysed by dynamic light scattering for particle size, enabling the identification of those combinations that form nano-dispersions. An example of such a ternary phase diagram is presented in Figure 2.7 (63), where combinations of medium-chain or long-chain triglycerides (lipid phase), Cremophor<sup>®</sup> RH 40 (surfactant), and Akoline MCM or Peceol<sup>®</sup> (co-surfactant) are examined. The area within the dotted line represents the microemulsion region for different mixtures of these excipients dispersed in 250 mL water at 37° C (particle size <100 nm).

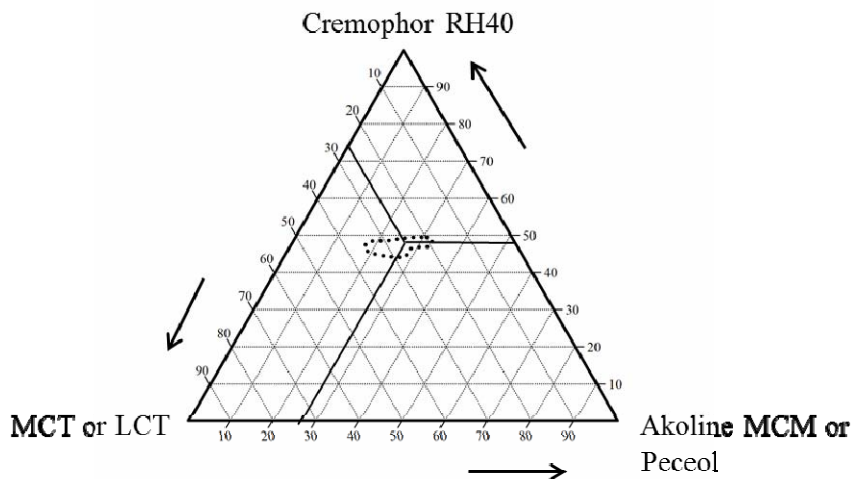


**Figure 2.7:** The marked area in the ternary phase diagram represents microemulsions obtained upon dispersion of 1 g of SMEDDS containing surfactant (Cremophor<sup>®</sup> RH40), oil (MCT or LCT) and co-surfactant (Akoline MCM or Peceol<sup>®</sup>) in 250 mL water. Droplet size of microemulsions was less than 100 nm. MCT-medium-chain triglycerides, LCT-long-chain triglycerides. Adapted from reference (63).

Although phase diagrams are of great interest to formulators, there is much time needed for experimental construction of such diagrams. Therefore, much effort was directed in recent years to shorten the formulation selection process. This involved development of artificial neural network models for computer simulation and optimization of microemulsion systems to minimize the experimental workload (64-67).

### 2.6.2. *In vitro* testing of SMEDDS

*In vitro* testing of selected formulations is often used to help predict the fate of the drug upon formulation dispersion and digestion in the GIT. There are several useful *in vitro* analyses that are commonly employed, such as dilution, dispersion, and *in vitro* lipolysis (68). Firstly, simple and fast dilution tests are normally used to evaluate the formulation performance in contact with aqueous media (69). Visual assessment of the diluted systems seems to be reliable for the estimation of oil droplet size (52, 63, 70). Namely, transparent to slightly bluish, opalescent dispersions possess oil droplets between 20-40 nm, whereas larger oil droplets ( $\geq 100$  nm) are characteristic of opaque, milk-white dispersions.

In comparison to simple aqueous dilution, *in vitro* dispersion testing better mimics the physiological conditions in the GIT. A compendial dissolution apparatus (United States Pharmacopoeia-USP 2) and various biorelevant media are often used to simulate gentle agitation of the GIT and its physiological environment. The general method for this test is analogous to dissolution testing, *i.e.* samples are taken from the vessels at various time points, and before assaying they are filtered or centrifuged to remove any precipitated drug. *In vitro* dispersion testing is of major importance particularly for hydrophilic LBF. The hydrophilic formulation components are likely to partition in the aqueous bulk, which in turn decreases the solubilization capacity of the formulation and increases the risk of drug precipitation. Formulations can be analysed regarding particle size in the course of their aqueous dispersion (usually at fixed time points) (71). Measuring particle size in formulations dispersions may detect drug precipitates but are often just meant to characterize the type of lipid-based formulations. However, the importance of droplet size is a debated topic when comparing different nano-dispersions (72). Most important is certainly drug solubilization.

As soon as the dispersed formulation enters the upper small intestine, the digestion of formulation components begins. The solubilizing properties of LBFs can change

dramatically following dispersion and digestion, so the fate of the drug depends on more factors than just the initial droplet size upon dispersion. *In vitro* lipolysis testing is generally of high importance for the development of LBFs (73, 74). However, it can be argued that for SMEDDS, the influence of digestion is often limited. Especially for this formulation type, rather simple dispersion tests may provide a good first estimate of the biopharmaceutical performance.

There are some specific factors to consider in the development of LBF with weak bases. Namely, weak bases may be dissolved at the low pH in the stomach, but when they enter the intestinal environment, they could precipitate. The fate of the weak base in the intestinal fluid will greatly depend on the solubilization capacity of the formulation or the intestinal mixed micelles. In the last decade, *in vitro* tests simulating drug transfer from the stomach to the intestine showed that the precipitation of weak bases depends on the rate of gastric emptying (75, 76). Therefore, for weak base formulations additional *in vitro* tests which mimic gastric emptying would be useful.

As mentioned earlier, the primary mechanism through which LBFs promote drug absorption is by providing a high concentration of solubilized drug in the GI lumen. However, depending on the LBF composition, the solubilization capacity of the formulation may decrease following dispersion and digestion and this creates the risk of drug precipitation. In the following paragraph drug precipitation, and focused beam reflectance measurement (FBRM) an *in vitro* analytical technique for studying drug precipitation, will be discussed.

## **2.7. Drug precipitation**

Drug precipitation is a complex process that involves three phases (77). In the first phase, a drug is in a supersaturated solution, *i.e.* the actual concentration of solubilized drug exceeds its equilibrium solubility. Such a supersaturated solution is associated with an

increased chemical potential ( $\mu$ ) compared to a thermodynamically stable, saturated solution ( $\mu_{eq}$ ). The difference in this chemical potential ( $\Delta\mu = \mu - \mu_{eq}$ ) is the driving force for drug precipitation. If we assume that there is no difference in the activity coefficients of the solute in the supersaturated and saturated state, the relationship between the difference in chemical potential ( $\Delta\mu$ ) and supersaturation ( $S$ ) can be presented as follows:  $\Delta\mu = kT\ln(S)$ , where  $k$  presents Boltzmann constant,  $T$  the temperature, and  $S$  the supersaturation ratio (78). Once a critical supersaturation is reached, the second phase of the drug precipitation process (nucleation) begins. It is important to differentiate between “primary” and “secondary” nucleation (Figure 2.8). In absence of solid drug, primary nucleation can occur, whereas secondary nucleation describes that nuclei are often formed in close proximity of crystals already existing in a supersaturated solution (79).

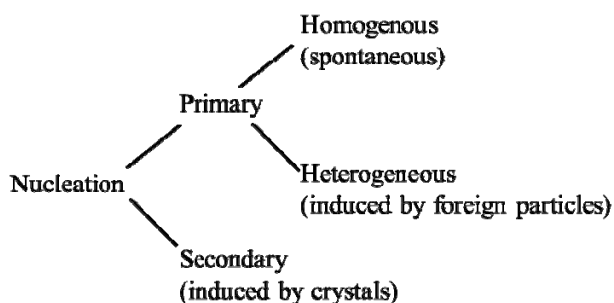


**Figure 2.8:** Schematic diagram of nucleation nomenclatures. Adapted from reference (77).

During this nucleation phase, drug molecules form small clusters/aggregates, which grow to macroscopic crystals (crystal growth) in the third phase of precipitation. As presented in Figure 2.9, precipitation from a supersaturated solution is thermodynamically favoured (decrease in Gibbs free energy). However, the nucleation step requires activation energy. During the nucleation phase, small aggregates grow until they become critical in size (with a critical radius  $r^*$ ). Such critical nucleus size is required for further particle growth. If this activation energy is too high, new crystals will not be formed and the

supersaturated solution will remain in a metastable zone (for a certain period of time) (79).

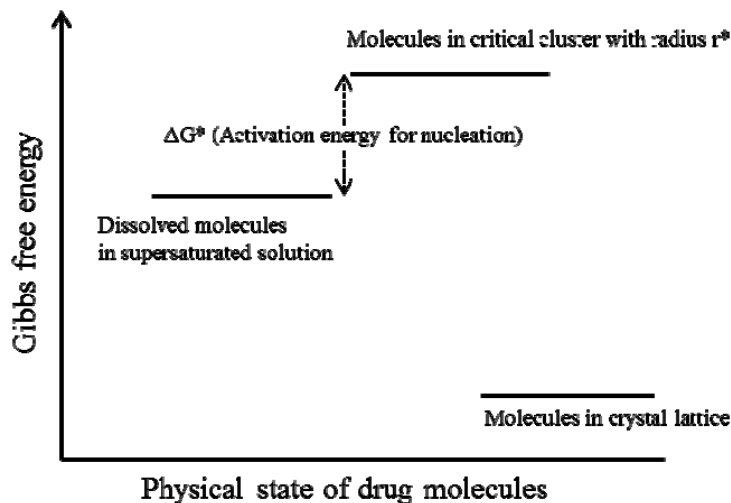


**Figure 2.9:** Schematic diagram of the Gibbs free energy of dissolved molecules in supersaturated solution. Adapted from reference (79).

Homogeneous nucleation may occur at rather high supersaturation, but is rarely found at comparatively lower supersaturation and in presence of impurities and other foreign particles. In the GI lumen, mostly heterogeneous nucleation may occur, which can be influenced by excipients such as surfactants (79).

Once the activation energy is reached (stable nuclei with critical radius  $r^*$  are formed), critical clusters can grow to macroscopic crystals. Crystal growth is the last phase of the precipitation process and consists of two steps: diffusion of molecules from the supersaturated solution to the crystal interface, and integration of the molecule in the crystal lattice (79).



## 2.8. Focused beam reflectance measurement (FBRM)

Focused beam reflectance measurement (FBRM) is a rather novel *in vitro* analytical technique for real time *in situ* analyses. Gao *et al.* were first to use this technique for studying drug precipitation during LBF dispersion (80). FBRM utilizes a focused beam of laser light that scans across a particle passing in front of the probe window (Figure 2.10). Based on the back-scattered light, the chord length distribution of particles is determined (81). The lowest detectable chord length of the particles is around 1  $\mu\text{m}$ . In this PhD thesis (Chapter 5) FBRM was successfully employed for the detection of the onset of drug precipitation following aqueous dispersion of solid lipid-based systems. This technique offers several advantages, such as ease of use, minimum maintenance requirements and, as mentioned beforehand, capability of *in-situ* measurements. In addition, FBRM can be coupled with other analytical techniques (*e.g.* Raman or infrared spectroscopy) for better characterisation of formed precipitates (82, 83).

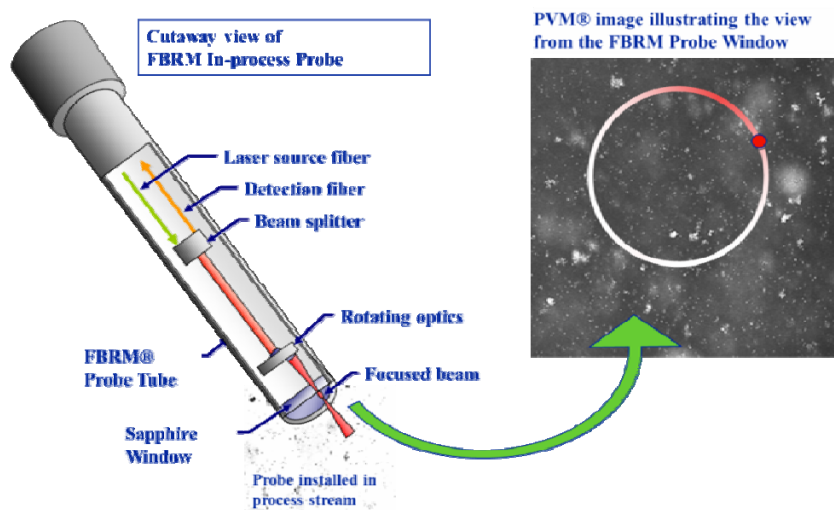


**Figure 2.10:** In-process probe for focused beam reflectance measurements (Source: Mettler-Toledo, Switzerland).

## 2.9. Drug supersaturation

### 2.9.1. Drug supersaturation triggered by oral administration of LBF

The intraluminal concentration of a drug is not necessarily limited by its solubility in GI fluids. Drugs may be in solution in a supersaturated state, which means at a concentration above their saturation solubility ( $C_{eq}$ ). However, as mentioned earlier, a supersaturated drug solution is thermodynamically unstable and has the tendency to return to the equilibrium state by drug precipitation. This period of drug supersaturation is of major importance from a biopharmaceutical perspective. Namely, if it is sufficiently long, it may enable drug absorption and prevent intestinal drug precipitation. Additionally, it would be beneficial if drug supersaturation occurs close to the site of absorption. Recent studies showed that LBFs could be a successful formulation strategy in this respect, since they induce moderate supersaturation within the GI lumen. Four different mechanisms have been suggested by which LBFs generate supersaturation along the GIT (84). Dispersion-triggered supersaturation (*mechanism 1*) usually appears when LBFs that contain high amounts of water-miscible co-solvents and hydrophilic surfactant are employed (85). In case the decreased solubilization capacity of the dispersed formulation does not immediately result in drug precipitation, the solubilized drug can reside in a supersaturated state. Similarly, excipient digestion can also induce drug supersaturation (*mechanism 2*) as digestion products are less lipophilic and a drop in formulation solubilization capacity is expected (86). Interestingly, Yeap *et al.* (87, 88) demonstrated that further dilution of digestion products with bile salt also caused a decrease in drug solubility (*mechanism 3*) and this was particularly crucial for basic drugs. Finally, drug supersaturation can also be generated at the intestinal unstirred water layer, which is more acidic compared to the bulk lumen (pH 5.5 vs. 6.5). This acidic microclimate promotes fatty acid absorption, since they become protonated and dissociate from bile salt mixed micelles. As a consequence, supersaturation is induced, since fatty acids are no longer

accessible for drug solubilization (*mechanism 4*) (89). In summary, LBFs present a promising formulation approach not only to promote GI drug solubilization, but also to enhance drug absorption by generating moderate supersaturation within the GIT.

The degree of supersaturation can be defined by the supersaturation ratio (*SR*):

$$SR = \frac{C_{sol}}{C_{eq}} \quad (2.1)$$

where  $C_{sol}$  represents the actual concentration of solubilized drug, and  $C_{eq}$  the equilibrium solubility of the drug. According to the degree of supersaturation, a system can be unsaturated ( $SR < 1$ ), saturated ( $SR = 1$ ), or supersaturated ( $SR > 1$ ) (79). As the *SR* value exceeds 1, there is an increasing likelihood of drug precipitation. As mentioned earlier, drug supersaturation is a typical outcome of LBF dispersion and lipolysis. Therefore, research effort has been recently directed in determining the critical *SR* for a range of PWSD formulated using various LBFs. It has been demonstrated that drug precipitation was unlikely to occur in a physiologically relevant time span when  $SR < 2$  was obtained upon formulation dispersion (85, 86). However, this limit might not be a general rule, since another study presented drug precipitation at lower *SR* values (90). The critical *SR* value could be considerably different upon formulation digestion, especially in the case of type I, II, and IIIA formulations, as their solubilizing properties change tremendously upon hydrolysis. Recent studies for a range of PWSD and LBFs reported that the risk of drug precipitation following digestion is high when the *SR* determined in digestion medium was higher than 3 (91). The determination of the critical *SR* value following dispersion and digestion might be a useful tool for comparison of different formulations and drug-loads. However, some care is needed as it seems that these values are rather drug-specific. Moreover, for the prediction of the risk of drug precipitation *in vivo*, an absorptive environment should be considered (92).

### **2.9.2. Supersaturatable (S-SEDDS) and supersaturated (super-SNEDDS) drug delivery systems**

In the last decade, the concept of supersaturation in the GIT as a formulation strategy to promote the intestinal absorption of PWSO has raised a lot of interest. To utilize drug supersaturation it is important to generate supersaturation and to maintain the metastable supersaturated state for a sufficient period of time. Yet, for some highly permeable drugs, the induction of supersaturation is more critical than stabilization of the supersaturated state (93, 94). Guzman *et al.* proposed the “spring and parachute” approach where a high energy form of the drug (“spring”) is generated and in the presence of precipitation inhibitors (“parachutes”) these drugs are kept in a metastable supersaturated state (Figure 2.11) (93). Based on the supersaturating strategy, Gao *et al.* introduced supersaturatable self-emulsifying drug delivery systems (S-SEDDS), which differ from the standard SEDDS as they contain a reduced amount of surfactant and a polymeric precipitation inhibitor (95). SEDDS have a high surfactant quantity to assure drug solubilization following formulation dilution and digestion in GI fluids. However, as mentioned earlier these high surfactant levels can lead to undesirable toxic effects. Smaller amounts of solubilizing excipients in S-SEDDS normally result in lower toxicity.

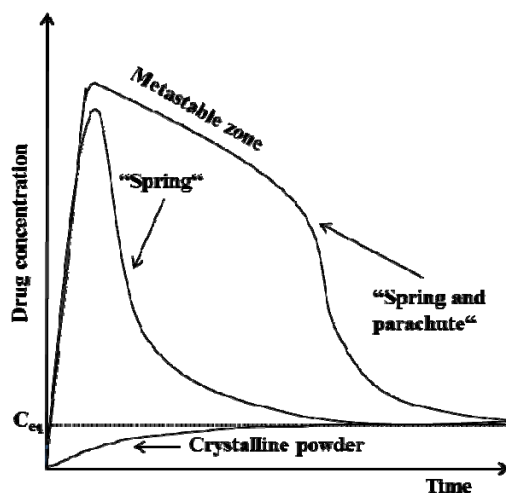


**Figure 2.11:** Schematic presentation of the “spring and parachute” approach of supersaturatable drug delivery systems. A high energy form of the drug (*e.g.* crystalline salt, the “spring”) provides the driving force to solubilize the drug at a concentration greater than its equilibrium solubility ( $C_{eq}$ ). Some excipients can act as a “parachute” and inhibit and/or retard drug precipitation. Adapted from reference (93).

Several additives from different groups of pharmaceutical excipients (*e.g.* polymers, surfactants, and cyclodextrins) exhibited the function of drug precipitation inhibitors when incorporated into S-SEDDS. From the group of polymers, water-soluble cellulosic polymers (*e.g.* HPMC-hydroxypropyl methylcellulose, MC-methylcellulose) were reported to be the most effective at suppressing drug precipitation (79, 96, 97). The underlying mechanisms by which they inhibit precipitation were proposed by Raghavan *et al.* (98). The authors suggested a mechanism based on hydrogen bonding between drug molecules and the polymer, which increased the activation energy for nucleation. Additionally, HPMC molecules adsorbed on the crystal surface (via hydrogen bonds), which hindered crystal growth. Other studies demonstrated that low concentrations of some surfactants (Pluronic- ethylene oxide/propylene oxide block copolymers, TPGS- d-

alpha tocopheryl polyethylene glycol 1000 succinate) also successfully prevented drug precipitation (99, 100). These surfactants might have improved the solvation of dissolved drug, and hence increased the activation energy required for desolvation during nucleation and crystal growth. Recently, Brewster *et al.* studied the influence of cyclodextrins (HP $\beta$ CD-hydroxypropyl- $\beta$ -cyclodextrin, SBE $\beta$ CD-sulfobutylether- $\beta$ -cyclodextrin) on stabilization of supersaturated drug solutions (100). These cyclodextrins were shown to be more effective in drug precipitation inhibition compared to the tested surfactants. The authors suggested that cyclodextrins might have acted as surfactants here and improved the solvation of the dissolved drug. In addition, they also behaved similarly to polymers, as they formed hydrogen bonds with drug molecules and therefore decreased both nucleation and crystal growth. To date, only a few animal studies have correlated *in vitro* supersaturation with *in vivo* intestinal drug absorption. However, they all inevitably showed that S-SEDDS provide higher oral bioavailability when compared to the standard SEDDS (101).

Another interesting supersaturation formulation approach was recently proposed by Müllertz *et al.* (102). These authors developed a supersaturated self-nanoemulsifying drug delivery system (super-SNEDDS), where the drug in the formulation was already present in a supersaturated state. Although these systems are thermodynamically unstable, the supersaturation could have been maintained for several months. These findings emphasized the potential for a higher drug loading capacity of super-SNEDDS. In a pharmacokinetic study in beagle dogs, these systems showed considerably higher bioavailability than multiple units of conventional SNEDDS (with the same dose) (103). However, uncertain long-term stability of the super-SNEDDS might limit them from becoming commercially viable delivery systems.

## **Chapter 3**

# **Novel starch-based PVA thermoplastic capsules for hydrophilic lipid-based formulations**

### **Summary**

For decades, gelatin has been used in the rotary die process as a shell-forming material of soft capsules because of its unique physicochemical properties. However, with respect to the encapsulation of comparatively hydrophilic lipid-based formulations, gelatin has one considerable drawback: Immediately after production, the capsule shell contains a large amount of water (up to 35% w/w). There is the potential for water to migrate from the capsule shell into the formulation, which will lead to a decrease in drug solubility and, in turn, the potential for drug crystallization. The present study introduces a novel capsule material that was obtained from extrusion. The starch-based polyvinyl alcohol thermoplastic capsules (S-PVA-Cs) mainly comprised a blend of starch and PVA. Gelatin and the novel material were used to encapsulate a hydrophilic lipid-based system of fenofibrate. Considerable water migration was observed from the soft gelatin shell to the hydrophilic formulation during drying and drug crystallization resulted in soft gelatin capsules. In contrast, S-PVA-Cs displayed no substantial water exchange or drug crystallization upon storage. The thermoplastic capsule material further exhibited larger

surface roughness and higher resistance to mechanical deformation compared with gelatin. In conclusion, S-PVA-C provided a robust drug product following encapsulation of a rather hydrophilic lipid-based formulation.

### 3.1. Introduction

The production of soft capsules from gelatin has a long tradition in pharmaceuticals (25). However, gelatin also has a number of drawbacks: Ingestion of gelatin as an animal-derived material can be an issue for patients living under religious or dietary (vegetarians or vegans) restrictions. Moreover, identification of transmissible spongiform encephalopathies in animals (especially bovine spongiform encephalopathy, first case in UK, 1986) raised anxiety among gelatin manufacturers and consumers. Today, most national and international authorities have guidelines (*i.e.*, in the EU EMA/410/01 rev.3, (31)) that ensure the safety of gelatin raw material by inspecting the geographical origin, the manufacturing method, and the quality system.

Another potential issue of unmodified gelatin is its susceptibility to cross-linking. It can affect *in vitro* drug release depending on whether or not the dissolution medium contains enzymes that are able to digest gelatin (*e.g.*, pepsin). This *in vitro* effect of gelatin capsules seems, however, to be of lesser importance for drug absorption *in vivo* (104). Another critical aspect of gelatin is that its mechanical properties depend greatly on temperature and moisture content. Thus, climatic conditions of hot and humid regions can soften capsules, which is unfavourable for their handling by patients (105). A considerable drawback of soft gelatin capsules (SGCs) is also the potential migration of the drug into the shell. This diffusion depends on the amount of water in the shell, the formulation, as well as the properties of the drug (6). Such drug migration may be promoted by marked water partitioning between the capsule shell and a hydrophilic lipid-based formulation. Apart from the drug migration, the water exchange between the shell and the formulation can also be critical. Substantial water partitioning is especially



expected with gelatin shells and hydrophilic formulations. Even temporary water uptake of the formulation is a risk for drug precipitation in the fill mass. Small amounts of water can already be sufficient to greatly reduce the drug solubility in the formulation (13).

To overcome the disadvantages of gelatin, a great deal of effort has gone into finding gelatin substitutes for soft capsules during the last decade. However, only a few non-gelatin soft capsule prototypes and methods of encapsulation have been patented so far. All materials were based on plant-derived hydrocolloids, except one that mainly comprised a synthetic polymer. In 2002, the patent by Tanner *et al.* (15) was granted for combining iota carrageenan and modified starch to produce mechanically strong, elastic films. After the casting of polymer bands, the rotary die process was employed for encapsulation. Later Brocker *et al.* (14) described in their patent the production of soft capsules that were mainly based on potato starch with special amylopectin content. They suggested a single screw-type extruder for producing polymer films that directly feed into a conventional rotary die process. As a result of this research on thermoplastic shell materials, VegaGels<sup>®</sup> were introduced to the market as the first starch-based vegetarian soft capsule (106). In 2005, Fonkwe *et al.* (39) proposed another hydrocolloid based film consisting of iota and kappa carrageenan, and the subsequent research activities focused on the production of this shell formulation. It appears that options for manufacturing capsules from carrageenan or starch-based materials are limited due to the technical difficulties. Carrageenan, like other hydrocolloids, requires a large fraction of water for full hydration, which in turn reduces the strength of the film. Therefore, Archibald *et al.* (19) presented a method for extracting a portion of water from the film-forming composition, leading to the production of a dried film with 8-25% w/w water. To avoid these water-related complications, as early as 2002, Brown proposed using polyvinyl alcohol (PVA) for the encapsulation process (16). Although PVA is less hygroscopic than hydrocolloids or gelatin, it lacks the gelling properties. Therefore, Brown suggested using preformed rolls of almost water-free films that can be fed into the rotary die encapsulation.

In summary, the research of novel shell materials has brought to light the difficulties of replacing gelatin. In particular, the production step remains a technical challenge for alternative materials. Further, it remains uncertain as to whether such alternative soft capsules have any pharmaceutical advantages other than their non-animal origin. This stresses the need for more pharmaceutical research in the area of identifying new shell materials. A particular rationale for new material is to obtain a robust drug product for the encapsulation of comparatively hydrophilic lipid-based formulations, such as self-microemulsifying drug delivery systems (SMEDDS). Such pre-concentrates exhibit favourable dispersion behaviour when in contact with water or gastrointestinal fluids, but it comes at the cost of employing large amounts of hydrophilic surfactant(s) and/or cosolvent(s). Thus, an optimal formulation is often incompatible with gelatin, so that current capsule technology actually limits the freedom to select the best system from a biopharmaceutical viewpoint. It would be desirable first to focus on the development of an optimal formulation with respect to drug absorption and stability and then still have a sufficient choice of a viable capsule technology.

This article describes a new soft capsule material that is extruded to films for the subsequent rotary die encapsulation process. The starch-based PVA (S-PVA) material combines the thermoplastic properties of starch with the characteristics of PVA. We expected this material to be specifically suited for encapsulation of hydrophilic lipid-based formulations.

More recently, there has been an increasing interest in “hydrophilic formulations” of PWSD. These lipid-based formulations containing a high proportion of hydrophilic surfactant and cosolvent are classed as type IIIB and type IV of the lipid formulation classification system (LFCS) proposed by Pouton in 2006 (50). The addition of small amounts of water to these systems can lead to the loss of drug solubility in the formulation. SGCs bear a particular risk of drug crystallization in such a hydrophilic fill because of water uptake from the shell during production (2, 13).

The present work compared the encapsulation of a rather hydrophilic SMEDDS (type IIIB formulation) in starch-based PVA thermoplastic capsules (S-PVA-Cs) and SGCs. We aimed to determine whether the novel shell material is associated with less water exchange between the capsule shell and the fill compared to gelatin, thus, preventing drug precipitation in the fill mass. Other potentially beneficial physical properties of the novel shell material were analysed as well.

## **3.2. Materials and methods**

### **3.2.1. Materials**

Fenofibrate (Sigma–Aldrich, St. Gallen, Switzerland) was selected as a poorly water-soluble model drug. Solvents for Karl Fischer titrimetry [HYDRANAL<sup>®</sup>-Formamide dry, HYDRANAL<sup>®</sup> Solvent, HYDRANAL<sup>®</sup>-Composite 5, and dimethyl sulphoxide (DMSO)] and ammonium acetate were purchased from Sigma–Aldrich, Buchs, Switzerland. Polyoxyethylene (80) sorbitan monooleate (Tween<sup>®</sup> 80), medium-chain triglycerides (Miglyol<sup>®</sup> 812), and sodium dodecyl sulphate (SDS) were supplied by Hänseler AG, Herisau, Switzerland. Transcutol<sup>®</sup> HP [2-(2-ethoxyethoxy)ethanol] was obtained from Gattefosse, Nanterre, France, and hydrochloric acid (0.1N) was purchased from Scharlab Ltd., Barcelona, Spain. Acetonitrile of high-performance liquid chromatography (HPLC) grade was purchased from Mallinckrodt Baker, St. Louis, Missouri.

### **3.2.2. Methods**

#### **3.2.2.1. Production and physical characterization of the S-PVA and soft gelatin films**

The S-PVA films were manufactured using extrusion technology. These films were a mixture of potato starch, PVA, and plasticizers (sorbitol solution and glycerol) in a ratio

of 40%:30%:30% (w/w). First, potato starch and PVA were premixed in a blender. This mixture was then mixed with the plasticizers by constant feeding of a double-screw extruder at approximately 135° C under high pressure of 115-120 bar to form granules. Formed granules were again extruded using a single-screw extruder at approximately 100-135° C at 22 rpm. The obtained extrudate was pressed through a slit die at 115° C to form an S-PVA film.

Gelatin films were obtained using casting technology. A mixture of bovine gelatin (type B, Bloom 160 limed bone/limed hide), glycerol, and water (47.4%:17.1%:35.5%, w/w) was heated while stirred gently in a stainless-steel vessel at approximately 55-65° C for approximately 60 min. Subsequently, the heated gelatin solution was poured onto a cooled casting drum using a spreader to form a homogeneous gelatin film.

Both S-PVA and gelatin films were left in a climate chamber for at least 2 weeks at 20° C/40% relative humidity (RH) to equilibrate. The film properties of both materials were subsequently analysed using various physical methods.

#### **3.2.2.1.1. Surface texture measurements**

Surface texture was assessed using a confocal laser scanning microscope (CLSM, LEXT OLS3100; Olympus, Southend-on-Sea, Essex, UK). The CLSM was equipped with a semiconductor laser at a wavelength of  $\lambda=408\pm 5$  nm. Magnification of  $\times 1200$  with a field of view of  $256 \times 256 \mu\text{m}^2$  was used. Both films were cut into rectangular pieces ( $2 \times 4 \text{ cm}^2$ ). These samples were then fixed to glass slides with transparent tapes to avoid any curvatures caused by the film specimens. Each film was scanned at six different positions in one line. The noise signal arising from flat surfaces in the three-dimensional images was removed, and the plane roughness was calculated using the LEXT OLSTM software (Olympus). For each region of interest, the following roughness parameters were calculated in accordance with DIN EN ISO 4287 (107):

- Average roughness ( $SR_a$ ) defined as the arithmetic average of absolute profile ordinate values  $Z(x)$  within the analysed area.
- Root mean square roughness ( $SR_q$ ) defined as the root mean square value of profile ordinate values within the analysed area.
- Maximum peak height ( $SR_p$ ) defined as the maximum profile peak height within the analysed area.
- Maximum valley depth ( $SR_v$ ) defined as the maximum profile valley depth within the analysed area.

The  $SR_a$  is a representative estimate of surface roughness, but it does not provide explicit information about variation in peak height and depth of the valleys. Therefore, it is important to calculate other roughness parameters, such as  $SR_q$  that is more influenced by the high amplitudes of peaks and valleys in the surface. Moreover, the extreme values were assessed in terms of the  $SR_p$  and  $SR_v$ .

#### **3.2.2.1.2. Residual water content**

Karl Fischer titrimetry was used for residual water determination. HYDRANAL<sup>®</sup>-Solvent (Sigma-Aldrich) (20 mL) and HYDRANAL<sup>®</sup>-Formamide dry (Sigma-Aldrich) (20 mL) were added to a heated titration vessel (50° C), and HYDRANAL<sup>®</sup>-Composite 5 (Sigma-Aldrich) was titrated to assure initial dryness. A gelatin sample (200 mg) was accurately weighted, and its water content was titrated with HYDRANAL<sup>®</sup>-Composite 5 (Sigma-Aldrich). Because a S-PVA sample (200 mg) could not be dissolved in the same solvents as a gelatin sample, it was prepared by dissolving in 2 mL of DMSO for 1 h in an ultrasonic bath at 60° C. Finally, the water content of DMSO was measured for correction of the sample values.

### 3.2.2.1.3. X-ray diffraction (XRD)

X-ray diffraction was used to determine which excipient contributed the most to crystallinity in an S-PVA film. A diffractometer Phaser D2 (Bruker, Karlsruhe, Germany) with LYNXEYE detector and the EVA software application was employed. The source of radiation was Co K $\alpha$  at 30 kV, 10mA, and the measurement range was  $2\theta$  7°–40°. The sample was automatically rotated on a holder at 15 rpm.

X-ray diffraction was also used to determine crystallinity of fenofibrate after precipitation caused by water in the formulation. Fenofibrate (60 mg/mL) was dissolved in the mixture of Miglyol<sup>®</sup> 812, Tween<sup>®</sup> 80, and Transcutol<sup>®</sup> HP (15%:60%:25%, w/w) by stirring at 800 rpm at room temperature (RT). Water was added to the formulation at a concentration of 32% w/w, which was still a realistic amount that can occur during production of SGC (consistent with method in the section 3.2.2.2.1.). The mixture was gently mixed and left at 5° C for 24 h. In the second step, the mixture was stirred at 800 rpm and RT for 5 days. These sample conditions were used to increase the crystallization yield. After this cyclic test the mixture contained crystals, which were analysed by X-ray diffraction in the measurement range  $2\theta$  5-40° without sample rotation. Subsequently, a fenofibrate reference was analysed and the diffractograms were compared.

### 3.2.2.1.4. Differential scanning calorimetry (DSC)

A differential scanning calorimeter DSC 30 (Mettler Toledo, Greifensee, Switzerland) was used to characterize the thermal properties of the PVA, potato starch, and S-PVA shell materials. Samples of PVA and potato starch (average weight: 9 mg) were placed in hermetically sealed aluminium pans (40  $\mu$ L) and heated at 10° C min<sup>-1</sup> from 25° C to 300° C in an inert environment (100 mL min<sup>-1</sup> Ar). Moreover, samples of S-PVA (average weight: 20 mg) were placed in bigger hermetically sealed aluminium pans (160  $\mu$ L) and also heated at 10° C min<sup>-1</sup> from 25° C to 300° C in an inert environment. Melting

temperature ( $T_m$ ) and heat of fusion ( $\Delta H_f$ ) of the S-PVA samples were determined from the peak maximum and the area under the peak, respectively. Finally, the degree of crystallinity of S-PVA was calculated using the following equation (108):

$$X_c = \left[ \frac{\Delta H_f}{w \times \Delta H_{f100}} \right] \times 100 \quad (3.1)$$

where  $X_c$  is the degree of crystallinity (%),  $\Delta H_f$  is the latent heat of fusion of the S-PVA sample (J/g),  $\Delta H_{f100}$  is the latent heat of fusion of a PVA with 100% crystallinity (161 J/g) (109) and  $w$  is the weight fraction of PVA in the S-PVA film.

### 3.2.2.2. Solubility studies and excipients phase behaviour

#### 3.2.2.2.1. Solubility studies of fenofibrate in excipients and mixtures with water

The solubility of fenofibrate in Miglyol<sup>®</sup> 812, Tween<sup>®</sup> 80, Transcutol<sup>®</sup> HP, and their mixture (*i.e.*, 15%:60%:25%, w/w) was determined as follows:

An excess amount of compound was added to 1 mL of each sample and the mixture was constantly stirred (750 rpm) in a glass vial at RT for 24 h and 7 days. The time point at 7 days was taken to assure that equilibrium was reached. The samples were then centrifuged at 13,362 g for 20 min using a Centrifuge 5415 R (Eppendorf AG, Hamburg, Germany). Finally, the concentration of the compound in the supernatant was determined after diluting the supernatant with acetonitrile (1:1000, v/v) by HPLC analysis (section 3.2.2.4.).

Drug solubility was also determined in the placebo formulation (Miglyol<sup>®</sup> 812, Tween<sup>®</sup> 80, and Transcutol<sup>®</sup> HP, 15%:60%:25%, w/w) with varying amounts of water at RT. The added water reflected a possible state after soft capsule production. Batches of SMEDDS (3 g in total) were prepared (in triplicate) to contain the following water levels: 1%, 2%, 4%, 8%, 16%, or 32% w/w. There was no visible change in mixtures containing 1%, 2%,

and 4% of water. The mixture with 16% w/w water showed more clouding than the mixture with 8% w/w water. In the mixture with 32% w/w water, phase separation was visible. An excessive amount of fenofibrate was added to each mixture and the glass vials were vortexed for 30 s. To mimic possible shipment and storage conditions, all mixtures were stored at 5° C for 24 h and then equilibrated at RT for 60 h under continuous stirring at 750 rpm. An aliquot (1 mL) was taken from each vial and centrifuged at 13,362 g for 20 min. The clear supernatant was diluted with acetonitrile (1:200, v/v) and the fenofibrate content was analysed using HPLC assay (section 3.2.2.4.).

#### **3.2.2.2.2. Preparation of the SMEDDS and particle size measurements**

Mixtures of Miglyol<sup>®</sup> 812, Tween<sup>®</sup> 80, and Transcutol<sup>®</sup> HP (Table 3.3) were compounded in glass vials by weight using an analytical balance (Mettler Toledo AB204-S; Mettler Toledo). The aim was to find SMEDDS resulting in a small particle size after aqueous dispersion (up to 50 nm) and at the same time to reach sufficient fenofibrate solubility. Quaternary mixtures containing oil, surfactant, cosolvent, and water (representing the lipid formulations after dilution) were prepared by the addition of water to a primary blend of oil, surfactant, and cosolvent (1:200, v/v). An aliquot (100 µL) of each mixture obtained from a calibrated automatic pipette Eppendorf Research<sup>®</sup> plus (Eppendorf) (20-200 µL) was diluted with 20 mL of water in a glass vial and gently mixed. Phase behaviour was assessed initially by visual observation, classifying the dispersion samples as either single phase or multiphasic (turbid) mixtures. Subsequently, all mixtures were analysed by means of dynamic laser light scattering using a Zetasizer Nano ZS (Malvern Instruments, Malvern, Worcestershire, UK). The mean particle size (Z-average diameter) was calculated from the volume size distribution. All experiments were repeated in triplicates from fresh samples at ambient temperature.



### **3.2.2.3. Characterization of the S-PVA-Cs and a comparison with SGCs**

#### **3.2.2.3.1. Production of the S-PVA-Cs and SGCs**

A continuous rotary die process was used for production of both S-PVA-Cs and SGCs at Swiss Caps (Kirchberg, Switzerland). For encapsulation of the S-PVA-Cs, an extrusion process was coupled with the capsule manufacture. Before encapsulation, the same granules used for the S-PVA films (section 3.2.2.1.) were extruded in two single-screw extruders (one for each half of the capsule shell) at approximately 135° C at 22 rpm, and ribbons were formed using flat film extrusion dies. These ribbons were feeding into the rotary die process. In the case of SGCs manufacture, the same gelatin solution as used for the production of gelatin films (section 3.2.2.1.) was used for the gelatin ribbons.

Both SGCs and S-PVA-Cs were filled with the same batch of fenofibrate formulation (drug concentration 60 mg/mL). The drug formulation (7.5 kg for each capsule type) was prepared in a stainless-steel vessel by mixing all excipients and fenofibrate at 20-25° C for 120-150 min using a paddle agitator. Subsequently, the formulation was transferred into the filling tank above the die rolls. Two ribbons (either S-PVA or gelatin) were continuously and simultaneously fed into the rotary die process. The formulation was injected between the converging ribbons and sealing of the capsules followed in matching dies of the counter-rotating rolls. The capsule size for both batches was 15 minims (R.P. Scherer volume units; 1 minim = 0.0616 mL). Gelatin capsules were filled with 1.0 g of drug formulation, whereas S-PVA-Cs contained 0.85 g of the drug formulation because of the less flexible material in comparison with gelatin. Each batch consisted of about 1000 capsules that were initially left for 50 h in a tumbler at RT/45% RH. Afterward, all capsules were stored in a climate chamber at 20° C/ 40% RH before analysis.

### 3.2.2.3.2. Drying kinetics-water activity measurement

During the drying process, samples of SGCs and S-PVA-Cs were taken at predetermined time points. Each capsule was opened with scissors and the fill mass was manually removed from the capsule shell. The shells were thoroughly dried with a cotton cloth. Both capsule shell and fill mass were used for analysis of water activity ( $a_w$ ) using a LabMaster-aw (Novasina AG, Lachen, Switzerland). The  $a_w$  is defined as the ratio of the water vapour pressure of the sample to that of pure water, which equals the relative equilibrium humidity (%) of the sample. The  $a_w$  values of the formulation fill and the capsule shells were measured in triplicates in the airtight chamber of the instrument.

The water activity was also measured in the mixtures of the drug-containing formulation (60 mg/mL of fenofibrate in a mixture of Miglyol<sup>®</sup> 812, Tween 80, and Transcutol<sup>®</sup> HP, 5%:60%:25%, w/w) with different amounts of water. The mixtures (10 g in total) contained the following water levels: 1%, 2%, 4%, 8%, 16%, or 32% w/w and, like in section 3.2.2.2.1., they reflected a possible state during soft capsule production.

### 3.2.2.3.3. Determination of the dissolved drug concentration in the capsule formulation

The concentration of fenofibrate in the formulation was determined immediately after the production and was used as the reference. The concentration of dissolved drug in SGC and S-PVA-C was determined after storing the capsules openly in a climate chamber and closed in glass vials for 4 months at 20° C/40% RH. The formulation was removed from each capsule ( $n = 5$ ) and centrifuged. The clear supernatant was diluted with acetonitrile (1:200, v/v) and used for HPLC assay (section 3.2.2.4.).

#### 3.2.2.3.4. Texture analysis

A texture analyzer (TAXT2i; StableMicro Systems, Godalming, UK) was used to study the capsule rupture strength. This mechanical test for soft capsules determines the bursting point of the film at the point of contact with a defined probe. The apparatus was equipped with a 5 kg load cell and fitted with a flat-bottomed cylindrical stainless-steel probe (P/2, 2mm in diameter). The capsule was placed in the centre of the testing platform with the capsule seam positioned perpendicularly to the probe. The speed of the probe was 1.0 mm/s until the surface of capsule was detected at the force of 0.049 N (threshold value for triggering the onset of texture analysis). The probe then penetrated the capsule to a maximal depth of 8 mm with a speed of 2.0 mm/s. The force dropped when the capsule was ruptured and the probe was automatically withdrawn at a speed of 10.0 mm/s. Tensile force (force applied at the rupture point) was recorded as an indicator of compressive capsule strength. From the area under the force-displacement curves, we obtained the work ( $W$ ) required to rupture the capsules. Both SGCs and S-PVA-Cs filled with fenofibrate formulation were tested ( $n = 4$ ), and the mechanical properties compared, that is, tensile forces, rupture distances, as well as the work required to rupture the capsules.

#### 3.2.2.3.5. *In vitro* disintegration and drug release testing

Disintegration times of SGCs and S-PVA-Cs were determined with six capsules in distilled water at  $37 \pm 0.5^\circ$  C using a DT-3 disintegration tester (SOTAX, Basel, Switzerland) according to United States Pharmacopeia (USP) 34 (110). Disintegration time was defined as the time necessary for complete opening of the capsules. A digital stopwatch was used, and only one capsule was analysed at a time. All results are presented as mean value  $\pm$  SD ( $n = 6$ ). Release testing with both capsule types was performed in 1000 mL of 0.05 M SDS in water using the USP dissolution apparatus II (DT 600; Erweka, Heusenstamm, Germany). The paddles were rotated at 75 rpm, and the

medium was heated to  $37 \pm 0.5^\circ \text{C}$ . At predetermined time points, a 2-mL sample of medium was drawn and centrifuged, and clear supernatant was subjected to drug analysis without dilution using HPLC analysis (described in the section 3.2.2.4.). The removed volume was replaced each time with 2 mL of fresh medium.

#### **3.2.2.4. HPLC method**

High-performance liquid chromatography analysis employed a LiChrospher 60, RP select B 125-4 (5  $\mu\text{m}$ ) column (Merck, Darmstadt, Germany). The mobile phase consisted of acetonitrile and 25 mM ammonium acetate buffer, pH = 3.5 (65:35, v/v). Flow rate was 1 mL/min with the injection volume of 20  $\mu\text{L}$  and the detection wavelength was 287 nm (111).

#### **3.2.2.5. Data analysis**

The concentration of dissolved drug in SGC and S-PVA-C stored openly and closed in glass vials for 4 months at  $20^\circ \text{C}/40\% \text{RH}$  was analysed with  $n = 5$ , and the results were expressed as mean values with lower and upper limits. The Statgraphics Centurion XVI ed. Professional Program from Statpoint Technologies Inc. (Warrenton, Virginia) was used for the analysis of variance (ANOVA) calculations. Significance was assumed if the  $p$  value was less than 0.05.

### **3.3. Results**

#### **3.3.1. Physical characterization of the S-PVA and gelatin films**

##### **3.3.1.1. Surface texture measurements**

To analyse the surface morphology of the different polymer materials (S-PVA and gelatin), confocal microscopy was used. Figure 3.1a presents the three-dimensional

surface profile of a soft gelatin film, which appeared to be less rugged and smoother than the surface of the S-PVA material (Figure 3.1b). This finding was also reflected by the calculated surface roughness parameters (Table 3.1). Thus, the  $SR_a$  of the SPVA film was almost four times higher than the corresponding value of gelatin. Even though the  $SR_a$  is the most widely used surface roughness parameter, it was also important to measure  $SR_q$ . This  $SR_q$  is more affected by rather high peaks and deep valleys on a surface compared with the  $SR_a$ . The  $SR_q$  also exhibited differences between the materials, but these were not more pronounced than with  $SR_a$ . This result already indicated that the difference in surface roughness was not because of few extreme profile values, but the result of a high number of peaks and valleys. To explore them more thoroughly, we studied the highest peak ( $SR_p$ ) and the lowest valley ( $SR_v$ ). The latter value of  $SR_v$  demonstrated a greater difference between the materials than in terms of  $SR_p$ . Figure 3.1b reveals that the surface roughness of S-PVA was to a great extent determined by valleys, which appeared to be characteristic for the new material.

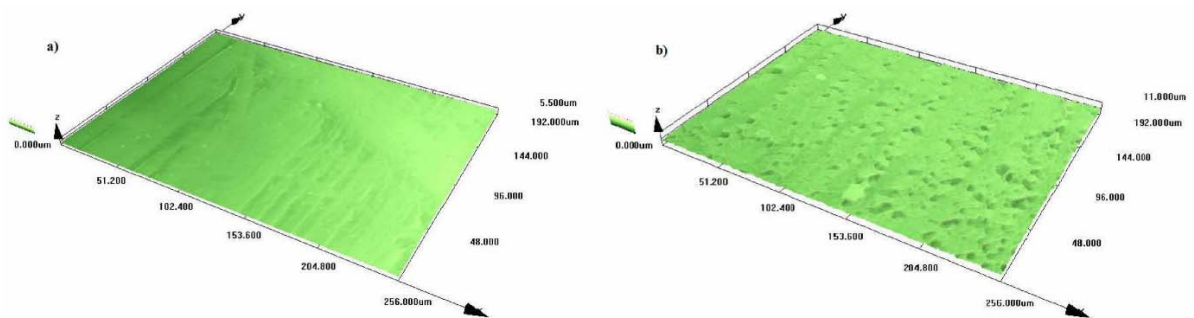


**Figure 3.1:** The three-dimensional surface profiles of (a) soft gelatin film (produced by casting) and (b) S-PVA film (extruded from a mixture of PVA, potato starch, and plasticizers, 40%:30%:30%, w/w) by using confocal laser scanning microscopy.

**Table 3.1:** Comparison of surface roughness parameters of soft gelatin and starch-based PVA (S-PVA) films (mean  $\pm$  SD,  $n=6$ ) calculated by confocal laser scanning microscopy (CLSM).

	$SR_a$ ( $\mu\text{m}$ )*	$SR_q$ ( $\mu\text{m}$ )*	$SR_p$ ( $\mu\text{m}$ )*	$SR_v$ ( $\mu\text{m}$ )*
soft gelatin	$0.089 \pm 0.010$	$0.131 \pm 0.024$	$1.875 \pm 0.995$	$0.971 \pm 0.231$
S-PVA	$0.327 \pm 0.057$	$0.435 \pm 0.066$	$2.546 \pm 0.242$	$2.719 \pm 0.450$

\* Surface roughness parameters:  $SR_a$ : the arithmetic average of absolute profile ordinate values  $Z(x)$  within the analysed area.  $SR_q$ : the root mean square value of profile ordinate values within the analysed area.  $SR_p$ : the maximum profile peak height within the analysed area.  $SR_v$ : the maximum profile valley depth within the analysed area.

### 3.3.1.2. Residual water content

Both soft gelatin and S-PVA films were stored for two weeks at  $20^\circ\text{C}/40\%\text{RH}$ , and were then analysed for residual water content by Karl Fisher titrimetry. As a result, the soft gelatin film provided a mean value of  $10.4 \pm 0.5\%$ , whereas the S-PVA film contained less water, that is,  $7.4 \pm 0.1\%$ . These values represent a total amount of water, which may be different from the fraction of water available for partitioning between the shell and the fill mass or the environment (112).

### 3.3.1.3. X-ray diffraction (XRD)

Figure 3.2 shows X-ray patterns of a PVA, a potato starch, and an S-PVA film. The main diffraction peak of PVA was at around  $22.5^\circ$ , which was already observed 2007 by Pal *et al.* (113). This peak was very intense indicating a highly crystalline structure of PVA. As expected, the diffractogram of the S-PVA film showed the peak at  $22.5^\circ$  as well. The distinct peaks of pure potato starch were observed at around  $17^\circ$  and  $20^\circ$ . This was in

agreement with van Soest *et al.* (114), who confirmed these peaks in potato starch back in 1996. They prepared thermoplastic starch from native starch by different manufacturing processes (*i.e.* kneading, extrusion, compression moulding, and injection). These process conditions were shown to affect the degree of starch crystallinity. In the present study, the absence of characteristic peaks of potato starch in the S-PVA films was interpreted as a lack of starch crystallinity following the extrusion process. Thus, crystallinity of the S-PVA film was obviously mainly because of the PVA.

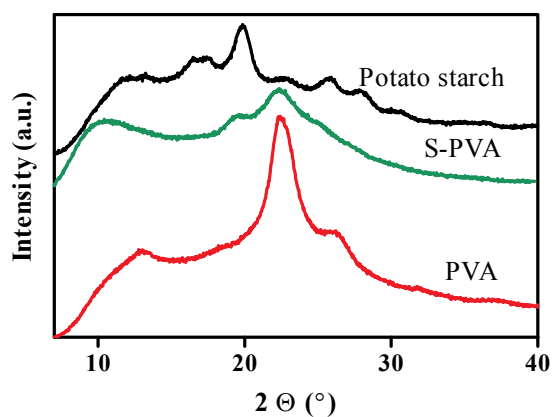


**Figure 3.2:** X-ray diffractogram patterns of PVA (red line), potato starch (black line), and S-PVA film (green line).

#### 3.3.1.4. Thermal analysis by DSC

Differential scanning calorimetry thermogram of potato starch exhibited two characteristic endothermic peaks (Figure 3.3). The first broad peak at about 100° C was attributed to the loss of adsorbed water, whereas the second peak (at about 280° C) corresponded to the melting of crystallites in starch, which was followed by immediate degradation. These findings were in good agreement with Zhao *et al.* (115). The melting point of PVA was observed at about 200° C and the same endothermic peak (at 200° C) was found in the S-PVA films (Figure 3.3). For calculation of the crystalline fraction in S-

PVA, the contribution of starch to crystallinity was neglected. This was based on the results of X-ray diffraction, where no distinct peaks were arising from starch. Therefore, only the contribution from pure PVA was considered for estimating crystallinity of the novel capsule material. The calculation in Eq. 3.1 (108) used the reference heat of fusion from pure PVA. Accordingly, the  $X_c$  of S-PVA yielded  $38.3 \pm 2.3\%$  ( $n = 4$ ), which indicated that a considerable fraction of the S-PVA polymer film was indeed crystalline.

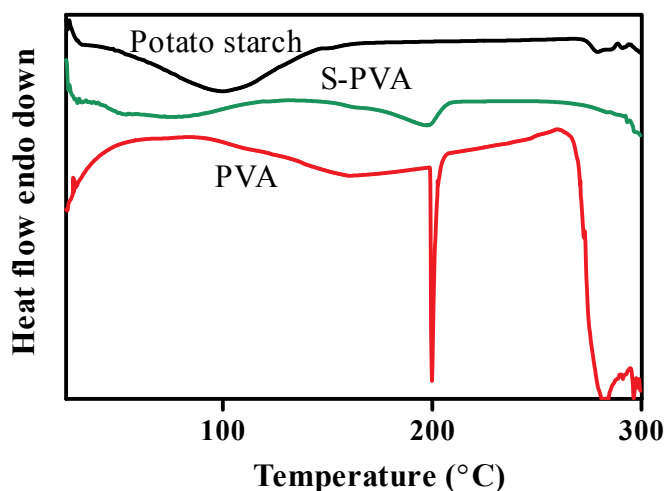


**Figure 3.3:** Differential scanning calorimetry thermograms of S-PVA film (green line), PVA (red line), and potato starch (black line).

### 3.3.2. Solubility studies and excipients phase behaviour

A broad range of excipients was initially evaluated with respect to maximal drug solubility. For this screening of excipients, fenofibrate was gradually added and solubility was visually assessed with respect to an onset of turbidity (data not shown). On the basis of this initial testing, favourable excipients (Miglyol<sup>®</sup> 812, Tween<sup>®</sup> 80, and Transcutol<sup>®</sup>



HP) were selected and the solubility of fenofibrate was then determined using HPLC analysis (section 3.2.2.4.). Table 3.2 displays the obtained fenofibrate solubilities in the chosen excipients (Miglyol<sup>®</sup> 812, Tween<sup>®</sup> 80, and Transcutol<sup>®</sup> HP). Miglyol<sup>®</sup> 812 and Tween<sup>®</sup> 80 demonstrated remarkable drug solubility, which was in agreement with the data previously reported by Patel and Vavia (116). However, Transcutol<sup>®</sup> HP exhibited the highest capacity to dissolve fenofibrate.

Our next step was to find the model formulation that had self-microemulsifying properties (particle size upon aqueous dispersion with a diameter of  $\leq 50$  nm) and the capability of dissolving rather large amounts of fenofibrate. To meet these two criteria, comparatively higher amounts of the cosolvent Transcutol<sup>®</sup> HP were considered. Mixtures of Miglyol<sup>®</sup> 812 (5-20% w/w), Tween<sup>®</sup> 80 (50-90% w/w), and Transcutol<sup>®</sup> HP (5-30% w/w) (Table 3.3) were prepared and dispersed in water at a physiologically relevant dilution level (1:200, v/v) to check for potential self-microemulsification. Within the tested ranges, excipients could be freely mixed resulting in macroscopically homogenous solutions. Dynamic laser light scattering was used to assess a range of microemulsification. Table 3.3 shows particle size results of obtained colloidal systems together with their polydispersity index.

The formulation with 15% w/w Miglyol<sup>®</sup> 812, 60% w/w Tween<sup>®</sup> 80, and 25% w/w Transcutol<sup>®</sup> HP was selected as a model system because of a very small particle size upon aqueous dispersion. Moreover, the composition contains good solvents of fenofibrate in rather high amounts and the surfactant concentration was limited to 60% w/w. The selected model formulation falls in category type IIIB of the LFCS and is rather hydrophilic compared with other lipid formulations (49, 50).

**Table 3.2:** Solubility of fenofibrate in Miglyol<sup>®</sup> 812, Tween<sup>®</sup> 80, Transcutol<sup>®</sup> HP, and their mixture (*i.e.* 15% : 60% : 25%, w/w) at RT after 24 h and 7 days under constant stirring at 750 rpm ( $n=3$ ).

	drug solubility in mg/mL	
	24 h	7 days
Miglyol <sup>®</sup> 812	80.4 ± 2.6	84.3 ± 3.4
Tween <sup>®</sup> 80	61.9 ± 2.9	61.1 ± 1.5
Transcutol <sup>®</sup> HP	160.3 ± 8.9	160.7 ± 3.8
Mixture*	91.2 ± 9.7	90.4 ± 2.4

\* Mixture with the following content: Miglyol<sup>®</sup> 812, Tween<sup>®</sup> 80, and Transcutol<sup>®</sup> HP (15% : 60% : 25%, w/w)

**Table 3.3:** Particle size (*Z*-average diameter) of the microemulsions prepared by gentle mixing of lipid components with water (1:200 v/v) at RT and measured by dynamic laser light scattering using a Zetasizer Nano ZS (Malvern).

Miglyol <sup>®</sup> 812 (% w/w)	Tween <sup>®</sup> 80 (% w/w)	Transcutol <sup>®</sup> HP (% w/w)	<i>Z</i> -average (nm)	PDI <sup>a</sup>
5	90	5	9.6	0.06
5	80	15	9.7	0.04
20	60	20	38.8	0.52
20	55	25	110.4	0.27
<b>15</b>	<b>60</b>	<b>25</b>	<b>15.9</b>	<b>0.17</b>
5	65	30	10.6	0.03
20	50	30	109.7	0.27

The microemulsion indicated **bold** contains the optimal ratio of cosolvent and surfactant and was selected for encapsulation of S-PVA-C and SGC.

<sup>a</sup>PDI, polydispersity index.

To assess the relevance of water migration from capsule shell to formulation, we studied the effect of added water to the formulation regarding fenofibrate solubility. Thus, drug solubility was determined in mixtures of the model formulation (Miglyol<sup>®</sup> 812, Tween<sup>®</sup> 80, and Transcutol<sup>®</sup> HP, 15%:60%:25%, w/w) with water (1%, 2%, 4%, 8%, 16%, or 32% w/w). We found that solubility of fenofibrate decreased nonlinearly with increasing water content in the formulation (Figure 3.4). A first-order model was selected to describe the solubility decay in line with previous work reported by Serajuddin *et al.* (13). In our study, an excellent model fit with an  $R^2$  value of 0.992 was obtained.

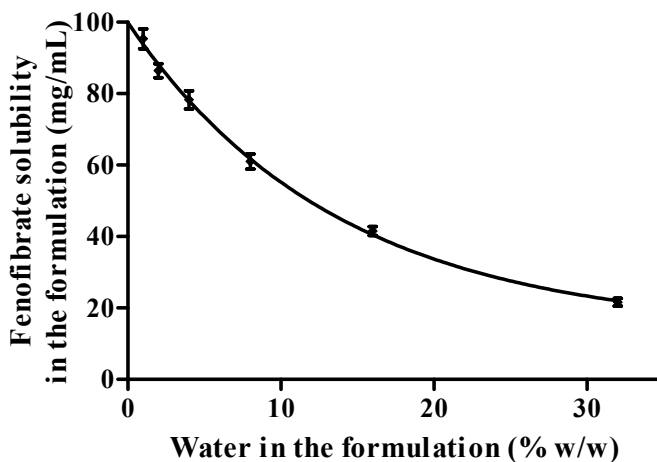


**Figure 3.4:** Solubility of fenofibrate in placebo formulation-water mixtures stored at 5° C for 24 h, and then equilibrated at RT for 60 h under continuous stirring at 750 rpm. Placebo formulation was mixture of Miglyol<sup>®</sup> 812, Tween<sup>®</sup> 80, and Transcutol<sup>®</sup> HP (15%:60%:25%, w/w). An exponential model was fitted (solid line). Data are presented as mean  $\pm$  SD ( $n = 3$ ).

### 3.3.3. Characterization of the S-PVA-Cs and a comparison with SGCs

#### 3.3.3.1. Drying kinetics-water activity measurement

Drying kinetics of SGCs is displayed in Figure 3.5a. Initially pronounced water partitioning between capsule shell and formulation was observed, which continued gradually until an equilibration of shell with environment was reached. In contrast to that, water migration between the S-PVA shell and the formulation was rather slight (Figure 3.5b).

The obtained RH data indicated that even after 50 h of drying, equilibrium had not been reached in both capsule types. Subsequently, the capsules were stored openly in a climate chamber at 20° C/40% RH. Measurements after 3 months exhibited that equilibrium was finally reached. Water activity ( $a_w$ ) of the shell and the fill of both capsule types was then  $\sim 0.4$ , that is, equal to the RH of the environment.

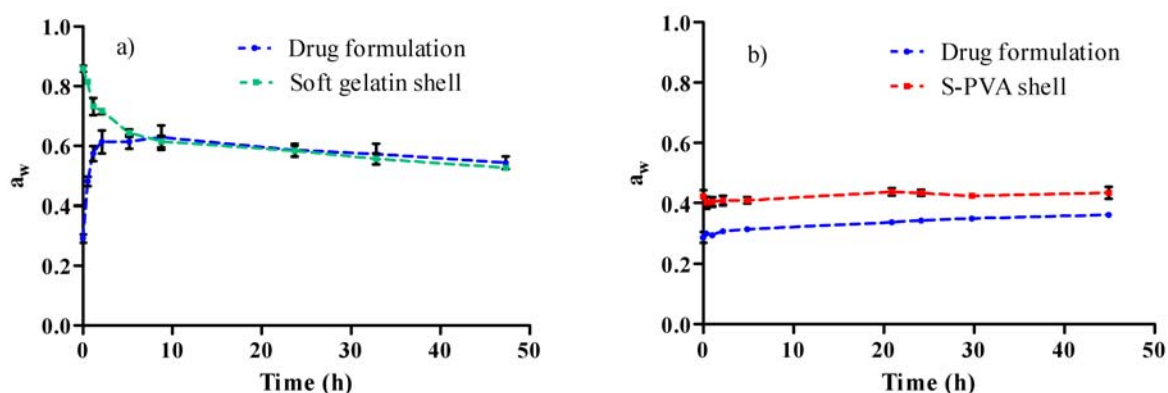


**Figure 3.5:** Measured water activity ( $a_w$ ) during drying of (a) drug formulation (blue line) with soft gelatin shell (green line) and (b) drug formulation with S-PVA shell (red line). In both capsule types the equilibrium was not reached within 50 h of observation time. Data are presented as mean  $\pm$  SD ( $n = 3$ ).

To link the water activity measurements (Figure 3.5) with the drug solubility in the formulation (Figure 3.4), we further measured the water activity of the drug containing formulation with different water amounts added (Figure 3.6). Because the water activity of the formulation in SGCs after encapsulation was around 0.7, the corresponding water content was roughly 8% w/w in the formulation. Therefore, drug solubility in the encapsulated formulation decreased temporarily close to about 60 mg/mL, which means close to the solubility limit with the given drug load.

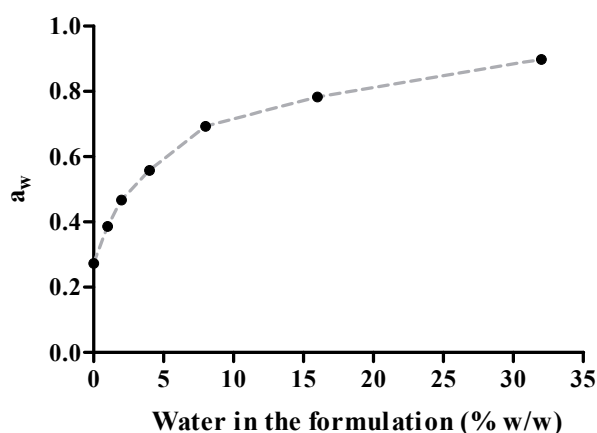


**Figure 3.6:** Water activity measurements of mixtures of drug-containing formulation (60 mg/mL of fenofibrate in a mixture of Miglyol<sup>®</sup> 812, Tween<sup>®</sup> 80, and Transcutol<sup>®</sup> HP, 15%:60%:25%, w/w) and water. Data are presented as mean  $\pm$  SD ( $n = 3$ ). Standard deviations are included within the labels.

### 3.3.3.2. Determination of the dissolved drug concentration in the capsule formulation

Soft gelatin capsules and S-PVA-Cs were stored openly and closed in glass vials for 4 months at 20° C/40% RH. Visual observation of the formulation in SGCs, stored both openly and closed, revealed drug precipitation. This physical instability was best observed after centrifugation. In contrast, the drug-containing formulation in S-PVA-Cs, stored

openly or closed, remained clear without visual signs of any drug precipitation. The concentration of dissolved drug in the formulation of both capsule types was analysed and compared with the initial drug content in the formulation, which was determined immediately after the production ( $60.6 \pm 1.6$  mg/mL) (Table 3.4). A reduced content of dissolved drug in SGCs was found for both storage conditions, whereas S-PVA-Cs always maintained the drug quantitatively in solution. The ANOVA demonstrated a significant effect of the shell material ( $p < 0.0001$ ) and the storage conditions ( $p = 0.0008$ ). Moreover, a significant factor interaction was revealed ( $p < 0.0001$ ; Table 3.4). Thus, the stability effect of the shell material was depending on storage conditions or vice versa. The storage conditions obviously did not affect the drug content of S-PVA-Cs, whereas the drug content of SGCs was even lower after storing the capsules in the closed condition than after storing them openly.

**Table 3.4:** The concentration of dissolved drug in SGC and S-PVA-C stored openly and closed in glass vials for 4 months at 20° C/40% RH ( $n=5$ ) with 95% confidence interval.

Storage condition	Mean (%)	Lower limit (%)	Upper limit (%)
<b>Open</b>			
S-PVA-C	99.46	98.05	100.87
SGC	86.64	85.23	88.05
<b>Closed</b>			
S-PVA-C	100.62	99.21	102.03
SGC	80.00	78.59	81.41

To study the solid state of precipitated material, X-ray analysis was conducted. Because the analysis required larger amounts of the solid material than obtained from the SGCs, water was added to the drug formulation as outlined in the method section 3.2.2.1.3. The diffractograms in Figure 3.7 demonstrate analogous distinct peaks from the precipitated material in the formulation as compared with a reference sample of crystalline fenofibrate. Thus, most of the precipitated material was obviously crystalline fenofibrate.

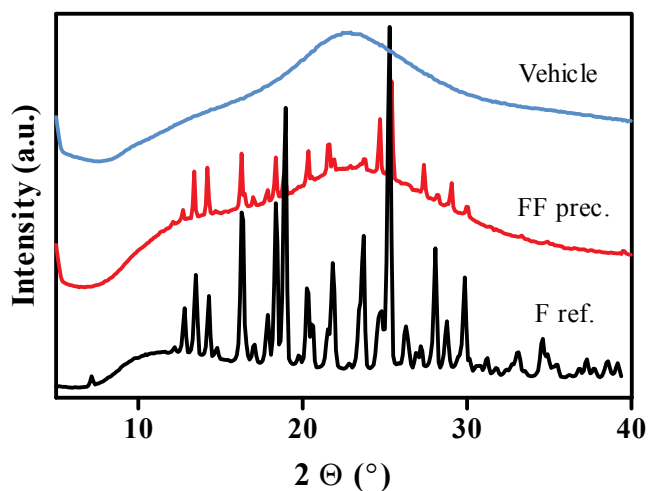


**Figure 3.7:** X-ray diffractogram patterns of fenofibrate powder as reference (F ref.) (black line), fenofibrate precipitated (FF prec.) from the formulation with 32% (w/w) (red line), and formulation without fenofibrate (vehicle) (blue line). FF prec. after preparation was stored for 24 h at 5° C, then left for 5 days at RT continuously stirring at 750 rpm and analysed. Formulation without fenofibrate (vehicle consisted of Miglyol<sup>®</sup> 812, Tween<sup>®</sup> 80, and Transcutol<sup>®</sup> HP (15%:60%:25%, w/w).

### 3.3.3.3. Texture analysis

To study the mechanical properties of SGCs and S-PVA-Cs, texture analysis was used. Four important parameters were considered: elastic stiffness (slope of linear region of the curve), tensile force (force applied at the rupture point), elongation at break (deformation at which a capsule breaks), and the area under the force-displacement curve (work required to rupture the capsules). These mechanical properties were obtained from force-displacement profiles of both capsule types (Figure 3.8). Comparison of the slopes of linear portion of the profiles of SGCs and S-PVA-Cs revealed lower elasticity of SGCs than of S-PVA-Cs. The tensile force at rupture point was about the same (SGC,  $F = 40.8 \pm 3.1$  N; S-PVA-C,  $F = 37.0 \pm 2.3$  N) indicating similar strength of both capsule types. Elongation at break was considerably greater with S-PVA-Cs, showing that these capsules accommodated more deformation before the rupture point was reached compared with SGC (S-PVA-C,  $d = 6.8 \pm 0.2$  mm; SGC,  $d = 3.7 \pm 0.3$  mm). The amount of  $W$  required to rupture the capsules was higher for S-PVA-C than determined with SGC (S-PVA-C,  $W = 107.8 \pm 7.9$  Nmm; SGC,  $W = 61.0 \pm 9.9$  Nmm).

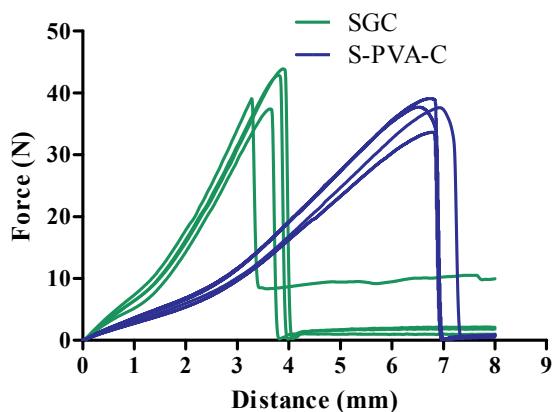


**Figure 3.8:** Comparison of the force-displacement profiles of SGCs (green lines) and S-PVA-Cs (blue lines), both filled with fenofibrate formulation and equilibrated for 2 weeks at 20° C/40% RH before measurements. Profiles of  $n = 4$  for each capsule type were measured.



### 3.3.3.4. *In vitro* disintegration and drug release testing

For disintegration testing, we measured the time necessary for complete opening of the capsules in water at 37° C. SGCs showed much faster disintegration ( $3.2 \pm 0.5$  min) than S-PVA-Cs ( $15.4 \pm 0.4$  min). This was partially attributed to the higher amount of work required to rupture the S-PVA-Cs than SGCs. We observed that S-PVA-Cs were first swelling before rupture at the seam occurred. On the contrary, SGCs exhibited fast opening when in contact with the disintegration medium. The different disintegration behaviour was also reflected by the drug release profiles. Figure 3.9 depicts the dissolution behaviour of both capsules types in 0.05 M SDS. The SGCs showed almost immediate drug release during first 15 min of analysis. A short lag time was noted for the S-PVA-Cs, which was due to the delayed opening time of these capsules.

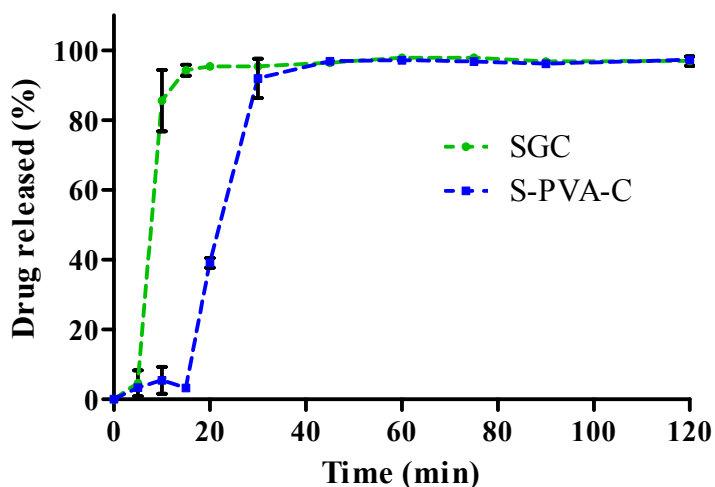


**Figure 3.9:** Drug release profiles of fenofibrate formulation encapsulated in SGCs and S-PVA-Cs in United States Pharmacopeia (USP) 2 in 0.05 M SDS, 75 rpm, at  $37 \pm 0.5^\circ$  C.

### 3.4. Discussion

One of the most critical points for encapsulating a hydrophilic lipid-based formulation in SGCs is water partitioning between the capsule shell and the fill (2). Water in the formulation typically reduces the solubility of poorly soluble drugs (13). In the present study, this reduction was shown to obey an exponential decay so that already small amounts of water in the formulation greatly lowered fenofibrate solubility (Figure 3.4). However, a precipitation is only observed when drug supersaturation occurs in the formulation for a sufficient time to induce nucleation of drug molecules and particle/crystal growth (117). The fenofibrate concentration of approximately 60 mg/mL was considerably lower than the solubility value of the water-free formulation. However, Figure 3.4 indicates that water concentrations higher than approximately 8% w/w in the formulation would lead to supersaturation of fenofibrate. It was possible to relate the amount of water in the formulation to the water activity of the formulation (Figure 3.6). Thus, the water activity of about 0.7 would already correspond to the solubility limit of fenofibrate in the formulation. During the SGCs manufacture, the high water activity of the gelatin shell decreased and approached that of the formulation ( $\sim 0.6-0.7$ ). This value was much higher than the water activity of around 0.3 that was obtained during the production of S-PVA-Cs. Only the SGCs exhibited a greatly reduced solubility that was in proximity of the drug loading. Any further reduction in solubility due to the temperature decrease or migration of the cosolvent to the gelatin shell would result theoretically in drug precipitation. Instead, much more robustness was expected for the S-PVA drug product based on the observed water activity changes during its soft capsule production.

On the basis of the observed water exchange pattern of SGC, it was not surprising to find precipitated drug in these capsules following production and storage. Such drug precipitation is in any case considered as a serious quality defect. It can influence the *in vivo* drug release even though the effects may not always be seen under *in vitro* release testing conditions. Especially a crystalline precipitate is problematic from a

biopharmaceutical viewpoint. It was proven by solid-state analysis that most of the solid material in the SGCs was indeed crystalline fenofibrate. The redissolution of this dose fraction is expected to be critically slow so that incomplete drug absorption can result.

Drug precipitation, as a consequence of water migration during the SGCs production, is even problematic when it is only temporary. It can be argued that drying upon storage can reduce the water content in the formulation and, therefore, the solubility would be shifted to a higher value allowing the precipitate to redissolve. However, such redissolution in an unstirred, viscous formulation is rather slow. Because any partitioning of water affects the equilibrium, it is expected that also packaging conditions influence the water content in the formulation and thereby also affect drug solubility. For example, fast packaging in hermetically sealed blisters may stop initial drying under open environment, thus keeping the water contained in the formulation.

For more formulation robustness, soft capsules should exhibit another water migration pattern. Our study suggested an advantage for the S-PVA-Cs compared with SGCs. By measuring the water activity of the shell and the fill in both capsule types, it was possible to monitor water migration during drying and storage (Figure 3.5). In SGCs, the initial fast water partitioning between the shell and the formulation was followed by a slow equilibration with the shell and the environment. This process may take days, and the final water content in a hydrophilic lipid-based formulation is typically higher than that measured before encapsulation. In line with the concerns of losing drug solvent capacity in the formulation, differences were found in the stability data of the two capsule types. Visual observation of the drug formulation in the SGCs (stored openly and in closed glass vials for 4 months at 20° C/40% RH) revealed drug crystallization, which was further confirmed by HPLC analysis (Table 3.4). In contrast, S-PVA-Cs exhibited only slight water partitioning between the shell, the formulation, and the environment leading to slow equilibration. Another benefit of the S-PVA-Cs is that the low water activity (approximately 0.4) is close to a typical environmental humidity at RT, which enables S-

PVA-Cs to be packaged shortly after production. Such fast packaging is not possible with the SGCs, so the novel capsule material enables a faster production of the final dosage form.

It was mentioned before that the SGCs demonstrated a lacking robustness of the drug product with the given hydrophilic lipid-based formulation. The water-exchange pattern was shown to reduce the fenofibrate solubility close to the given drug loading in the formulation. It was assumed that an additional migration of a hydrophilic excipient into the gelatin shell occurred. Especially, the cosolvent Transcutol<sup>®</sup> HP was a candidate for such solute diffusion because of its hydrophilic nature and because of a comparatively small molecular size. Migrations of excipients or of the drug into the gelatin shell were reported earlier (6, 8). The authors studied the diffusion of solutes through interstices in the gelatin matrix (8). They proved these interstices were too large to act as physical barriers to diffusing molecules. Our study results could indicate that the thermoplastic shell material had an advantage over gelatin regarding solute diffusion. However, it is theoretically also possible that similar amounts of the cosolvent diffused from the formulation to the shell, but given the different water exchange patterns, only the SGCs exhibited drug crystallization during storage.

The capsule materials also differed in their mechanical behaviour. As shown by the force-displacement profiles (Figure 3.8), tensile force for both types of capsules was about the same indicating similar compressive strength. The typical force-displacement profile for soft capsules consists of an initial linear range, followed by a nonlinear behaviour (118). The linear range presented deformation according to Hook's law, indicating that the applied compression force was directly proportional to probe displacement. This part of the profile represents the elastic range of deformation, which is followed by irreversible plastic deformation. Interestingly, the S-PVA-Cs accepted more deformation than SGCs and had larger elongation at break. Moreover, the work required to rupture the S-PVA-Cs

was considerably higher than that of SGCs. Such mechanical robustness of S-PVA-Cs is advantageous for direct bulk storage on trays or storage in large bins after capsule filling.

Apart from the mechanical differences between the capsule types, surface morphology differed as shown in Figure 3.1. The films of S-PVA were considerably rougher than those of gelatin, which may be beneficial for capsule coating. S-PVA-C has the potential for simpler and more robust coating than SGC because of the slow water migration, high temperature resistance (up to 150° C), and rougher surface (Table 3.1). However, further technical studies are needed to better understand the relevance of the different capsule properties for additional manufacturing steps such as coating.

### **3.5. Conclusion**

We have successfully introduced a novel thermoplastic material for soft capsules. The S-PVA-Cs were manufactured on a pilot scale using a coupled extrusion and rotary die encapsulation. The water migration pattern of these thermoplastic capsules was markedly superior to that of SGCs. The novel shell material was found to be suitable for encapsulation of a hydrophilic lipid-based formulation (SMEDDS, type IIIB) without exhibiting any drug crystallization. Thus, a promising soft capsule technology was obtained for the production of a stable drug product when using hydrophilic lipid-based formulations that may otherwise not be suitable for SGCs. Moreover, the high resistance to mechanical deformation of the novel shell material may shorten manufacturing times as compared with the soft capsules made of gelatin. Other characteristics of the new material, such as surface roughness and thermal stability can be advantageous for a subsequent coating step.

The hydrophilic lipid-based system in this study profited from the new capsule technology, but other formulations might be less critical with respect to encapsulation. Future studies are needed to investigate more formulations with different drugs at varying

dose strengths. Especially, the effects of cosolvent migration would have to be studied to finally assess the potential of the novel thermoplastic S-PVA-C in pharmaceuticals.

## Chapter 4

# Understanding biorelevant drug release from a novel thermoplastic capsule by considering microstructural formulation changes during hydration

### Summary

The objective of this study was to explore the biorelevant drug release from novel starch-based polyvinyl alcohol capsules (S-PVA-Cs). The effect of the shell material is studied by considering microstructural formulation changes during hydration. Two different self-emulsifying systems containing either fenofibrate or probucol were filled in S-PVA-Cs, as well as capsules of gelatin (SGCs) and starch (VegaGels<sup>®</sup>). Release analysis employed a BioDis<sup>®</sup> apparatus, while disintegration was studied by texture analysis. For microstructural analysis we used small angle x-ray scattering (SAXS).

S-PVA-Cs opened only partially in biorelevant media compared to completely opened SGCs and VegaGels<sup>®</sup>. In case of the fenofibrate formulation, this opening mechanism caused only a short lag time, while the probucol formulation in S-PVA-Cs resulted in a sustained release. The latter formulation demonstrated much higher viscosity upon hydration compared to the fenofibrate system. Such a rheological effect on drug release was barely noted for SGCs or VegaGels<sup>®</sup> and SAXS revealed differences in the hydrated

microstructure. Even though S-PVA-Cs are highly attractive for encapsulation of rather hydrophilic formulations, some care is needed regarding an immediate release form. The type of formulation hydration must be considered for adequate selection of the capsule material.

#### **4.1. Introduction**

There has been a great interest in finding gelatin substitutes for soft capsules in the last decade. This is due to known gelatin drawbacks, for example animal sources, potential issues of cross-linking, drug migration, or high water exchange during drying between a hydrophilic fill mass and the gelatin shell (25). Recently, we introduced (thermoplastic) starch-based polyvinyl alcohol capsules (S-PVA-Cs) in pharmaceuticals (119). This soft capsule technology appeared to be especially promising for encapsulation of rather hydrophilic lipid-based systems. A typical problem of many self-microemulsifying or nano-emulsifying drug delivery systems is that the presence of hydrophilic formulation components can lead to issues of capsule compatibility when gelatin is used as shell forming material. The problem might be alleviated by addition of excipients to the soft gelatin shell, but a more versatile alternative is to employ the novel S-PVA-C technology. This thermoplastic capsule material was found to be suitable for rotary die encapsulation and the previous study demonstrated adequate drug release in a quality-control (QC) drug release test (119).

Compendial drug release methods are used either in QC testing or to predict *in vivo* drug release with regards to the absorption process. Depending on the focus, the appropriate dissolution media and conditions need to be selected. For example, simplified aqueous media are typically used for routine QC purposes and more complex media might be required for predicting *in vivo* absorption (120). Such more complex media are especially needed for lipid-based formulations. The presence of bile salts and phospholipids, as natural surfactants, has a special importance in these drug release media. Due to their



amphiphilic nature, there can be an effect on drug solubilization as well as on reduction of interfacial oil/water tension, which would affect formulation dispersion. To better simulate the environment of gastro-intestinal (GI) fluids, many biorelevant dissolution media have been developed and tested over the last decade (21). Moreover, standard dissolution methodology (paddles or baskets) may not adequately mimic the hydrodynamics occurring in the GI tract, which was one of the reasons to develop the reciprocal cylinder, *i.e.* USP apparatus 3 (BioDis<sup>®</sup>). Although it is the most attractive method for testing extended-release products, some immediate release products were also successfully analysed (121). It seems to be attractive for *in vivo* absorption prediction to combine the use of a USP apparatus 3 with selecting biorelevant media. This is especially the case for poorly soluble, lipophilic drugs as demonstrated by Jantratid *et al.* (20, 122). One could argue that the most physiological for lipid-based systems is to test *in vitro* lipolysis (26, 123). Such tests are advantageous with formulations that are extensively digested. However, there is currently no standardized vessel defined for lipolysis testing so that hydrodynamics may differ from one equipment to another. Another drawback compared to compendial testing is that the final dosage form cannot be assessed with current lipolysis assays. Since we focused rather on the effect of the shell material on drug release, we selected biorelevant media in a USP apparatus 3.

In the last decade self-emulsifying lipid-based systems have attracted increasing interest among scientists. These systems are dosed as pre-concentrates in a capsule and upon administration they disperse to microemulsions with a large surface area. The process of self-emulsification is a complex and still debated topic. Excellent reviews on the mechanisms of spontaneous emulsification were written by Lopez-Montilla *et al.* and others (124-127). Three principal mechanisms have been proposed for spontaneous emulsification. A first mechanism is based on interfacial turbulence, while another is called “diffusion and stranding” and finally, the transient occurrence of a negative interfacial tension has been discussed. It is also possible that combinations of these principal mechanisms dominate the aqueous dispersion of a self-emulsifying formulation.

The aqueous dilution of a pre-concentrate can possibly exhibit a phase separation along the dilution line. Interesting is the work of Regev *et al.* (128) who demonstrated that even in case of a resulting one-phase system, the aqueous dilution of the pre-concentrate typically passes through liquid crystalline structures and/or a bicontinuous microemulsion area. Only recently, small angle x-ray scattering (SAXS) was used in pharmaceuticals to study the intermediate hydration phases of self-emulsifying drug delivery systems (129-132).

In the present work, we addressed the need to study the biorelevant drug release from S-PVA-Cs. Self-emulsifying systems were used as model formulations and results were compared to the release from soft capsules made of gelatin and of a thermoplastic starch (VegaGels<sup>®</sup>). A particular aim was to evaluate the interaction of the shell material and the type of formulation hydration by studying microstructural changes.

## **4.2. Materials and methods**

### **4.2.1. Materials**

Fenofibrate (Sigma-Aldrich Chemie GmbH, Buchs, Switzerland) and probucol (Euroasian Chemicals Pvt Ltd, Mumbai, India) were selected as poorly water-soluble model drugs. Medium-chain triglycerides (Miglyol<sup>®</sup> 812) were supplied by Hänseler AG (Herisau, Switzerland), soybean oil refined from Georges Walther AG (Pfäffikon, Switzerland) and Transcutol<sup>®</sup> HP (2-(2-ethoxyethoxy)ethanol) by Gattefosse (Lyon, France). Imwitor<sup>®</sup> 742 (medium-chain partial glyceride) was obtained from SASOL (Witten, Germany) and macrogol-glycerolhydroxystearat (Cremophor<sup>®</sup> RH 40) from BASF (Ludwigshafen, Germany). Polyoxyethylene (80) sorbitan monooleate (Tween<sup>®</sup> 80) and acetonitrile of high-pressure liquid chromatography (HPLC) grade were purchased from Sigma-Aldrich Chemie GmbH (Buchs, Switzerland).

For the preparation of the fasted state simulated gastric fluid (FaSSGF) and the fasted state simulated intestinal fluid (FaSSIF), we purchased sodium chloride and sodium hydroxide from Sigma-Aldrich Chemie GmbH (Buchs, Switzerland), pepsin and maleic acid from Hänseler AG (Herisau, Switzerland), sodium taurocholate from Prodotti chimici e alimentari S.p.A. (Basaluzzo, Italy), phosphatidylcholine from Lipoid GmbH (Ludwigshafen, Germany), and hydrochloric acid (1 N) and sodium hydroxide (1 N) from Scharlab (Barcelona, Spain).

The air-filled and oil-filled capsules (Table 4.1), used for the release testing, and the disintegration testing, were produced at the technical facility at Swiss Caps AG, (Kirchberg, Switzerland).

**Table 4.1:** Characteristics of different capsule types.

Type of capsule	Capsule shell material	Method of production	Fill mass <sup>1</sup>
<b>Soft gelatin capsules</b>	bovine gelatin, glycerol, and water 47.4%: 17.1%: 35.5% (w/w)	casting and rotary die method <sup>2</sup>	soybean oil
<b>VegaGels<sup>®</sup></b>	potato starch, glycerol, sorbitol, carrageenan, and water 66%: 18%: 10% : 1% : 5% (w/w)	extrusion and rotary die method <sup>3</sup>	soybean oil
<b>S-PVA-Cs<sup>4</sup></b>	potato starch, PVA, plasticizers (sorbitol solution and glycerol) 40 % : 30% : 30% (w/w)	extrusion and rotary die method <sup>2</sup>	Miglyol <sup>®</sup> 812

1 Fill mass for those capsules used for the texture analysis of dosage form disintegration

2 Methods of production are described in Mistic et al. (119).

3 Method of production of VegaGels<sup>®</sup> is the same as for S-PVA-Cs.

4 S-PVA-Cs: starch-based polyvinyl alcohol thermoplastic capsules

## 4.2.2. Methods

### 4.2.2.1. Preparation and hydration of the formulations

Two different self-emulsifying systems consisting of Tween<sup>®</sup> 80, Transcutol<sup>®</sup> HP, Miglyol<sup>®</sup> 812, Imwitor<sup>®</sup> 742 (45%: 15%: 20%: 20% w/w; TTMI) and Cremophor<sup>®</sup> RH 40, Transcutol<sup>®</sup> HP, Miglyol<sup>®</sup> 812 (60%: 25%: 15% w/w; CrMTrans) were used as model formulations. Since lipid-based systems are generally tailor-made for each drug substance, we also employed two different formulations for the active substances, *i.e.* TTMI for fenofibrate and CrMTrans for probucol. Both mixtures (TTMI and CrMTrans) were compounded in glass vials (by weight) using an analytical balance (Mettler Toledo AB204-S). A magnetic stirring was employed at 40° C until a clear solution was obtained. We carefully checked for the absence of residual particles following the cooling at room temperature. The prepared formulations were hydrated with deionized water at water levels in the range of 5-90% w/w and stored for 24 h at room temperature (RT) before analysis.

### 4.2.2.2. Preparation of drug-containing formulations (solubility studies)

For the system of fenofibrate in TTMI as well as probucol in CrMTrans, an excess amount of drug was added. The mixtures were constantly stirred (750 rpm on a magnetic stirrer) in glass vials at RT. To ensure that equilibrium was reached, the solubility was determined after 18 h, 24 h, and 72 h. The samples were then centrifuged at 13,362 g for 20 min using a Centrifuge 5415 R (Eppendorf AG, Hamburg, Germany). Finally, the concentrations of the active compounds in the supernatant were determined after diluting the supernatant with acetonitrile (1:500 v/v) by HPLC analyses.

Drug-containing formulations were prepared by adding fenofibrate to a clear solution of TTMI (FF-TTMI), and probucol to CrMTrans (Pro-CrMTrans), both in drug concentration of 60 mg/mL.

### **4.2.2.3. Characterisation**

#### **4.2.2.3.1. Particle size measurements**

Particle size of the diluted self-emulsifying systems was analysed by means of dynamic laser light scattering using a Zetasizer Nano ZS (Malvern, Worcestershire, United Kingdom). For individual measurements, an aliquot (100  $\mu\text{L}$ ) of each preconcentrate was obtained from a calibrated automatic pipette Eppendorf Research<sup>®</sup> plus (20-200  $\mu\text{L}$ ) and dispersed in 20 mL of water using a glass vial. Both formulations were assessed for their ease of self-emulsification and qualitatively described as “good”, “moderate” or “poor” (129). The diluted samples were measured in dynamic light backscattering (173° angle) and the mean particle size (*Z*-average diameter) was calculated from the volume size distribution. All experiments were repeated in triplicates from fresh samples at RT.

#### **4.2.2.3.2. Rheological studies**

The rheological properties of low-viscous lipid-containing colloids can be difficult to measure. For adequate measurements using a cone-plate rheometer, there must be a uniform force transmission in the sample. A loss of grip between the cone and the sample shear plane is a problem that especially occurs at comparatively high shear forces. For the measurements of the hydrated formulations, we therefore employed a new mechanical chip-based (MEMS) capillary rheometer (mVROC<sup>™</sup> RheoSence, San Ramon, CA, USA). m-VROC<sup>™</sup> (Viscometer-Rheometer-on-Chip) is a microfluidic slit rheometer used for fast and accurate measurements of the viscosity of microliter sample volume solutions. It measures the viscosity from the pressure drop of a sample as it flows through a rectangular slit. The glass syringe (Hamilton 1010 C SYR 10 mL or Hamilton 81260 SYR 500  $\mu\text{L}$ , depending on the viscosity of the sample) was loaded with sample and placed inside of the thermal jacket ( $25 \pm 0.5^\circ \text{C}$ ). When the measurement temperature was stable, the sample was pumped to flow (at shear rate  $200 \text{ s}^{-1}$ ) through the flow channel of the chip. The pressure drop was detected by a sensor (cell m-VROC A-10 or D-10) and

the viscosity was calculated using m-VROC Control Software™. The viscosities of TTMI and CrMTrans were measured for hydration levels of 5-90% w/w. Results were based on experiments in triplicates.

#### 4.2.2.3.3. Small angle x-ray scattering (SAXS) studies

SAXS was measured using a Bruker NANOSTAR setup with an Incoatec I $\mu$ S-microfocus Cu-K $\alpha$  anode (wavelength 1.54 Å) and a Bruker VANTEC-2000 detector. The samples were measured in flame-sealed glass capillaries with a diameter of 1.5 mm and a wall thickness of 1  $\mu$ m. The 2D detector images were taken at ambient temperatures and were azimuthally averaged to produce 1D intensity profiles.

**Fitting.** The SAXS data were fitted using a Teubner-Strey model for microemulsions (131, 133). The Teubner-Strey model is based on the Landau theory for microemulsions, where the order parameter is associated with the “water-to-oil ratio” (133). This model predicts a single broad maximum and a  $q^{-4}$ -dependence towards higher  $q$ -values (higher scattering angles).

Within this model the scattering intensity has the following form:

$$I(q) \propto \frac{1}{a + c_1 q^2 + c_2 q^4} \quad (4.1)$$

The obtained parameters  $a$ ,  $c_1$  and  $c_2$  are used to calculate the two characteristic length scales  $d$  and  $\xi$ .

$$d = 2\pi \left[ \frac{1}{2} \left( \frac{a}{c_2} \right)^{\frac{1}{2}} - \frac{1}{4} \frac{c_1}{c_2} \right]^{\frac{1}{2}} \quad (4.2)$$

$$\xi = \left[ \frac{1}{2} \left( \frac{a}{c_2} \right)^{\frac{1}{2}} + \frac{1}{4} \frac{c_1}{c_2} \right]^{\frac{1}{2}} \quad (4.3)$$

Here,  $d$  is the domain size (or periodicity) whereas  $\xi$  is the correlation length, both together providing an indication of the order in the system. The ratio  $\xi/d$  is a measure of the correlation length in units of the periodicity.

#### 4.2.2.3.4. Biorelevant drug release studies

Drug release was studied using the BioDis<sup>®</sup> apparatus (RRT 8, CALEVA Ltd, Dorset, England) at  $37 \pm 0.5^\circ$  C using 220 mL of test medium in each vessel, mesh sizes of 420  $\mu$ m for both the top and bottom mesh of the glass cylinders and a dip rate of 10 dpm or 30 dpm, respectively (134, 135). Prior to each experiment, the air-filled capsules were weighed before and after manual filling with FF-TTMI or Pro-CrMTrans, to obtain an exact fill mass in each capsule. The experimental set-up in this study was supposed to mimic the fasted gastrointestinal tract (GIT). Therefore we used FaSSGF (30 min) followed by FaSSIF (60 min), prepared as described by Jantratid *et al.* (136). At predetermined time points, a 2-mL sample was taken by a syringe, immediately filtered through a 0.45  $\mu$ m Nylon filter (Titan 2 Syringe Filter, SUN SRi, Rockwood, TN, USA) and analysed by HPLC. The removed volume was replaced each time with 2 mL of fresh medium. All experiments were performed in triplicates.

#### 4.2.2.3.5. Texture analysis of dosage form disintegration

A texture analyzer (TAXT2i; Stable Micro Systems, Surrey, United Kingdom) was assembled with a disintegration rig (originally developed for fast-melting tablets) to study the disintegration of capsules. This mechanical test mimics the gastric disintegration conditions, while constantly maintaining the force and measuring the distance as the sample disintegrates. The apparatus was equipped with a 5 kg load cell and fitted with a 20 mm diameter cylindrical probe. The capsule was attached with a strip of 3 mm wide

double-sided tape to the underside flat region of the probe end. Each capsule type was filled with oil at the technical facility of Swiss Caps AG, (Kirchberg, Switzerland) (Table 4.1) and was analysed in triplicates. A double-jacketed glass vessel was connected with tubes to a thermostat system to keep the disintegration medium (FaSSGF, 100 mL) at  $37 \pm 0.5^\circ \text{C}$ . On the bottom of the double-jacketed glass vessel was a (30 mm diameter) platform, which was perforated to allow ingress of water beneath the capsule. The speed of the probe with an attached capsule was initially 2.0 mm/s until the surface of perforated platform was detected at the force of 0.029 N (threshold value for triggering the onset of texture analysis). Subsequently, the force of the probe was 0.098 N with a speed of 3.0 mm/s and the distance was measured to obtain a capsule disintegration profile. The time of analysis was 30 min (consistent with section 4.2.2.3.4.). All capsules were produced either on pilot- (S-PVA-Cs) or on a production-scale (SGCs, VegaGels<sup>®</sup>) using rotary die filling machines at the Swiss Caps facility in Kirchberg, Switzerland (Table 4.1).

#### **4.2.2.4. HPLC method**

The drug content of each sample was determined by HPLC (Agilent Technologies 1200 Series) using a degasser (G1379 B), an isocratic pump (G1310A), an autosampler (G1329A), a variable wavelength detector (G1314B), and a LiChrospher 60, RP select B 125–4 (5  $\mu\text{m}$ ) column (Merck, Darmstadt, Germany) at a flow rate of 1 mL/min. The HPLC conditions are described in Table 4.2.



**Table 4.2:** Overview of HPLC methods used for active compounds quantification.

<b>Active compound</b>	<b>Mobile phase</b>	<b>Injection volume</b>	<b>UV detection</b>
Fenofibrate	Acetonitrile : ammoniumacetate buffer (pH 3.5; 25 mM) (65:35, v/v)	20 $\mu$ L	287 nm
Probucol	Acetonitrile : water (90:10, v/v)	10 $\mu$ L	241 nm

## 4.3. Results

### 4.3.1. Characterization

#### 4.3.1.1. Particle size measurements

The self-emulsifying systems (CrMTrans and TTMI) used in our study showed different spontaneous dispersion behaviour in water (ratio 1:200 v/v) at room temperature. We checked each of the evolving dispersions visually and qualitatively classified the ease of their self-emulsification as “good”, “moderate” or “poor”. Since TTMI spontaneously formed a transparent dispersion, it was categorized as “good” emulsifying system. This ease of spontaneous self-emulsification behaviour was already described by Groves and Pouton (137, 138). In contrast to that, the formulation CrMTrans was rated as rather “poor” emulsifier, since it formed flakes upon gentle agitation, while following short vigorous stirring, the mixture became completely transparent. This result was obviously caused by the formation of viscous structures, which required higher shear forces to disperse the system. Despite the differences in their ease of self-emulsification, both systems resulted in nanodroplets. The droplet sizes of CrMTrans and TTMI were found to

be  $23.0 \pm 1.6$  nm (PDI = 0.15) and  $17.9 \pm 1.7$  nm (PDI = 0.07), respectively. A statistically significant difference between the droplet sizes of diluted formulations was confirmed with  $p < 0.01$  (t-test following an F-test that demonstrated the homogeneity of sample variances).

#### 4.3.1.2. Rheological studies

Figure 4.1 shows differences in viscosities of the hydrated self-emulsifying systems (TTMI and CrMTrans). We observed that, in the case of CrMTrans, the viscosity at lower water contents (10-25% w/w) increased with dilution. It may be related to the swelling of the amphiphilic film as part of the generated microstructure. This increase in viscosity, caused by instantaneous formation of a transparent gel upon hydration, was already visually observed during sample preparation. With further increase in water volume fraction, continuous hydration of the structure was observed. There was a sharp increase in viscosity observed with the CrMTrans system demonstrating a maximum at 30% w/w water, followed by a decrease with further hydration. In contrast, TTMI exhibited only a slight increase in viscosity at the hydration levels of 40-50% (w/w).

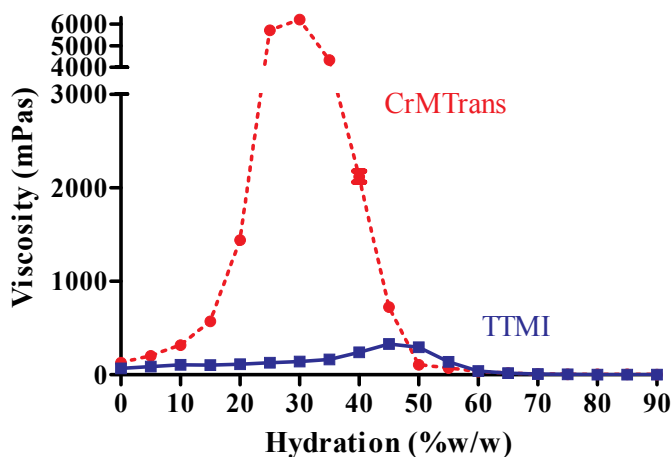


**Figure 4.1:** Viscosity profiles of the self-emulsifying systems upon hydration measured at  $200 \text{ s}^{-1}$  and  $25^\circ \text{ C}$  by m-VROC<sup>TM</sup> rheometer [CrMTrans (red line), TTMI (blue line)]. The lines are presented as guides to the eye.

#### 4.3.1.3. Small angle x-ray scattering (SAXS)

SAXS was used to study microstructural changes in hydrated formulations over the whole hydration range. We did not expect a marked effect of the compounds on hydration, because both drugs are neutral, highly lipophilic and low concentrated. Therefore, the controlled hydration was studied using placebo formulations. The peak positions of hydrated TTMI shifted to smaller  $q$ -values with increasing water content and became narrower up to 55 % w/w water content (Figure 4.2). For the hydrated CrMTrans, with the increasing water content from 10 to 25% w/w, a shift of the peak to lower  $q$ -values and a narrowing of the peak could be observed. The narrowest peak was obtained at a water content of 30% w/w. Further water increase resulted in only slight shifts of the peak positions, while a broadening of the peak with increasing water content was noted. Both formulations exhibited at higher hydration levels (for TTMI from 60% up to 90% w/w and for CrMTrans from 35% to 70% w/w) an additional change in SAXS intensity for smaller  $q$  values ( $0.01$ - $0.02 \text{ \AA}^{-1}$ ). The appearance of an additional SAXS signal can be attributed to a coexistence of an additional colloidal phase with the general microemulsion structure.

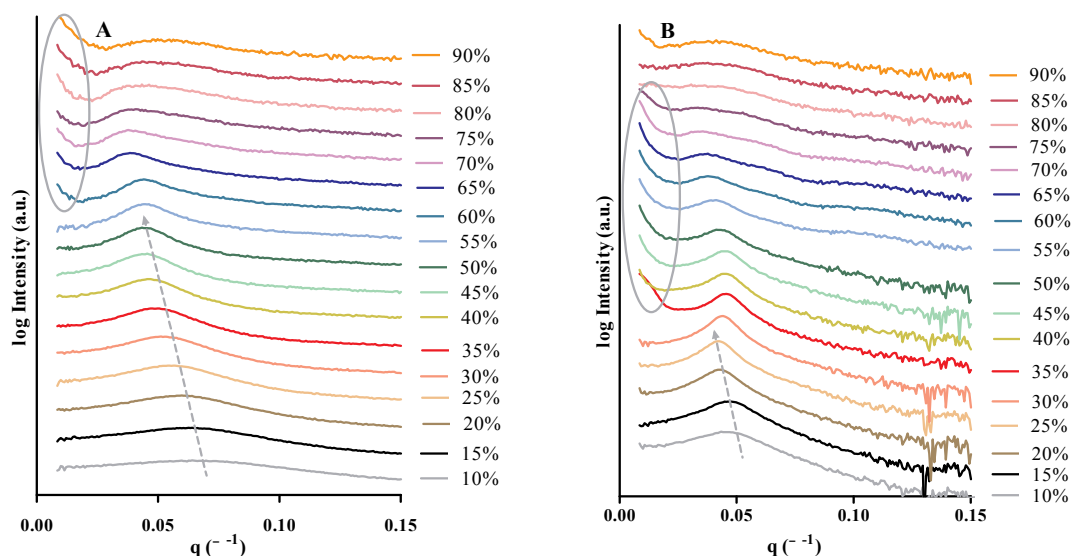


**Figure 4.2:** SAXS intensity profiles (logarithmic scale) for microemulsions consisting of (a) TTMI and water and (b) CrMTrans and water. The numbers next to the each curve indicate different water concentrations in the mixtures. Each curve is shifted by one order of magnitude with respect to the previous one.

The calculated domain sizes  $d$  and correlation lengths  $\zeta$  are shown in Figures 4.3 and 4.4. For CrMTrans hydrated from 15% to 25% w/w, and from 45% up to 60% w/w an increase in  $d$  was found, which was followed by a slight decrease for water contents up to 90%. In contrast to that, a strong (linear) increase of the correlation length  $\zeta$  with increasing water content from 10% to 30% w/w could be seen. After reaching a maximum in  $\zeta$  at 30% w/w water content ( $\zeta \approx 190 \text{ \AA}$ ),  $\zeta$  sharply decreased between 30% and 65% w/w with a subsequent slower decrease towards higher water contents. Both the calculated domain size  $d$  and the correlation length  $\zeta$  of hydrated TTMI demonstrated a linear increase with rising water content up to 50% w/w, followed by slight decrease at higher water contents. The exception was at 65% w/w hydration level when  $d$  showed some increase compared to other hydration levels.

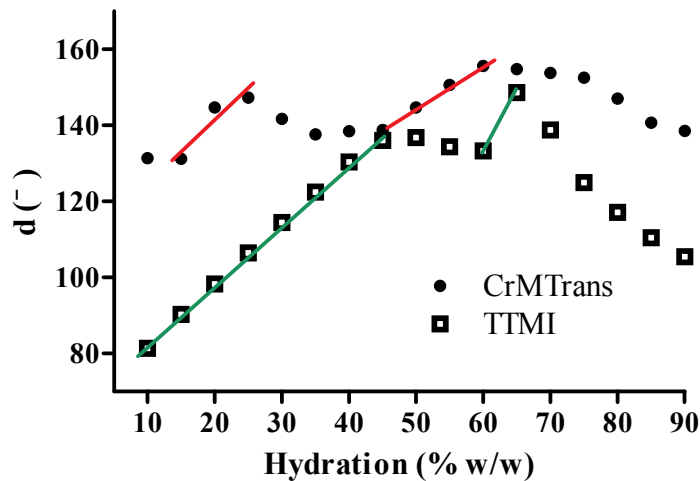


**Figure 4.3:** Plot of domain size (periodicity)  $d$  versus hydration levels for both model formulations (TTMI and CrMTrans). [CrMTrans (red line), TTMI (green line)]. The lines are presented as guides to the eye to point at increase in periodicity.

Both formulations exhibited a maximum value in  $d$  as well as with respect to the correlation length  $\zeta$ . This scattering behaviour was reflecting a hydration process that induced the formation of a more ordered phase. Following the maximum domain size and correlation length, a reverse trend in the swelling process started, which can be viewed as a phase transition. Thus, dominance of a bicontinuous microemulsion structure (with possible existence of local lamellar structures) was receding to evolving colloids of a droplet type.

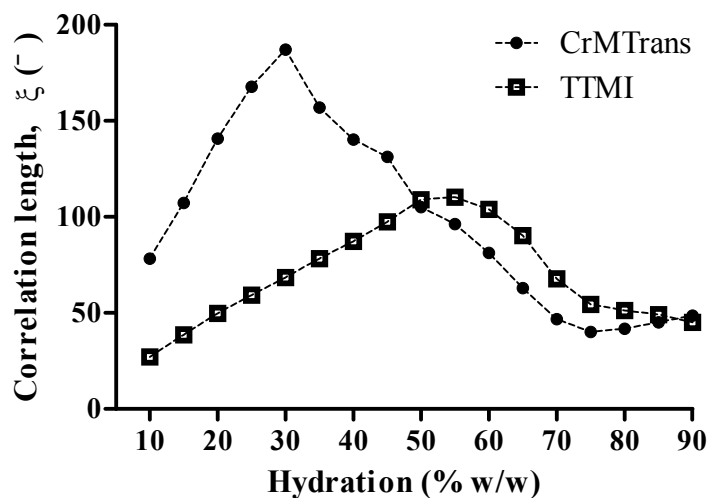


**Figure 4.4:** Plot of correlation length  $\xi$  versus hydration levels for both model formulations (TTMI and CrMTrans). The connecting lines are for the ease of visualization.

#### 4.3.1.4. Analysis of capsule disintegration and drug release

To better characterize the mechanical changes of the shell material, we used a capsule disintegration testing rig of texture analysis. Thus, the capsule filled with oil (Table 4.1) was placed in biorelevant test medium (FaSSGF) at  $37 \pm 0.5^\circ \text{C}$  and a plate was kept at constant force to monitor changes in distance. Such changes of displacement were caused by the specific hydration and capsule disintegration mechanisms (Figure 4.5). Both S-PVA-Cs and VegaGels<sup>®</sup> were first swelling before rupture at the seam occurred. For S-PVA-Cs partial opening at the seam was noticed by visual observation, whereas for VegaGels<sup>®</sup> there was a fast and complete opening along the seam. This difference in opening can also be seen in their disintegration profiles. VegaGels<sup>®</sup> appeared to disintegrate in a two-steps process. A first stage corresponded to the opening at the capsule seam, while the second stage was given by the disintegration of the residual

capsule halves. SGCs exhibited a very fast and complete opening prior to dissolution of the gelatin fragments.

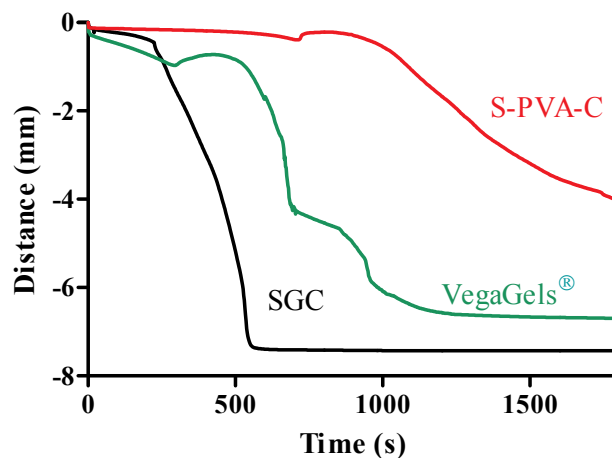


**Figure 4.5:** Comparison of disintegration profiles of oil-filled SGC, VegaGels<sup>®</sup>, and S-PVA-C analysed by texture analyzer in biorelevant medium (FaSSGF) at  $37 \pm 0.5^\circ \text{C}$ . Each curve is a single representative example of  $n = 3$  experiments.

The different disintegration behaviour was also reflected by the drug release profiles. Figure 4.6 depicts the release behaviour of fenofibrate formulation (FF-TTMI) in all three capsule types using the biorelevant media. SGCs and VegaGels<sup>®</sup> showed an almost immediate drug release within the first 10 min, which was in agreement with the disintegration profiles confirming a complete capsule opening. A short lag time was noted for the S-PVA-Cs, which was due to the partial opening of these capsules.

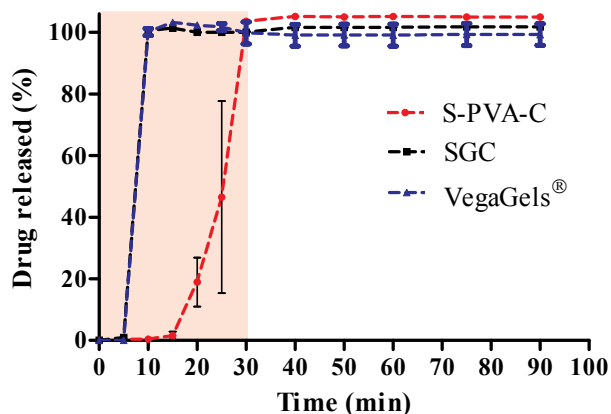


**Figure 4.6:** Release behaviour ( $n = 3 \pm \text{SD}$ ) of fenofibrate formulation (FF-TTMI) from S-PVA-Cs, SGCs, and VegaGels<sup>®</sup> using the BioDis<sup>®</sup> apparatus in biorelevant media at  $37 \pm 0.5^\circ \text{C}$ , 10 dpm (shaded part represents drug release in FaSSGF, and non-shaded in FaSSIF).

Figure 4.7 presents the release behaviour of the probucol formulation (Pro-CrMTrans) in all three capsule types using biorelevant media. The drug release of Pro-CrMTrans filled in S-PVA-Cs in FaSSGF was incomplete with high variations (10-30%). A subsequent change to FaSSIF exhibited sustained and comparatively slow drug release also with high variability. This observation may be attributed to the differences in viscosity of Pro-CrMTrans compared to FF-TTMI. The drug release of Pro-CrMTrans filled in SGCs and VegaGels<sup>®</sup> was complete after 30 min with a short delay.



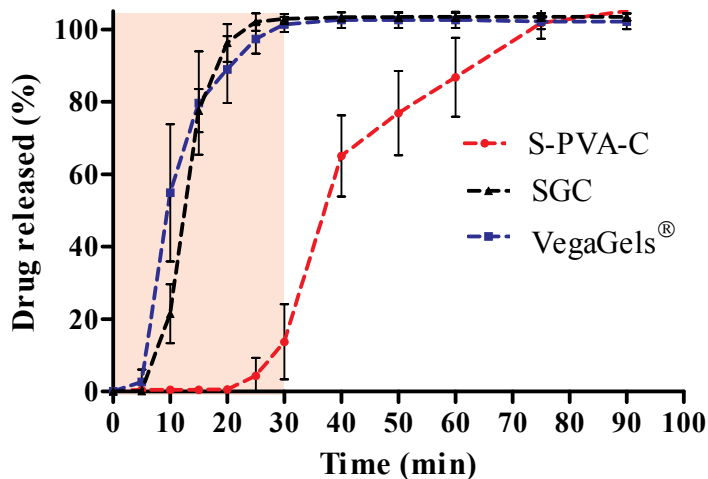


**Figure 4.7:** Release behaviour ( $n = 3 \pm \text{SD}$ ) of the probucol formulation (Pro-CrMTrans) from S-PVA-Cs, SGCs, and VegaGels® using the BioDis® apparatus in biorelevant media at  $37 \pm 0.5^\circ \text{C}$ , 10 dpm (shaded part represents drug release in FaSSGF, and non-shaded in FaSSIF).

To evaluate the effect of mechanical force on release behaviour of the probucol formulation in S-PVA-Cs, we increased the dipping rate from 10 dpm to 30 dpm. A rate of 10 dpm provided an agitation that is generally considered as physiological for dosage form release in the USP 3 (139). An increase of the dip rate was therefore primarily of interest to mechanistically study the probucol system. We targeted higher shear forces caused by an increased agitation of the reciprocal cylinder. However, the probucol formulation CrMTrans barely revealed a difference in drug release when comparing the two dip rates (Figure 4.8).

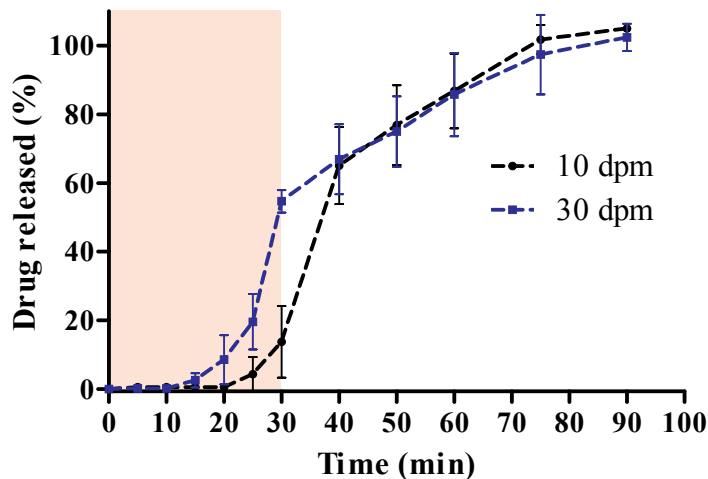


**Figure 4.8:** Effect of the mechanical force on release behaviour of probucol formulation (Pro-CrMTrans) in S-PVA-C in BioDis<sup>®</sup> apparatus in the biorelevant media at  $37 \pm 0.5^\circ \text{C}$  (shaded part represents drug release in FaSSGF, and non-shaded FaSSIF).

#### 4.4. Discussion

For any new capsule technology it is important to study drug release not only in standard buffer solutions but also using biorelevant media. Although these media only approximate the composition of gastro-intestinal fluids, they still contain the most important components, namely bile salts and phospholipids, which facilitate solubilization of lipophilic drugs in micelles. So the release of poorly soluble, lipophilic drugs is usually enhanced compared to the release rate in simple aqueous solutions (20).

In our previous work we focused on manufacturability and general characterization of the novel thermoplastic soft capsules (S-PVA-Cs). Benefits were shown for the encapsulation of rather hydrophilic formulations and drug release was studied in water only (119). Considering the importance of more physiological drug dissolution, we focused in the

present study on biorelevant drug release using the USP apparatus 3. A special aim was to better understand how the shell material affects drug release by considering changes in the hydrated microstructure of selected self-emulsifying formulations.

#### **4.4.1. Effect of the shell material**

Disintegration in a compendial sense is defined as the state in which any residue of the unit, except fragments of the capsule shell, is a soft mass having no palpably firm core (140). The process of disintegration consists theoretically of two steps: opening of the capsules and the disintegration of the capsule shell, which may overlap in time. In case of the gelatin capsules, the opening process was usually fast (within the first 5 min) and seemed not to limit the drug release. In contrast to gelatin, there was a general lack of knowledge about disintegration of thermoplastic capsules or their drug release in biorelevant media. This was not only true for the novel S-PVA-Cs but also for other thermoplastic capsules such as VegaGels<sup>®</sup>. Since the thermoplastic capsules may have a specific opening mechanism, depending on the nature of the polymer, their disintegration profiles can vary. Both VegaGels<sup>®</sup> and S-PVA-Cs are starch-based thermoplastic capsules that are similar in their qualitative composition (Table 4.1). Their similarity was also reflected by the observed disintegration profiles in biorelevant media. Texture analysis of their disintegration process revealed a swelling (pre-disintegration) before a rupture occurred at the seam of the capsules (Figure 4.5). Following an initial swelling, VegaGels<sup>®</sup> demonstrated a step-wise disintegration pattern. It was clearly possible to distinguish a complete opening of the capsule from the disintegration of the residual shell material. In contrast to that, S-PVA-Cs first partially opened and then started to disintegrate, while they continued to open. This different opening pattern was visually observed and was supported by the texture analytical profiles. Moreover, this finding was in agreement with the observed release profiles of S-PVA-Cs. In the case of the fenofibrate formulation, a short lag time was noted, which was attributed to the partial

capsule opening. For the probucol formulation, the interaction of the opening mechanism and poor formulation dispersibility resulted in sustained and comparatively slow drug release. Furthermore, there was no influence noted of a varied hydrodynamics on the release profile (Figure 4.8). This was similar to the results of a previous study in which a difference in typical dip rates of the USP apparatus 3 barely affected drug release of tablets (141). A complete and fast opening of SGCs and VegaGels<sup>®</sup> assured an immediate drug release, which was not depending on the nature of the formulation with its hydration process.

In summary, the fenofibrate system easily self-emulsified and drug release was therefore practically independent of the used capsule shell. However, the model formulation of probucol was critically depending on the type of capsule opening. The partial opening of the S-PVA-Cs in combination with the highly viscous hydrated formulation obviously sustained the drug release. Such hindered drug diffusion was not observed with the same formulation using the other tested capsules that opened rapidly along their entire seam.

#### **4.4.2. Effect of microstructural formulation change**

The results of the capsule opening as well as the drug release testing showed, especially for S-PVA-Cs, that formulation changes during water hydration can be critical. To better understand such effects during self-emulsification, we studied the pre-concentrates at different hydration levels. The drug-free formulations were studied while assuming that the compounds would have a neglectable effect on hydration at the rather low concentrations used in this study.

Both model formulations (CrMTrans and TTMI) exhibited along the different hydration levels some similarities. Until the viscosity maximum was reached, the system remained a clear single phase. The drop of viscosity in both systems resulted in slightly turbid mixtures that became practically transparent as the water hydration levels increased. The

probucol system (CrMTrans) revealed a sharp increase in viscosity at an intermediate hydration (10-25%, w/w), which was quite different from the hydrated fenofibrate system (TTMI). Such a viscosity peak was previously observed by Fanun (142) in hydrated pre-concentrates that were fully dilutable (as a single-phase). It was assumed that structural transitions occurred from water-in-oil to bicontinuous to oil-in-water microemulsions. This view of structural transitions has also been reported by other authors who studied similar self-emulsifying formulations (85). However, the microstructural changes may still be specific for a given system so that different rheological properties evolve during hydration.

For the swelling of an amphiphile, the polar head group is expected to play a key role. Both model systems comprised rather hydrophilic surfactants with a substantial amount of ethylene oxide units. However, the Cremophor-containing formulation (CrMTrans) had a much higher surfactant concentration than the Tween-system (TTMI). This probably contributed to the more viscous structures that were formed upon water addition. Unfortunately, we could not compare surfactant effects at the same concentration levels, because of the individual phase behaviour of the formulations that were tailor-made for the different model drugs.

A better understanding of the microstructure was targeted by the analysis of SAXS data. Both systems demonstrated a typical peak for the hydrated systems as it has been observed before in hydrated microemulsion pre-concentrates (130-132). Recently, Patil *et al.* discussed the possibility that at least a part of such structure was consisting of local lamellar structures (131). Such structures can be viewed as small stacks of randomly oriented lamellar structures. Local lamellar structures were initially reported in microemulsions by Cabos *et al.* (143). Since there is a lack of long-range and orientational order, no macroscopic birefringence would be expected. Kogan *et al.* described the existence of “ordered bicontinuous structures” as bicontinuous microemulsions based on lamellar phases that have lost the long-range order due to

thermal distortions but kept the short-range order (144). In our case, the SAXS diffractograms of both systems developed comparatively ordered structures at an intermediate hydration regime. This increase in ordering has been seen in a shift of the peak maxima to the lower angles ( $q$ ) and a sharpening of the peaks. The samples at intermediate hydration levels were also examined by a polarized light microscope and did not reveal any birefringence, which indicated that no marked liquid crystalline structures were present. The obtained structures were considered to be microemulsions with some short-range order. For such intermediate hydration levels, a bicontinuous microemulsions type is expected. Our data showed in case of TTMI some linearity of  $d$  as a function of different water amounts. More complex were changes in the domain size of the CrMTrans system upon addition of water. This formulation showed a maximum in  $\zeta \approx 190 \text{ \AA}$  at 30% w/w, whereas TTMI exhibited a strong linear increase and reached its maximum only at  $\zeta \approx 110 \text{ \AA}$  at 55% w/w. It was a notable finding that the maximum in the correlation length of the CrMTrans system corresponded to the observed sharp viscosity peak. In contrast to that, hydrated TTMI demonstrated neither a sharp peak in correlation length nor in viscosity.

Our systems also exhibited a typical bell-shaped curve of  $\zeta$  as a function of the hydration level (Figure 4.4). As earlier reported by Fanun (132, 142) this behaviour could be correlated with structural transitions. Another interesting property is the ratio of the correlation length to the domain size  $\zeta/d$ , which indicates a length of order that is relative to a typical domain size. It has been argued that the product  $2\pi$  times  $\zeta/d$  might be used to differentiate a bicontinuous microemulsion from another type of a Windsor type IV system (128). However, some care is needed with this theoretical argument because real Windsor type IV systems can be difficult to assign to an ideal structural type. Structures of different colloidal nature can also co-exist. As explained earlier, it is well possible that stacks of local lamellar structures were present in our model systems. However, they could have been part of a bicontinuous microemulsion at intermediate hydration levels.

A co-existence of different structures was also an interpretation of the additional SAXS features at very low  $q$ , which was observed at relatively higher water amounts in both systems. This signal was likely due to larger colloidal structures such as oil-swollen micelles. Hence, it may hold for the onset of a transition to oil in water microemulsion.

In summary, the SAXS data demonstrated clear differences in the microstructures of the model systems in terms of how the domain size  $d$  and the correlation length  $\zeta$  changed at different hydration levels. Interesting was the more complex hydration process of the CrMTrans system, which was inferred from the non-linearity of  $d$  as a function of increasing water amounts. Our data suggested that different colloidal structures can co-exist in hydrated self-emulsifying systems. The higher structural ordering might have caused an increased viscosity. Although, the microstructural analysis using SAXS effectively complemented the rheological studies of the hydrated formulations, it did not fully explain the huge differences in viscosity between the two hydrated systems. More research is needed to better understand how the microstructure of hydrated self-emulsifying systems is affecting rheological properties.

## 4.5. Conclusions

This study focused on the biorelevant drug release from S-PVA-Cs. Texture analysis of capsule disintegration revealed interesting findings. A clear difference was noted in the mechanism of how the novel S-PVA-Cs opened compared to soft capsules of gelatin or of another thermoplastic material (VegaGels<sup>®</sup>). The different opening mechanism was relevant for the drug release depending on the given formulation. We studied two model formulations which were both pre-concentrates of microemulsions, but they significantly differed in their hydrated microstructure. A better understanding of these microstructures was achieved by SAXS analysis. An interaction of the hydrated structures and the shell material was identified for the drug release from the novel thermoplastic capsules.

Our results support the view that a capsule shell material may not be freely selectable for a given formulation. While initial formulation development is typically optimizing the biopharmaceutical performance, some care is needed with selecting an appropriate capsule technology. The choice of a suitable shell material has to be based on improved knowledge of formulation characteristics. Quality control failures in drug release can be avoided by a better understanding of the mechanisms of capsule opening and the microstructural formulation changes during hydration. Ultimately, such knowledge contributes to designing quality into a capsule dosage form. This is a step in the right direction towards the desired state of the quality by design initiative as it is targeted by regulatory authorities as well as by developers of drug products.



---

## Chapter 5

# Understanding interactions of oleic acid with basic drugs in solid lipids on different biopharmaceutical levels

### Summary

Recently, the impact of intestinal supersaturation on absorption of poorly water-soluble drugs has raised much interest among researchers. A focus has been mostly to study excipient effects on maintenance of drug supersaturation. The aim of the present study was to better understand the effects of drug-excipient interactions on different levels, *i.e.*, in the anhydrous formulation, upon dispersion in simple buffer media and, in particular, regarding precipitation kinetics. As a model system a solid lipid-based formulation was developed, comprising PEG-32 stearate and oleic acid (OA) (8:2 w/w). Loratadine ( $pK_a = 4.33$ ) and carvedilol ( $pK_a = 8.74$ ) were chosen as basic drugs. UV/FTIR spectroscopy and viscometry were used to characterize drug-OA molecular interactions in solution, while solid formulations were studied using x-ray diffraction, thermal analysis and van't Hoff solubility-temperature plots. Precipitation kinetics of drug formulations was real-time monitored in phosphate buffer (pH = 6.5) by focused beam reflectance measurements. It was found that the addition of OA in the formulations resulted in substantial drug solubility increase. Although the drug-OA interactions appeared to be partially lost upon formulation dispersion, the extent of precipitation was markedly lowered compared to the

formulations without OA. A Precipitation number ( $P_{nc}$ ) was introduced as a ratio of a relevant residence time of drug in the gastrointestinal tract (GIT) to the induction time (the onset time of crystalline precipitation). Without OA,  $P_{nc}$  was already taking critical values ( $>1$ ), while the anhydrous formulation was still below saturation for both model drugs. Interestingly, the addition of OA resulted in amorphous instead of crystalline precipitates, which is advantageous for drug absorption. In conclusion, this study provides an improved understanding of OA and basic drug interactions on different levels of *in vitro* performance for more rational oral formulation development.

## 5.1. Introduction

Poorly water-soluble drugs (PWSD) present a challenge for drug development because of a typically reduced systemic exposure upon oral administration. A key approach to enhance oral bioavailability of PWSD is to employ lipid-based formulations (LBFs) that may consist of oils, surfactants, and co-solvents (26). The latter excipients are often added to solubilize the dose of rather hydrophobic drugs, while primarily lipophilic compounds may be incorporated in oils alone. A high solvent capacity of the anhydrous formulation generally decreases upon formulation dispersion and digestion in the gastrointestinal tract (GIT), thereby resulting in drug supersaturation. This supersaturated state is thermodynamically unstable and its extent constitutes the driving force for drug precipitation. In the last decade, there has been a growing interest in: 1) development of different types of supersaturating drug delivery systems (SDDS) (79, 145) that stabilize supersaturation, and also in 2) understanding the mechanisms by which LBFs generate supersaturation (84, 87, 89). Maintenance of drug supersaturation upon aqueous formulation dispersion was demonstrated in several studies by inclusion of some polymers (96, 97), surfactants (99), and cyclodextrins (100) in drug formulations. As a result of a sufficiently long and stable period of drug supersaturation, intestinal drug absorption and oral bioavailability can be enhanced (101).

Many studies on drug supersaturation are not mechanistically oriented and there is a need to better differentiate excipient effects on drug solubility (upon dispersion) from an influence on the kinetics of drug precipitation. Much needed is a better holistic understanding of drug-excipient interactions starting already on the level of the anhydrous formulation to the fate of the drug delivery system *in vitro* and *in vivo*. Such a systematic study of drug-excipient interactions, to the best of our knowledge, has not been reported for solid lipid-based formulations. The present study is following such an approach by studying the excipient interactions up to an *in vitro* level as outlined in Figure 5.1.

This study employs a solid lipid-based excipient that has recently been introduced for oral use. Polyethylene glycol 32 stearate (PEG-32 S) is a waxy lipid-based excipient, with a melting point of 48° C and a HLB of 16. It belongs to a group of the polyoxyl stearates, consisting of PEG-32 mono- and diesters of mainly stearic (octadecanoic), and/or palmitic (hexadecanoic) acid, and free PEG-32 (146). Since PEG-32 esters are hydrophilic surfactants and free PEG-32 is a hydrophilic solvent, this excipient alone would correspond to a type IV formulation of Lipid Formulation Classification System (50).

The present study is focused on the mechanistic understanding of oleic acid (OA) and basic drug interactions in anhydrous solid lipid-based formulations, and upon aqueous dispersion of these systems. In particular, drug-excipient interactions were studied with respect to drug precipitation kinetics. Since it has been demonstrated earlier that various hydrodynamics may have an impact on precipitation kinetics (147), a comparison between two different mixing techniques was made (magnetic stirring and standard USP 3 apparatus). As a model system, we developed a solid lipid-based formulation, comprising PEG-32 stearate and OA in the optimal ratio. Loratadine ( $pK_a = 4.33$ ,  $\log P = 4.55$ ) (148) and carvedilol ( $pK_a = 8.74$ ,  $\log P = 3.42$ ) (149) were selected as basic drugs and were incorporated at different saturation levels in LBFs with and without OA. The formulations were dispersed in phosphate buffer ( $pH = 6.5$ ) and the precipitation kinetics was studied

using a laser scanning technique (focused beam reflectance measurement, FBRM). Gao and co-workers (80) were first to use this technique to analyse drug precipitation. Compared to commonly used light scattering techniques (*e.g.* nephelometry), FBRM allows *in situ* monitoring of both dimension and number of precipitated particles. Finally, we introduced the concept of a biopharmaceutically relevant parameter, *i.e.* a Precipitation number ( $P_{nc}$ ), by the ratio of a relevant residence time of drug in the gastrointestinal tract (GIT) to the induction time (the onset time of crystalline precipitation).

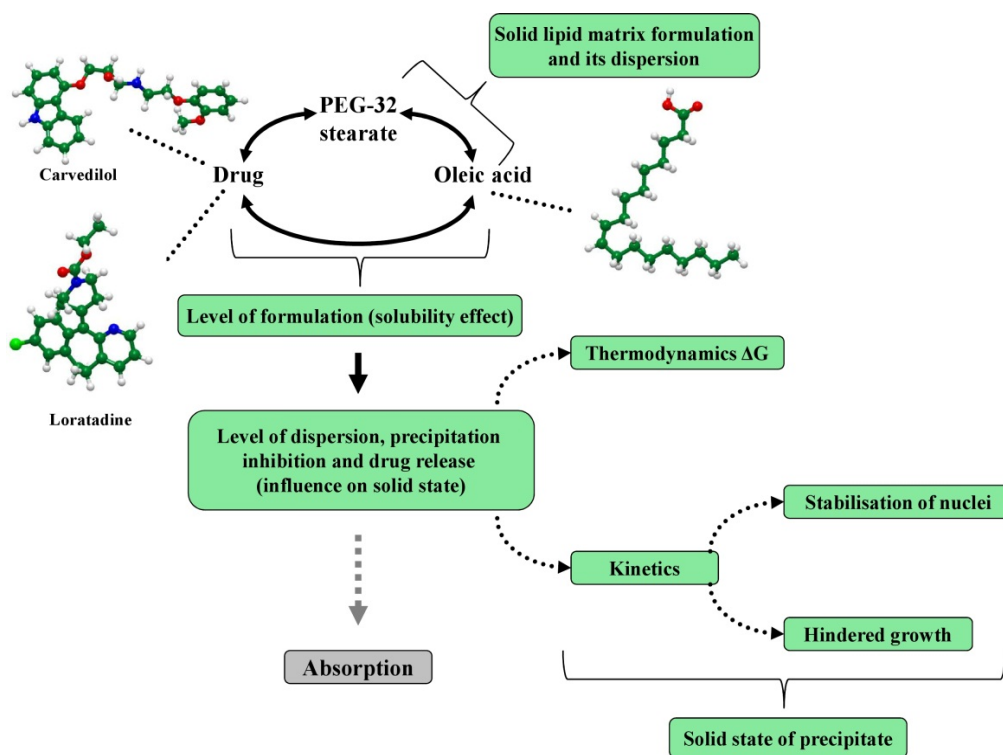


**Figure 5.1:** Scheme highlighting the different biopharmaceutical levels of formulation *in vitro* performance.

## **5.2. Materials and methods**

### **5.2.1. Materials**

Loratadine and carvedilol were purchased from AK Scientific Inc. (Union city, CA, USA) and PEG-32 stearate was a gift from Gattefosse SAS (Lyon, France). Oleic acid vegetable (extra pure) was supplied by Merck (Darmstadt, Germany). Sodium phosphate monobasic anhydrous and sodium hydroxide (pellets) were obtained from Sigma-Aldrich (Steinheim, Germany), hydrochloric acid (0.5 M) from J. T. Baker (Deventer, Holland), and potassium phosphate monobasic from Sigma-Aldrich (St. Louis, MO, USA). Acetonitrile of high-pressure liquid chromatography (HPLC) grade was purchased from Sigma-Aldrich Chemie GmbH (Buchs, Switzerland). The air-filled thermoplastic capsules (VegaGels<sup>®</sup>), used for the drug release testing (5.2.2.6.2.), were produced at Aenova facility at Swiss Caps AG (Kirchberg, Switzerland).

### **5.2.2. Methods**

#### **5.2.2.1. Preparation of solid systems**

Mixtures of PEG-32 S with OA at different weight ratios (10:0, 9:1, 8:2, 7:3, 6:4) were prepared by heating 20° C above their melting points, mixing and cooling to room temperature (RT). The other ratios of PEG-32 S and OA did not solidify and remained liquid or semisolid at RT, which were therefore not further considered in this study.

## **5.2.2.2. Characterization of solid systems**

### **5.2.2.2.1. X-ray diffraction (XRD)**

XRD of PEG-32 S and of PEG-32 S/OA mixtures was analysed at RT using a diffractometer Phaser D2 (Bruker, Karlsruhe, Germany) with LYNXEYE detector and the EVA software application. The source of radiation was Co K $\alpha$  at 30 kV, 10 mA, the measurement range was 5-50° 2 $\theta$  using a step size of 0.02° and a count time of 0.5 s per step. The sample was automatically rotated on a holder at 15 rpm. We also used XRD and polarizing light microscopy PLM (Olympus BX61, Tokyo, Japan) to determine the solid-state properties of precipitated drugs upon formulation dispersion in phosphate buffer.

### **5.2.2.2.2. Differential scanning calorimetry (DSC)**

The thermal characteristics of PEG-32 S and of the solid mixtures were determined using a differential scanning calorimetry (DSC 8500, Perkin Elmer, Santa Clara, CA, USA). Samples (average weight: 8 mg) were accurately weighed in hermetically sealed aluminium pans (50  $\mu$ L), held at initial temperature (20° C) for 5 min, and then heated at 10° C min<sup>-1</sup> from 20° C to 80° C under nitrogen gas purging (20 mL/min). We also used DSC to examine the drug-loaded formulations (saturation level  $S = 1.5$ ; *i.e.* 150% w/w of drug equilibrium solubility at 37° C) to detect any crystalline drug.

### **5.2.2.2.3. Particle size measurements following aqueous dispersion of solid systems**

The PEG-32 S and PEG-32 S/OA mixtures were dispersed in 0.025 M HCl (pH = 1.6), or in phosphate buffer (pH = 6.5) at 37° C to measure particle size. Dynamic laser light scattering was used with a Zetasizer Nano ZS (Malvern, Worcestershire, United Kingdom). Each sample was accurately weighed in a dust-free glass vial and 20 g of dispersion medium (heated at 37° C) was added (1:200 w/w). Prior to measurements, we mixed the dispersions for 10 min at 100 rpm in a water bath (37° C), and passed the

dispersions through a coarse filter (0.45  $\mu\text{m}$ ) to assure absence of dust particles. The mean particle size ( $Z$ -average diameter) of each dispersed sample was calculated from the volume size distribution. For these measurements aqueous viscosity provided a good approximation of the diluted dispersions. All experiments were repeated in triplicates from fresh samples. This method was also used to examine the particle size of dispersed drug-loaded PEG-32 S/OA (8:2 w/w) formulations (at saturation level  $S = 0.8$ ).

### **5.2.2.3. Spectroscopic and rheological characterization of drug-exciptient molecular interactions**

#### **5.2.2.3.1. UV spectroscopy**

The UV spectra of OA and of drug-OA mixtures were scanned using a SpectraMax M2e microplate reader (Molecular Devices, Sunnyvale, CA, USA). Both loratadine and carvedilol were mixed in dark glass vials with OA at 80% w/w of their  $S_{eq}$  (equilibrium solubility in OA at 37° C), purged with nitrogen, and left for one hour at 37° C while magnetically stirring (300 rpm). An aliquot (300  $\mu\text{L}$ ) of each sample was added to a 96-well microplate and UV spectra were recorded over a wavelength range of 200-700 nm. Additionally, UV spectroscopy was employed to examine the drug-OA molecular interactions in dispersed formulations (at saturation level  $S = 0.8$ ).

#### **5.2.2.3.2. Mechanical chip-based rheology**

The viscosity profiles of drug-OA mixtures were analysed using a new mechanical chip-based (MEMS) capillary rheometer (mVROC™ RheoSence, San Ramon, CA, USA). It measures the viscosity from the pressure drop of a sample as it flows through a rectangular slit. Each drug was dissolved in OA in dark glass vials at following concentrations: 0%, 5%, 10%, 15%, 20%, and 25% w/w. The mixtures were purged with nitrogen and left for one hour at 37° C on magnetic stirrers at 300 rpm. A glass syringe (Hamilton 81260 SYR 500  $\mu\text{L}$ ) was loaded with the sample and placed inside of the

thermal jacket ( $25 \pm 0.5^\circ \text{C}$ ). When the measurement temperature was stable, the sample was pumped to flow (at shear rate  $500 \text{ s}^{-1}$ ) through the channel of the chip. The pressure drop was detected by a sensor (cell m-VROC A-10) and the viscosity was calculated using the m-VROC Control Software™. All experiments were conducted in triplicates.

#### **5.2.2.3.3. FTIR**

The infrared spectra of the drugs, OA, and of both drug-OA mixtures (prepared as described in section 5.2.2.3.1.) were recorded using a Diamond ATR (attenuated total reflection) accessory (MKII Golden Gate™, Specac Inc, Woodstock, GA, USA) on a Bio-Rad Excalibur FTS 3000 MX spectrophotometer (Bio-Rad, Cambridge, MA, USA). The drug-OA interactions in dispersed formulations (at saturation level  $S = 0.8$ ) were also studied using FTIR. The analysis depth of the surface was approximately  $1 \mu\text{m}$  and all spectra were calculated from 32 scans, (each containing 2038 points) in the wavelength number range of  $645\text{-}4000 \text{ cm}^{-1}$ . Data were acquired with the Resolutions Pro software (version 5.2.0; Agilent Technologies, Santa Clara, CA, USA).

#### **5.2.2.4. Testing of the anhydrous drug-loaded solid systems**

##### **5.2.2.4.1. Van't Hoff solubility study**

The PEG-32 S/OA mixture (8:2 w/w), which upon dispersion resulted into the smallest particle size with lowest polydispersity index (PDI) was selected for the solubility study. Drug solubility was determined at different temperatures ( $55^\circ \text{C}$ ,  $60^\circ \text{C}$ ,  $65^\circ \text{C}$ , and  $70^\circ \text{C}$ ), and the value at  $37^\circ \text{C}$  was extrapolated using van't Hoff plots. An excess amount of loratadine or carvedilol was added to dark glass vial containing approximately 5 g of melted vehicle. The vials were tightly closed with rubber cap under nitrogen purging (2 min). The mixtures were then left on magnetic stirrers at 300 rpm in water baths at controlled temperatures for 72 h. We measured drug solubility after 24 h, 48 h, and 72 h to assure that equilibrium was reached. Samples were withdrawn, filtered through 0.45



$\mu\text{m}$  PVDF syringe filters (Titan3, SMI-LabHut LTD, Gloucester, UK), and diluted with phosphate buffer (20 mM, pH = 2.5; in weight ratios) for HPLC analysis. All solubility values were determined in triplicates.

Loratadine solubility in OA was measured directly at 37° C, and these samples were prepared as for the drug solubility studies in the vehicles. In contrast to that, it was not feasible to determine carvedilol solubility in OA at 37° C using magnetic stirring in glass vials, due to the high viscosity of the mixture. Therefore, an excess amount of carvedilol was added to Eppendorf® tubes (1.5 ml) containing OA, and the mixtures were shaken using a Thermomixer comfort (Eppendorf AG, Hamburg, Germany) at 1400 rpm and 37° C for 72 h. Every 24 h, samples were centrifuged ( $n = 3$ ) at 16 100 x g (37° C, 30 min) using a Centrifuge 5415 R (Eppendorf AG, Hamburg, Germany). Finally, the concentration of the compound in the supernatant was determined by HPLC analysis following dilution.

The maximum supersaturation ratios,  $SR^M$ , of the dispersed formulations in phosphate buffer (pH = 6.5) were calculated according to  $SR^M = C/C^*$ , where  $C$  is the maximum concentration of solubilized drug and  $C^*$  is the solubility in the dispersion of formulation in phosphate buffer (1:100 w/w), respectively (150).

#### **5.2.2.4.2. Drug loading of solid systems**

The drug-loaded systems were prepared as follows: The PEG-32 S and PEG-32 S/OA mixture (8:2 w/w) were heated 20° C above their melting point, and added to previously weighed drug in dust-free dark glass vials. Following a heating phase (1 h at 80° C while stirring with magnetic stirrer), the samples were cooled to RT (102). Drug loads are expressed as saturation levels ( $S$ ) referring to the equilibrium solubility of loratadine or carvedilol (in the formulation at 37° C), respectively.

### 5.2.2.5. Zeta potential measurements of dispersed drug-loaded solid systems

For measurements of zeta potential we used a Zetasizer Nano ZS (Malvern, Worcestershire, United Kingdom). The PEG-32 S/OA (8:2 w/w), drug-free and drug-loaded (at 80% w/w of  $S_{eq}$ ), were dispersed (1:200 w/w) in 0.025 M HCl (pH = 1.6) or in phosphate buffer (pH = 6.5) at 37° C for 10 min at 100 rpm. Each dispersed sample was passed through a coarse filter (0.45  $\mu$ m), poured in a transparent cuvette with electrodes at each ends, and inserted in a slit through which was laser beamed. As an electric field was applied to the cell, the Zetasizer measured the electrophoretic mobility of particles. The zeta potential was calculated and all measurements were done in triplicates at 37° C.

### 5.2.2.6. Drug precipitation testing upon dispersion and release from capsules

#### 5.2.2.6.1. Drug precipitation upon aqueous dispersion

Drug precipitation upon dispersion in phosphate buffer (pH = 6.5, 1:100 w/w) was analysed using a Lasentec FBRM D600L probe (Lasentec, USA). This laser scanning technique employs an in-process probe, which detects the chord length distribution of particles. The general measurement principle of focused beam reflectance measurements (FBRM) was described by Ruf *et al.* (81). The detection is limited to particles with a chord length 1  $\mu$ m. For calculation of the induction time, we monitored only chord length of less than 10  $\mu$ m in order to follow the number of evolving particles over time, while avoiding the noise from counts of aggregated particles. In contrast to that, when we studied the effect of OA on precipitation, all chord lengths and their particle size distributions (PSD) were considered. Both PEG-32 S and PEG-32 S/OA (8:2 w/w) were loaded with loratadine or carvedilol at the following saturation levels: 0.6, 0.7, 0.8, 0.9, 1.0, 1.1, 1.3, 1.5, and 1.7. Due to the ranges of interest, these saturation levels were non-equally distributed. The probe was positioned at an angle of 30° in a thermostated glass vessel (37° C) and the accurately weighed drug formulation was added to the dispersion medium. The dispersion was stirred at 500 rpm and the particle size of precipitated drug was recorded every 2 s for 8 h using the iC FBRM software (version 4.0; Mettler-Toledo

AutoChem, Columbia, MD, USA). All formulations were dispersed and measured in triplicates. From each precipitation curve, the onset time of crystalline precipitation (induction time,  $\tau_{ind}$ ) was determined at the crossing point of the tangent of the precipitation curve and the time axis. Subsequently, the Precipitation number ( $P_{nc}$ ) was defined for each saturation level as follows:

$$P_{nc} = \frac{t_{res}}{\tau_{ind}} \quad (5.1)$$

where  $t_{res}$  is a relevant drug residence time in the gastrointestinal tract (GIT) and is approximated with 180 min according to Amidon *et al.* (45).

#### 5.2.2.6.2. Drug release testing

Compendial release testing from soft capsules was determined regarding a potential effect of the different hydrodynamics or of the shell material on drug precipitation kinetics. Drug formulations (PEG-32 S and PEG-32 S/OA (8:2 w/w)) loaded with loratadine or carvedilol were studied both at saturation level of 1.5. A reciprocal cylinder BioDis<sup>®</sup> apparatus (RRT 8, CALEVA Ltd, Dorset, England) was thermostated at  $37 \pm 0.5^\circ \text{C}$ . Each vessel contained 200 mL of phosphate buffer (pH = 6.5). A mesh size of 420  $\mu\text{m}$  was selected (top and bottom mesh) for the glass cylinders that were dipping at a rate of 20 dpm. Two manually filled soft capsules were placed in each glass cylinder, due to their lower fill mass ( $\sim 0.6 \text{ g}$ ) compared to the capsules obtained from a machine-filling process ( $\sim 1.0 \text{ g}$ ). Prior to each experiment, the air-filled capsules were weighed before and after manual filling with the drug formulations to determine an exact fill mass in each capsule. At predetermined time points, a 1-mL sample was taken by a syringe, immediately filtered through a 0.45  $\mu\text{m}$  PVDF syringe filter (Titan3, SMI-LabHut LTD, Gloucester, UK) and analysed by HPLC. The removed volume was replaced each time with 1 mL of fresh medium. The total time of analysis was 180 min with respect to a relevant residence time of the drug in the GIT. All experiments were performed in triplicates.

### 5.2.2.7. HPLC method

High-performance liquid chromatography analysis employed a LiChrospher 60, RP select B 125-4 (5  $\mu\text{m}$ ) column (Merck, Darmstadt, Germany), a degasser (G1379 B), an isocratic pump (G1310A), an autosampler (G1329A), and a variable wavelength detector (G1314B). The mobile phase consisted of acetonitrile and 20 mM phosphate acetate buffer, pH = 2.5 (40:60, v/v). Flow rate was 1 mL/min with the injection volume of 10  $\mu\text{L}$  and the detection wavelengths were 248 nm and 280 nm for loratadine and carvedilol, respectively.

### 5.2.2.8 Data analysis

The temperature-dependent drug solubility in solid systems (PEG-32 S and PEG-32 S/OA (8:2 w/w)) was analysed at different temperatures with  $n = 3$ . The Statgraphics Centurion XVI ed. Professional Program from Statpoint Technologies Inc. (Warrenton, Virginia, USA) was used for van't Hoff linear regression and prediction of the drug solubility at 37° C. A good correlation was assumed if the  $R^2$  value was higher than 0.99.

## 5.3. Results

### 5.3.1. Characterization of solid drug-free systems

In preliminary experiments, OA was incorporated in PEG-32 S at different w/w ratios to determine the physical consistency of the mixtures at RT. Visual observation of the mixtures (stored for two days at RT) indicated that when the concentration of OA was not higher than 40% w/w, the mixtures solidified and no phase separation occurred, whereas higher concentrations of the liquid OA were deemed less suitable for a solid lipid-based formulation.

### 5.3.1.1. X-ray diffraction (XRD)

Figure 5.2 displays x-ray diffractograms of PEG-32 S and PEG-32 S/OA mixtures. The presence of peaks in the mixtures at the same angle ( $2\theta$ ) as those of PEG-32 S confirmed that crystallinity of PEG-32 S was maintained in the formulations. We observed a gradual decrease in peak heights as the concentration of OA increased. This can be interpreted as lowering the concentration of crystalline lipid phase by increasing the amount of OA. The extent of crystallinity of PEG-32 S in PEG -2 S/OA mixtures could be approximated by the crystallite size(s). Determination of crystallite size(s) from XPD patterns are based on the widths of the diffraction peaks but due to the complexity of added OA, this task was beyond the scope of the present work. However, observations made by Patel *et al.* (151) could suggest that the addition of OA results in decrease of the crystallite size.

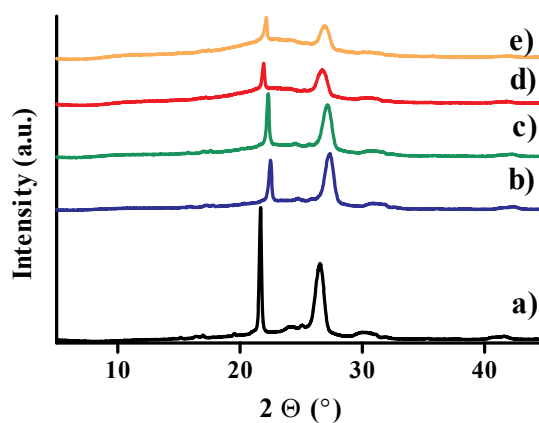


**Figure 5.2:** X-ray diffraction patterns of the solid systems containing different concentrations of oleic acid in PEG-32 S/OA mixtures (w/w). Oleic acid concentrations: (a) 0%, (b) 10%, (c) 20%, (d) 30%, and (e) 40% (w/w).

### 5.3.1.2. Differential scanning calorimetry (DSC)

The DSC thermogram of PEG-32 S exhibited a characteristic endothermic peak at 47° C (Figure 5.3a). We observed a gradual decrease in the onset of melting endotherms (Figure

5.3), as the concentration of OA in the mixtures with PEG-32 S increased. Similar changes were also observed for the melting peak maximum of the mixtures.

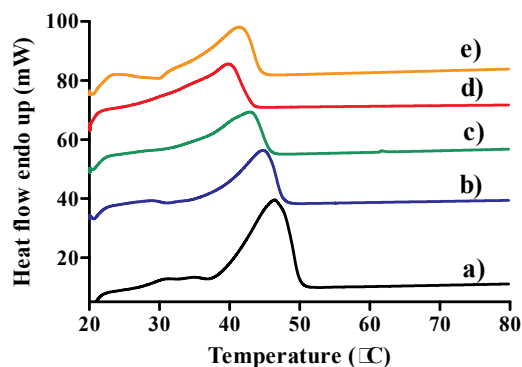


**Figure 5.3:** Differential scanning calorimetry (DSC) thermograms of the solid systems containing different concentrations of OA in PEG-32 S/OA mixtures (w/w). Oleic acid concentrations: (a) 0%, (b) 10%, (c) 20%, (d) 30%, and (e) 40% (w/w).

### 5.3.1.3. Particle size measurements following aqueous dispersion of solid systems

To select the optimal ratio of PEG-32 S and OA, we considered aqueous formulation dispersions. A minimal particle size and polydispersity index of prepared dispersions of PEG-32 S/OA mixtures were viewed as desirable from a biopharmaceutical viewpoint. Two aqueous media were selected that were mimicking an acidic stomach environment and an intestinal pH. As evident from the Figure 5.4, PEG-32 S : OA w/w ratio had a substantial influence on both particle size and polydispersity. The dispersed mixture with 20% w/w OA exhibited the smallest particle size, as well as the lowest polydispersity, in both dispersion media and was therefore selected for further evaluations.

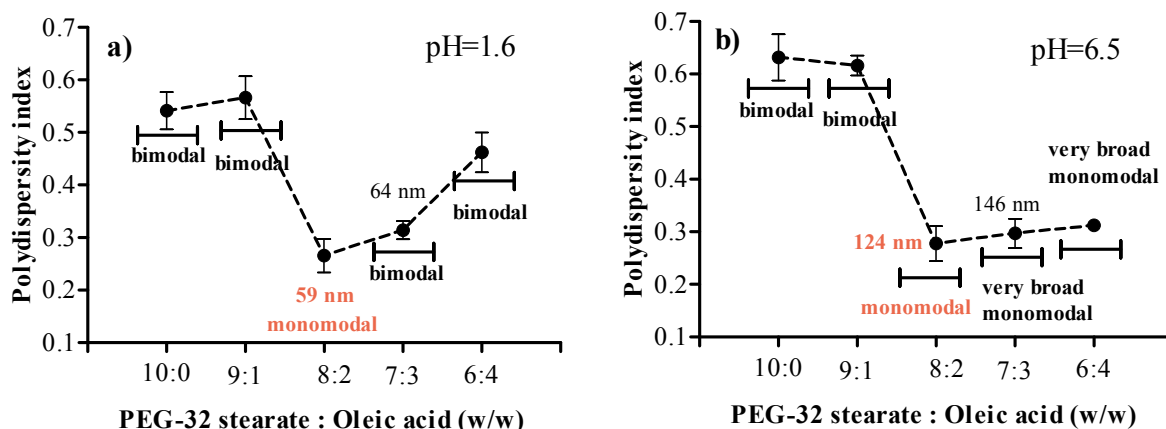


**Figure 5.4:** Effect of PEG-32 S : OA ratio on particle size and polydispersity index (PDI) analysed in (a) 0.025 M HCl (pH = 1.6) and in (b) phosphate buffer (pH = 6.5) ( $n = 3$ ). The particle size is specified only for systems with a PDI  $\leq 0.3$ .

### 5.3.2. Characterization of solid drug-loaded systems

#### 5.3.2.1. Drug-excipient interaction in oily mixtures

Loratadine and carvedilol typically absorb in organic solvents (*e.g.* methanol) at 288 nm and at 242 nm, respectively (152, 153). In the present study both drugs were dissolved in OA and a considerable shift in the peak maxima and a broadening of the UV bands, compared to the pure OA was revealed (Figure 5.5a). This indication of a molecular interaction between the excipient and the basic drugs was also supported by a rheological study. An increase in viscosity was noted for rising amounts of drug (Figure 5.5b). The oily system was probably becoming a partially organized system due to the interaction, which was more pronounced in the case of carvedilol- compared to loratadine-OA solutions. These findings indicated a molecular complex in oily mixtures.

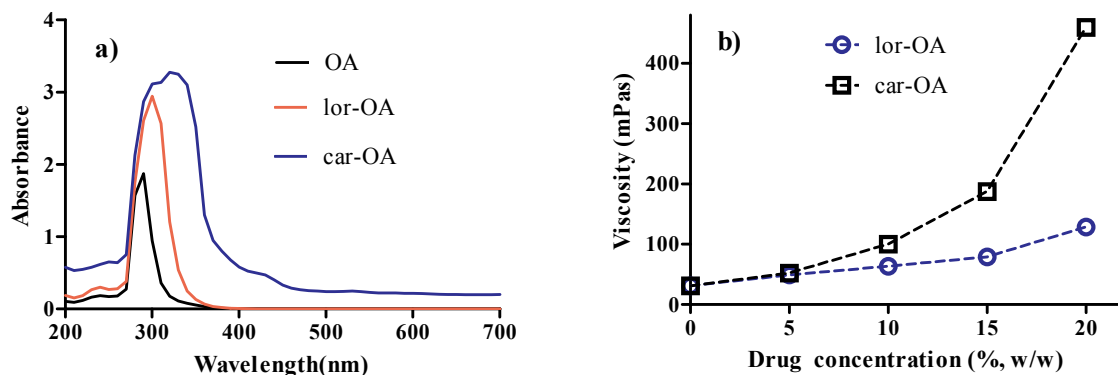


**Figure 5.5:** Shift of the maximum in UV spectrum and a broadening of the UV bands (a), and increase in viscosity profiles (b) indicate the presence of loratadine-OA and carvedilol-OA molecular complexes ( $n = 3$ , error bars are within markers).

The IR spectrum of OA showed characteristic vibrational bands at  $1700\text{ cm}^{-1}$  (C=O stretching vibrations) and at  $3000\text{-}2700\text{ cm}^{-1}$  (O-H stretching vibrations) (Figure 5.6). No changes for hydroxyl group band were observed in both spectra of drug-OA molecular complexes (lor-OA and car-OA). In contrast to that, the drug-OA interaction could be proposed from the changes of both drug spectra. In lor-OA spectrum we noted shifting and broadening of the characteristic bands at  $1200\text{ cm}^{-1}$  and  $1700\text{ cm}^{-1}$ , which represent stretching vibrations of C-O and C=O, respectively. Broadening/shifts of bands around  $1200\text{ cm}^{-1}$  could also indicate changes in amine ( $1250\text{-}1020\text{ cm}^{-1}$ ) and aromatic amine ( $1342\text{-}1266\text{ cm}^{-1}$ ) groups of loratadine. Additionally, changes in the  $1700\text{ cm}^{-1}$  region could be attributed to the stretching of the C=N group. This could suggest that the “basic” groups of the drug were also involved in some kind of interactions with OA, most probably hydrogen bonds with carboxyl groups of OA. In case of carvedilol, the relevant N-H bonds at  $1600\text{ cm}^{-1}$  and below  $3500\text{ cm}^{-1}$  practically disappeared in car-OA spectrum. Moreover, the car-OA spectrum displayed the changes in the region between  $1200\text{ cm}^{-1}$  and  $1000\text{ cm}^{-1}$  that correspond to C-O stretching in ethers and primary



alcohols. Both of these changes strongly indicate the interaction between ether and amino groups in carvedilol and carboxyl group of OA.

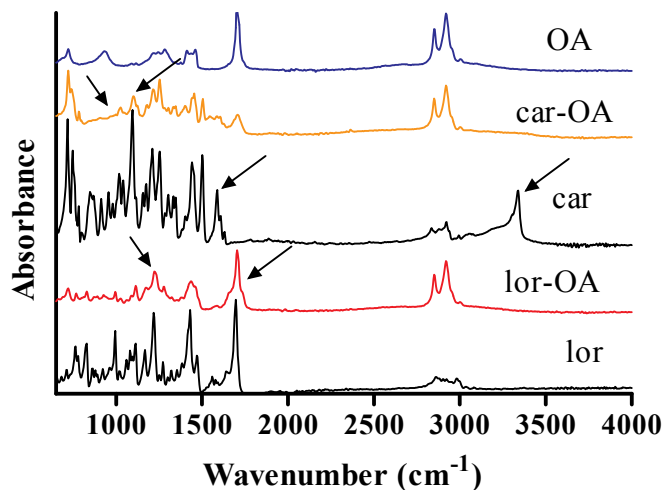


**Figure 5.6:** FTIR spectra of loratadine, carvedilol, OA and of their binary drug-OA mixtures (bands of interest are indicated by arrows).

### 5.3.2.2. Solubility study

PEG-32 S and PEG-32 S/OA (8:2 w/w) were solid at RT as well as at 37° C. To determine the drug solubility in these solid systems, it was measured at elevated temperatures and extrapolated to lower temperature by the van't Hoff model (Figures 5.7 and 5.8) (154). The extrapolated solubility at a temperature of 37° C was of interest regarding the biopharmaceutical fate of the formulation.

Table 5.1 displays the extrapolated drug solubility values in PEG-32 S and PEG-32 S/OA (8:2 w/w), as well as the drug solubility in OA determined at 37° C. OA demonstrated remarkable drug solubility for both loratadine and carvedilol.

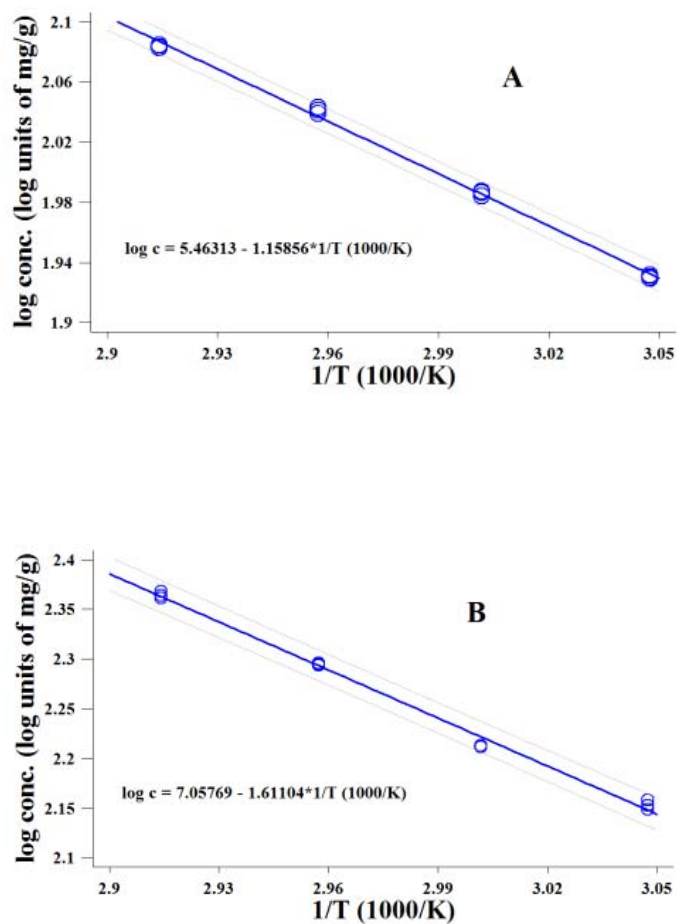


**Figure 5.7:** Plot of van't Hoff model of loratadine solubility in (a) PEG-32 S (linear regression,  $R^2= 0.9969$ ;  $p<0.05$ ) and in (b) PEG-32 S/OA (8:2 w/w) (linear regression,  $R^2= 0.9944$ ;  $p<0.05$ ). Outer lines show 95% prediction limits.

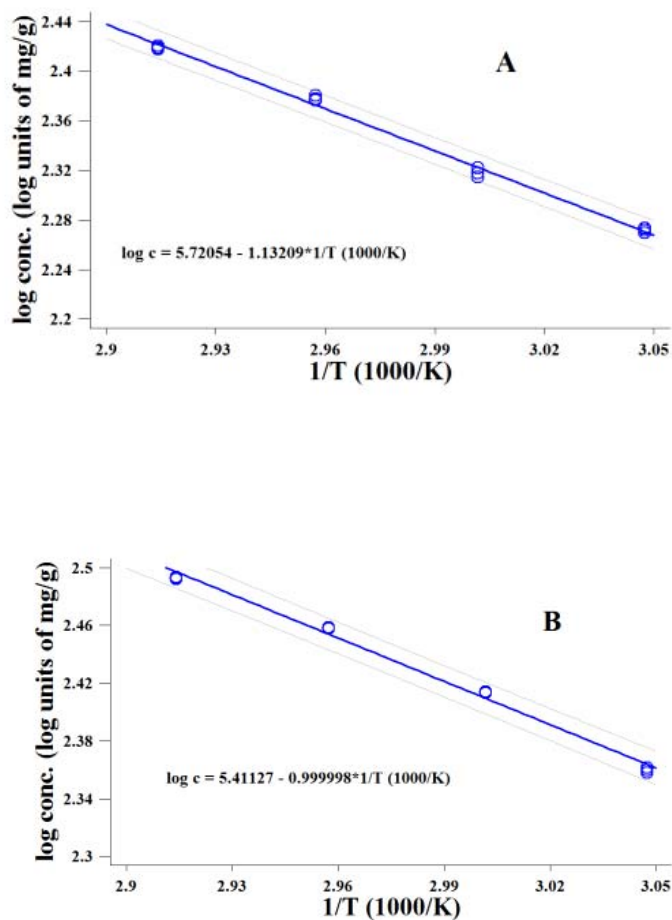


**Figure 5.8:** Plot of van't Hoff model of carvedilol solubility in (a) PEG-32 S (linear regression,  $R^2 = 0.9944$ ,  $p < 0.05$ ) and in (b) PEG-32 S/OA (8:2 w/w) (linear regression,  $R^2 = 0.9927$ ,  $p < 0.05$ ). Outer lines show 95% prediction limits.

**Table 5.1:** Comparison of carvedilol and loratadine solubility in PEG-32 S, OA, and PEG-32 S/OA (8:2 w/w) at 37° C.

	Solubility (mg/g)	
	Carvedilol	Loratadine
PEG-32 S *	117.7 ± 4.8	53.4 ± 1.7
OA	372.8 ± 11.3	253.2 ± 0.5
PEG-32 S/OA (8:2 w/w)*	153.9 ± 6.5	73.1 ± 4.3

\* extrapolated by linear van't Hoff regression from higher temperatures

Following solubility study, drug-loaded formulations at different saturation levels were prepared. The formulations loaded with drugs at supersaturated level ( $S = 1.5$ ) were analysed using DSC for the presence of crystalline drugs. The characteristic drug melting peaks in all tested formulations were not observed (Figure 5.9), which confirmed the absence of crystalline drug.

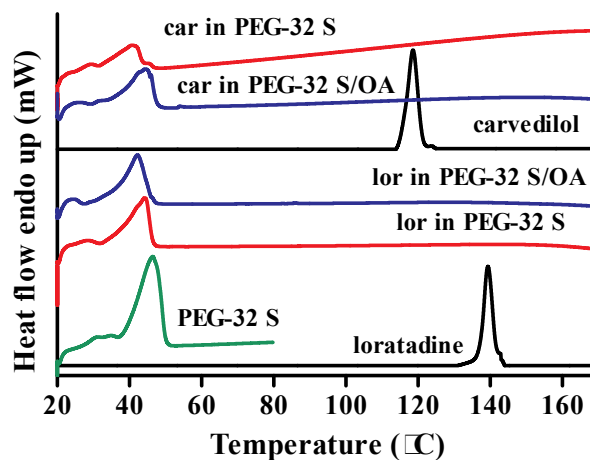


**Figure 5.9:** Differential scanning calorimetry (DSC) thermograms of the supersaturated solid lipid-based formulations ( $S = 1.5$ ) show the absence of the crystalline drug 2 h upon loading.

Drug-loaded PEG-32 S/OA formulations ( $S = 0.8$ ) were analysed for the particle size following aqueous dispersion. In contrast to the dispersed drug-free formulation, an increased polydispersity index (PDI = 0.4 for pH = 1.6, and PDI = 0.32 for pH = 6.5) and similar  $Z$ -average were observed for all examined dispersion. This indicated that the presence of the drug probably disturbed the optimized structure of the drug-free system.

### 5.3.3. Zeta potential measurements of dispersed drug-loaded systems

To explore the drug-OA interactions during an aqueous dispersion process, UV/FTIR spectroscopy and zeta potential were employed using drug-loaded and drug-free formulations. UV spectra of all drug-free and drug-loaded dispersed systems demonstrated no significant shift of the peak maximum, indicating probably a different quality of the drug-OA interactions (data not shown). Regarding FTIR, recorded spectra did not show any representative band either of the drugs or of oleic acid, suggesting that the analysis was not sensitive enough for this high dilution ratio. Therefore, we studied zeta potential of the dispersed systems (Table 5.2). Loratadine is a weak base ( $pK_a = 4.33$ ) and is expected to have a neutral form in phosphate buffer (pH = 6.5). The zeta potential of dispersed lor-PEG-32 S/OA in phosphate buffer was negative. The result was similar to the negative zeta potential of the drug-free formulation under the same conditions. In contrast to that, the dispersed carvedilol-loaded formulation (car-PEG-32 S/OA; carvedilol  $pK_a = 8.74$ , OA  $pK_a = 9.85$  (155)) resulted in a neutral zeta potential in phosphate buffer. A positive zeta potential was determined in 0.025 M HCl for both drug formulations, which was in line with the expected protonation and charge of the basic drugs at such a low pH. For the drug-free system dispersed in the acidic medium (HCl) zeta potential was almost neutral.

**Table 5.2:** Zeta potential of drug-free and drug-loaded PEG-32 S/OA (8:2 w/w), dispersed (1:200 w/w) in phosphate buffer (pH = 6.5) and 0.025 M HCl (pH=1.6) at 37° C.

	Zeta potential (mV)		
	PEG-32 S/OA (8:2 w/w)	PEG-32 S/OA (8:2 w/w) loaded with loratadine ( $S = 0.8$ )	PEG-32 S/OA (8:2 w/w) loaded with carvedilol ( $S = 0.8$ )
<b>Phosphate buffer (pH = 6.5)</b>	$-7.9 \pm 1.0$	$-6.6 \pm 1.5$	$-0.1 \pm 0.1$
<b>0.025 M HCl (pH = 1.6)</b>	$-0.8 \pm 0.5$	$3.9 \pm 0.5$	$11.2 \pm 0.4$

### 5.3.4. Drug precipitation testing upon dispersion and release from capsules

#### 5.3.4.1. Drug precipitation upon aqueous dispersion

We monitored drug precipitation by means of FBRM upon formulation dispersion in phosphate buffer (pH = 6.5). As a control, drug-free PEG-32 S and PEG-32 S/OA (8:2 w/w) were also dispersed, but either no FBRM signal or a very low signal (up to 50 counts) was detected. The drug-containing dispersion samples were analysed to determine the induction times that marked the onset of drug precipitation. Results for the dispersions of the formulations without OA are depicted in Figure 5.10. A decrease in the induction time was observed for both drugs with rising drug saturation. For loratadine loaded in PEG-32 S, the lowest saturation level in the anhydrous formulation to exhibit precipitation upon dispersion was 0.7 (considering 8 h limit of measurement). The corresponding results of carvedilol showed that only at a (formulation) drug saturation of 0.9 and beyond, there was a precipitation detected within the observation time.

Considering the physiologically relevant residence time of 180 min, it was possible to extrapolate a critical formulation saturation level for which drug precipitation is expected. These critical values were about 0.65 for the formulation of loratadine and 0.85 in case of the PEG stearate mixture with carvedilol.

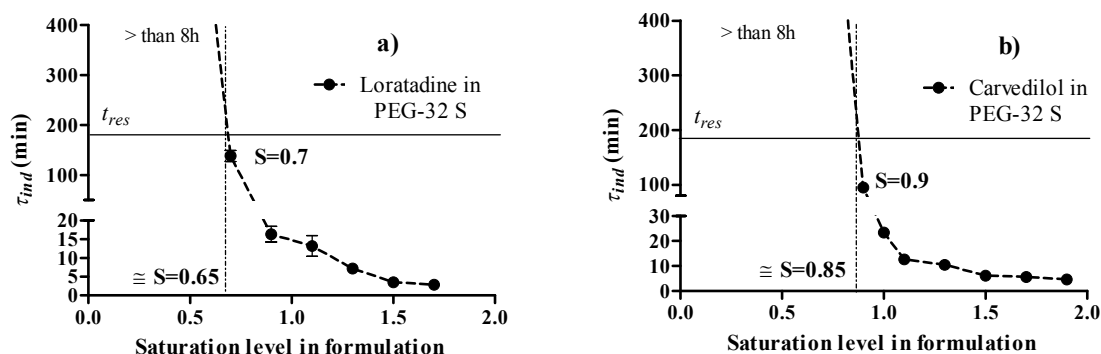


**Figure 5.10:** Effect of different saturation levels in the anhydrous formulation of (a) loratadine and (b) carvedilol on the induction times upon dispersion (pH = 6.5). The horizontal line presents a relevant residence time  $t_{res}$  (180 min) of the drug in the gastrointestinal tract. The vertical line determines the critical saturation level in the formulation for which drug precipitation starts within  $t_{res}$ .

Subsequently, dispersions of PEG-32 S/OA (8:2 w/w) were analysed to explore the effects of OA on drug precipitation. Formulations of both drugs did not show any precipitation in the range of unsaturated formulations. This marked effect of OA as potential precipitation inhibitor was also of interest to explore with supersaturated systems. A reference drug saturation of 1.5 was selected and FBRM results of the dispersions can be inferred from Figure 5.11. The particle size distribution (PSD) profiles from the supersaturated systems indicated that incorporation of 20% w/w of OA lowered the extent of drug precipitation but could not prevent it entirely. This effect was more pronounced in case of carvedilol formulations, as illustrated by Figure 5.11b. The chord length counts were greatly reduced

in the formulation containing OA and the maximum particle size may have been slightly shifted to  $\sim 10 \mu\text{m}$  (at  $t = 3\text{h}$ ). In case of loratadine, particle size distributions appeared to be very similar for both tested formulations (Figure 5.11a). Addition of OA demonstrated also in this system a reduction in the extent of drug precipitation.

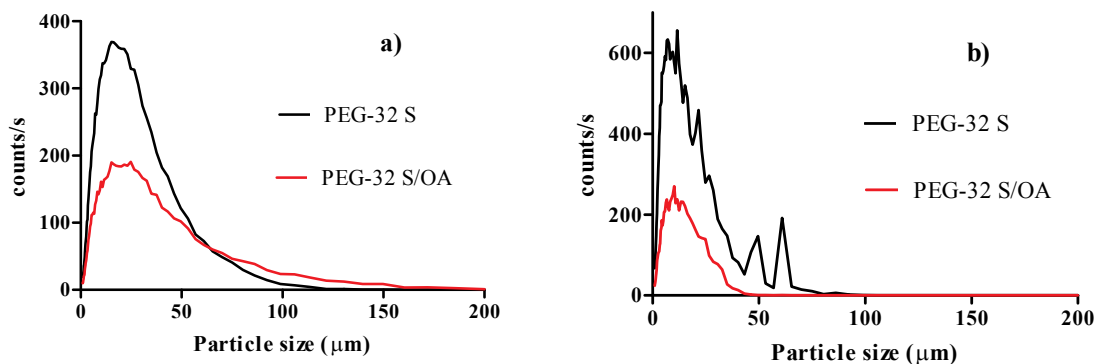


**Figure 5.11:** Mean particle size distribution (PSD) profiles observed at  $t = 3\text{h}$  upon dispersion of solid lipid-based formulations loaded with (a) loratadine and (b) carvedilol at  $S = 1.5$ .

The reference formulation at a drug saturation level of 1.5 was further explored regarding time evolution of particle counts. Counting of primarily short chord lengths ( $< 10 \mu\text{m}$ ) focused on the early particle growth phase with minimal noise from potential aggregates. Interestingly, a spontaneous nucleation was observed for both drugs loaded in PEG-32 S/OA (8:2 w/w). Figure 5.12a shows the precipitation kinetics of the dispersed loratadine formulation ( $S = 1.5$ ). A high initial count rate was detected that slowed down to a much lower plateau as compared to the formulation without OA. Also carvedilol in PEG-32 S/OA (8:2 w/w) ( $S = 1.5$ ) demonstrated only a high initial rate that was followed by almost constant count rates after about 20 min. The count rate plateau from this OA-containing formulation was again substantially lower than observed with carvedilol-loaded PEG-32 S. Interestingly, these mixtures of PEG stearate and drugs did not



precipitate spontaneously, but appeared to have short induction times. Therefore OA influenced the extent of drug precipitation and also the type of its kinetics.

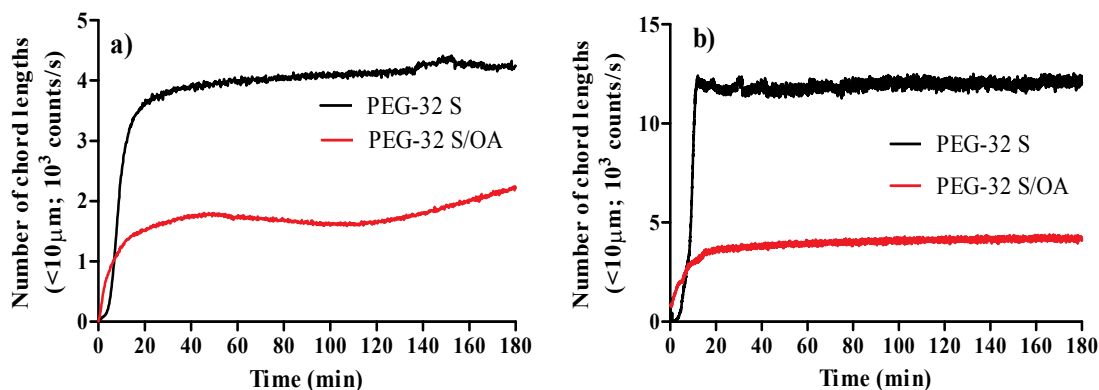


**Figure 5.12:** The effect of the drug-OA interaction on the type of precipitation kinetics of (a) loratadine and (b) carvedilol, both loaded at saturation level of 1.5 in PEG-32 S and PEG-32 S/OA (8:2 w/w), respectively.

Regarding oral drug delivery it was important to also analyse the solid-state properties of the precipitated drugs. Figure 5.13 displays the X-ray diffraction patterns of the precipitates and of crystalline drugs as used in the solid formulations ( $S = 1.5$ , at  $t=3h$ ). These X-ray patterns demonstrated that both drugs maintained their crystallinity following the precipitation of dispersed drug-loaded PEG-32 S. These precipitates were also investigated by polarizing light microscopy and no different crystal morphology was observed. We noticed birefringent needles and cubic shapes for loratadine and carvedilol precipitates, respectively. This situation was in contrast to adding OA, since the drug

precipitates from the dispersed PEG-32 S/OA (8:2 w/w) systems were amorphous according to X-ray patterns (Figure 5.13). However, in the case of loratadine precipitate some isolated crystals were also observed under polarized microscope, while no crystalline drug was found in the carvedilol precipitate. The amorphous precipitates demonstrated that OA not only changed the type of precipitation kinetics, but also influenced the solid state of both drugs upon dispersion.

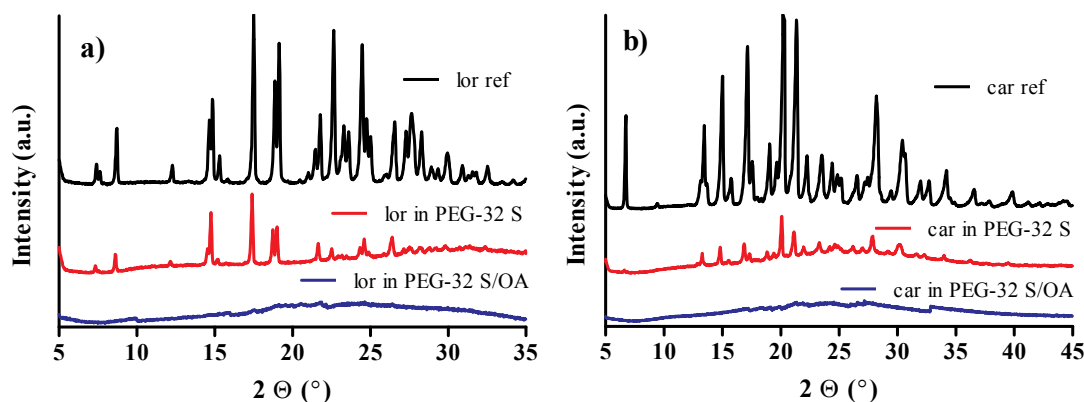


**Figure 5.13:** X-ray diffraction patterns of (a) loratadine powder as reference (black line), loratadine precipitated from PEG-32 S (red line), and from PEG-32 S/OA (blue line), and (b) carvedilol powder as reference (black line) and carvedilol precipitated from PEG-32 S (red line), and from PEG-32 S/OA (blue line). All solid formulations were supersaturated ( $S = 1.5$ ) and the precipitated drugs were analysed following 3 h of dispersion in phosphate buffer (pH = 6.5).

Tables 5.3 and 5.4 provide an overview of the drug saturation levels studied for their precipitation kinetics. For calculation of maximum supersaturation ratios ( $SR^M$ ) (150) determination of the equilibrium drug solubilities in the dispersion medium was needed. This solubility of loratadine was  $0.25 \pm 0.01$  mg/mL and  $0.52 \pm 0.02$  mg/mL for the dispersion medium containing PEG-32 S and PEG-32 S/OA (8:2 w/w), respectively. For carvedilol, the corresponding solubilities were  $0.91 \pm 0.03$  mg/mL and  $1.68 \pm 0.06$  mg/mL, respectively. Additionally, for each studied saturation level, the Precipitation number ( $P_{nc}$ ) was determined according to Eq. 5.1. This number assessed the biopharmaceutical relevance of a supersaturation following dispersion of a formulation. However, it is very important to note that we were focusing only on crystalline precipitates because amorphous precipitates were deemed as less problematic for drug absorption (102). For both drugs loaded in PEG-32 S, precipitation upon dispersion started already with anhydrous formulations below saturation. A critical saturation level was here for loratadine 0.7 and 0.9 for carvedilol. Observed drug precipitation within a relevant physiological time span was reflected by precipitation numbers becoming higher than unity as seen in Table 5.3 and 5.4.

**Table 5.3:** Loratadine doses, corresponding saturation levels of the anhydrous formulations, calculated maximum supersaturation ratios ( $SR^M$ ), and Precipitation numbers ( $P_{nc}$ ) used for the drug precipitation analyses.

<b>Model formulation</b>	<b>Dose (mg/g)</b>	<b>Saturation level in anhydrous formulation (<math>S</math>)</b>	<b>Maximum supersaturation ratio (<math>SR^M</math>) upon dispersion</b>	<b>Precipitation number (<math>P_{nc}</math>)</b>
<b>Loratadine in PEG-32 S</b>	32.0	0.6	1.3	< 1 (< 0.38)
	<b>37.4</b>	<b>0.7</b>	<b>1.5</b>	<b>&gt;1 (1.31 ± 0.10)</b>
	48.1	0.9	1.9	> 1 (11.15 ± 1.51)
	58.8	1.1	2.4	> 1 (14.08 ± 2.95)
	69.4	1.3	2.8	> 1 (25.63 ± 4.41)
	80.0	1.5	3.2	> 1 (52.14 ± 7.53)
	90.8	1.7	3.6	> 1 (64.00 ± 6.93)
<b>Loratadine in PEG-32 S/OA</b>	58.5	0.8	1.2	< 1
	65.8	0.9	1.3	< 1
	<b>80.4</b>	<b>1.1</b>	<b>1.6</b>	*
	95.0	1.3	1.9	*
	109.6	1.5	2.2	*
	124.3	1.7	2.5	*

\* Different type of kinetics and an amorphous precipitate.

**Table 5.4:** Carvedilol doses, corresponding saturation levels of the anhydrous formulations, calculated maximum supersaturation ratios ( $SR^M$ ), and Precipitation numbers ( $P_{nc}$ ) used for the drug precipitation analyses.

Model formulation	Dose (mg/g)	Saturation level in anhydrous formulation ( $S$ )	Maximum supersaturation ratio ( $SR^M$ ) upon dispersion	Precipitation number ( $P_{nc}$ )
<b>Carvedilol in PEG-32 S</b>	94.2	0.8	1.0	<1 (< 0.38)
	<b>105.9</b>	<b>0.9</b>	<b>1.2</b>	<b>&gt; 1 (1.97 ± 0.16)</b>
	117.7	1.0	1.3	> 1 (7.74 ± 0.50)
	129.5	1.1	1.4	> 1 (14.36 ± 1.81)
	153.0	1.3	1.7	> 1 (17.17 ± 0.82)
	176.5	1.5	2.0	> 1 (29.37 ± 2.91)
	200.1	1.7	2.2	> 1 (32.14 ± 4.18)
223.6	1.9	2.5	> 1 (39.24 ± 6.17)	
<b>Carvedilol in PEG-32 S/OA</b>	153.9	1.0	0.9	< 1
	<b>169.3</b>	<b>1.1</b>	<b>1.0</b>	*
	200.1	1.3	1.2	*
	230.9	1.5	1.4	*
	261.6	1.7	1.6	*
292.4	1.9	1.7	*	

\* Different type of kinetics and an amorphous precipitate.

#### 5.3.4.2. Drug release testing

Initial release tests (USP 3 apparatus) used anhydrous formulations with PEG-32 S or PEG-32 S/OA (8:2 w/w) that were below drug saturation. For both drug release tests, no drug precipitation was revealed (data not shown). It must be noted that the given aqueous formulation dilution (1:160 w/w), specific hydrodynamics, as well as the capsule made a difference to the dispersion experiments using FBRM. It was hence of primary interest to compare the formulations at a supersaturated reference level of 1.5. Figure 5.14 displays the drug release profiles of the formulations for the model drugs loratadine and carvedilol.

Both drugs precipitated during the drug release testing and clear differences were obtained in the kinetic profiles. A fast dispersion was observed with the different formulations once the thermoplastic capsules opened. Therefore, systems had in common that the maximum drug concentration was reached within 30 min (Figure 5.14). The OA-containing system reached a maximum of released drug at 90% for loratadine and for carvedilol it could be it levelled off at 70%. This plateau level of the drug concentration remained constant during the 3 h of analysis. In contrast to that, the maximum of released drug for PEG-32 S formulations was reached at around 60%, followed by fast drug precipitation and lowering of the drug concentration to 30% and 40% in case of loratadine and carvedilol, respectively. The resulting maximum supersaturation ratios ( $SR^M$ ) for both drugs during release testing were also calculated. For loratadine  $SR^M$  values were 3.2 and 2.1 for the PEG-32 S formulation and OA-containing formulation, respectively. For carvedilol, the corresponding values were 2.0 and 1.4, respectively.

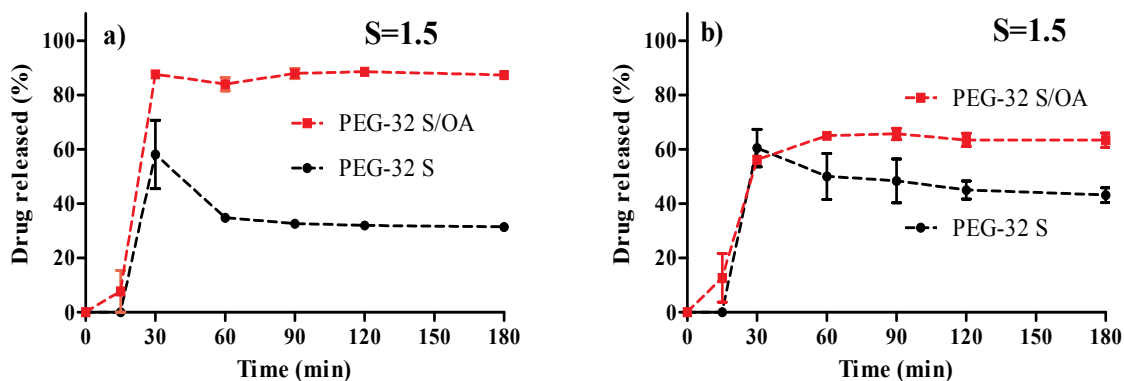


**Figure 5.14:** Drug release profiles of (a) loratadine, and (b) carvedilol, formulated in PEG-32 S and PEG-32 S/OA (8:2 w/w) and encapsulated in VegaGels<sup>®</sup>, analysed in USP 3 apparatus in phosphate buffer (pH = 6.5), 20 dpm, at  $37 \pm 0.5^\circ \text{C}$  ( $n = 3$ ).

## 5.4. Discussion

Mechanistic understanding of drug-excipient interactions on different biopharmaceutical levels could be a way to better develop oral dosage forms. However, until now there has been a lack of systematic studies of drug-excipient interactions in solid lipid-based systems. As detailed in Figure 5.1, we focused on OA interactions with basic drugs in the anhydrous formulation, upon aqueous dispersion, and particularly with respect to precipitation kinetics and the evolving solid state of the precipitate.

### 1) Level of the anhydrous formulation

Firstly, we developed the solid system containing PEG-32 S and OA in optimal ratio (8:2 w/w), which demonstrated optimal dispersion with respect to particle size and polydispersity. The reduction of particle size could indicate forming of mixed micelles

that may be beneficial for robust drug absorption. We targeted smallest particle sizes, as it proved to be relevant for enhanced bioavailability of some PWSD (72). However, such size effects may not always be relevant for drug bioavailability (71).

Secondly, we characterized the drug-OA interactions in oily mixtures. It is well known that the intermolecular forces are often strong enough to control physical properties such as viscosity (156). This effect was also confirmed in the present study. Namely, the pronounced intermolecular forces between OA and the basic drugs caused an increasing viscosity with rising amounts of both drugs (Figure 5.5a). The molecular interactions between OA and the model bases were also supported by the results of the spectroscopic studies. The shift and the broadening of the UV band of drug-OA mixtures clearly indicated interactions between the two components. The nature of the drug-OA interactions was further characterized using FTIR spectroscopy. As displayed in Figure 5.6, there were no changes in the band of the hydroxyl group of OA ( $3000\text{-}2700\text{ cm}^{-1}$ ). This could be attributed to the higher OA content in the mixtures ( $\sim 1\text{:}5$  w/w drug : OA ratio). A first intuitive assumption is that organic bases (drug) interact with organic acids (OA) *via* amino and carboxyl groups, where amino groups act as a proton acceptor and carboxyl groups as a proton donor. However, the complex systems such these may exhibit more complex interactions. Tertiary amines (as in loratadine) show no characteristic bands, but in case of their protonation, they would become secondary and the matching bands would appear. In the present study this was clearly not the case. We observed in the lor-OA spectrum shifting and broadening of the characteristic bands at  $1200\text{ cm}^{-1}$  and  $1700\text{ cm}^{-1}$ , which showed stretching vibrations of C-O and C=O, respectively. This can indicate hydrogen bonds between OA and both carboxyl groups of loratadine. Similar observations were also reported by Nacsa *et al.* in 2008 in a study of loratadine interacting with a cyclodextrin (157). As the oxygen atoms of loratadine are not sterically hindered, it could be expected that they were more exposed to an interaction compared to a basic nitrogen atom within the rings. Moreover, the point charge of the basic nitrogen in the pyridine ring was similar to the oxygen atoms (calculated using chemicalize.org,



ChemAxon Ltd., Hungary). Our findings therefore point to the well accessible oxygen groups of loratadine that interact with OA. However, broadening/shifts of IR bands in the same region (around  $1200\text{ cm}^{-1}$  and  $1700\text{ cm}^{-1}$ ) could also indicate changes in amine and the stretching of the (aromatic) C=N group. Therefore, it could not be excluded that the “basic” groups of loratadine were also involved in the interactions with OA, especially since OA was in excess in the lor-OA mixture. In case of carvedilol, the relevant N-H bonds at  $1600\text{ cm}^{-1}$  and below  $3500\text{ cm}^{-1}$  disappeared in the car-OA spectrum. Moreover, we observed the changes in the region between  $1200\text{-}1000\text{ cm}^{-1}$ , which correspond to C-O stretching in ethers and primary alcohols. In a classical sense, this could be interpreted as deprotonation of N-H groups and change of environment around C-O groups. Thus, spectroscopic results indicate several possible intra- and intermolecular interactions of drug and OA.

The drug-OA interactions were also observed with respect to the increased drug solubility. The excipient demonstrated a substantial influence on both loratadine and carvedilol solubility (Table 5.1). These results are in line with the observations reported by Patel *et al.* for lumefantrine-OA formulations (158). In summary, our findings indicate that the strong drug-OA interactions can be viewed as molecular complex formations on the level of the anhydrous formulation.

## 2) Level of dispersion, precipitation inhibition and drug release

To better understand the drug-OA interactions following aqueous dispersion, we studied zeta potential of dispersed drug-free and drug-loaded formulations in acidic environment ( $\text{pH} = 1.6$ ) and at an intestinal  $\text{pH}$  of 6.5 (Table 5.2). At the low  $\text{pH}$ , both drug bases were protonated, which resulted in a positive zeta potential of their dispersions and indicated that both drugs were associated with the surface of micelles. In the same acidic medium dispersion of drug-free formulation exhibited an almost neutral zeta potential probably because any fatty acids on the surface would be in neutral form. In phosphate buffer, zeta

potential of the dispersed drug-free formulation was slightly negative, which is a common observation for dispersed glyceride oils or other systems with low dielectric constant. Zeta potential of the dispersed loratadine-containing formulation was also slightly negative, reflecting the neutral form of the weak base ( $pK_a = 4.33$ ). For the dispersed carvedilol-loaded formulation (carvedilol  $pK_a=8.74$ ), the net charge was almost neutral. Here, the negative charge observed with the drug-free formulation was probably suppressed by the presence of protonated carvedilol at the surface of the micelles. Thus, a fraction of protonated drug was evidently interacting with the colloidal surfaces, while some other drug may have also partitioned as charged molecules into the bulk solution.

Subsequently, it was important to evaluate the effect of OA on drug precipitation. As evident from Tables 5.3 and 5.4, the dispersions of both model drugs loaded either in PEG-32 S or OA-containing systems resulted mostly in supersaturated solutions. While the dispersed PEG-32 S precipitated already as unsaturated formulations ( $S < 1$  in the anhydrous formulation), OA-containing systems precipitated only at formulation drug saturation of 1.1 and beyond. The addition of OA increased the equilibrium drug solubility in the dispersion medium. Therefore, the degree of supersaturation was decreased, which in turn inhibited drug precipitation. This mechanism of precipitation inhibition is well known for using surface active excipients.

Interesting findings were also inferred from a comparison of the maximum supersaturation ratios ( $SR^M$ ) between the different formulations for a given drug. As mentioned earlier, the addition of OA almost doubled the solubilizing capacity of the dispersion medium (see section 5.3.4.1.). As a consequence, although the drug loading was much higher for OA-containing formulations (at the same  $S$ ), the corresponding  $SR^M$  values upon dispersion were lower compared to  $SR^M$  of systems without OA. Moreover, both systems started to precipitate at analogous  $SR^M$  values (Tables 5.3 and 5.4). Interesting is the report of Rodriguez-Hornedo *et al.* (159) who studied a critical supersaturation regarding spontaneous drug precipitation. Such critical supersaturation for

spontaneous nucleation was compared between systems containing different solvents. When the drug solubility was in a two or threefold regimen (as in our case), such critical supersaturation was similar. However, when the drug solubility was fivefold or higher, clearly reduced values of critical supersaturation were observed. Recently, Anby *et al.* (86) showed danazol (practically spontaneous) precipitation upon dispersion of various formulations, when  $SR^M$  values were higher than 2. The authors differentiated this situation from lipolysis-induced drug precipitation, where another critical value of  $SR^M$  was proposed. Our results of the supersaturation upon dispersion demonstrated that for values lower than 2, the Precipitation number became critical (*i.e.*  $> 1$ ). Certainly, a different time span was considered here as opposed to nearly spontaneous precipitation. Interesting was the finding of a different critical  $SR^M$  value for the two bases. This implies that critical  $SR^M$  values for precipitation might be useful to compare formulations, but may be rather drug specific. In addition, our systems contained considerably higher drug amounts (especially all supersaturated formulations), which could have been relevant for precipitation kinetics.

As evident from Figures 5.11 and 5.12, OA influenced the extent of precipitation and its kinetics. It can be compared to findings of Gao *et al.* (80), who reported that the amount of surfactant (Tween<sup>®</sup> 80) in the formulation dictated the initial degree of drug (AMG 517) supersaturation, and therefore, its precipitation kinetics. In the present study, there was a substantially lower extent of precipitation when OA was added to the formulation. The precipitation kinetics of these OA-containing formulations was, however, characterized by a high initial rate. The portion of drug that precipitated almost spontaneously might have been primarily solubilized base in the bulk. Some drug-OA interactions might have occurred also in the bulk but it was mainly on the colloidal level, where the molecular interactions were assumed. This direct drug-OA interaction on the level of micelles was probably one mechanism of nucleation inhibition. OA could have further reduced the interfacial energy of forming drug nucleates and it may have

interfered with the particle growth process. The latter effect may, however, be more pronounced in case of polymeric precipitation inhibitors as reported elsewhere (97, 98).

Besides the extent of precipitation and its kinetics, the solid state of the evolving material can be of crucial biopharmaceutical importance. If drug precipitates in a crystalline form in the intestinal environment, it is often problematic, since re-dissolution of drug crystals is typically rather slow. In the present study, the precipitates of both drugs in PEG-32 S were crystalline (Figure 5.12). Interestingly, the presence of OA affected the solid state of precipitates, resulting in an amorphous material. Drug could have formed a solid dispersion or co-precipitate with the fatty acid. Such differentiation was not further attempted as it was deemed as less crucial from a biopharmaceutical perspective. Another recent study by Stillhart *et al* (160) found also an amorphous precipitate of carvedilol in a digested formulation medium, whereas pure formulation dispersion (no lipolysis) produced crystalline material. It might have been due to generation of fatty acids during lipolysis that an interaction with carvedilol enabled an amorphous precipitate. In our study the presence of a fatty acid in the anhydrous formulation could be a beneficial formulation strategy to target amorphous drug precipitates. The advantage of such amorphous precipitates from lipid-based formulations has for example been shown recently for halofantrine *in vivo* by Thomas *et al.* (102).

There is a high interest from biopharmaceutical perspective in intraluminal generated amorphous drug and supersaturation. Only few studies correlate *in vitro* supersaturation with *in vivo* absorption characteristics. For example, it was shown that for some drugs the initial production of a highly supersaturated system appeared to be more important for absorption enhancement as compared to long-term stabilization of supersaturation (93, 94). The reason for this might be that the model drugs used in these studies (celecoxib and tacrolimus) are fast permeating drugs, and the trans epithelial flux generated sink conditions, limiting the importance of long-term stabilization. Therefore, such drugs should be evaluated optimally with an absorption step as part of an *in vitro* test. In the

present study the precipitation kinetics was studied using FBRM, in a closed system. Although, both loratadine and carvedilol are fast permeating drugs, the focus was more on the effects of OA on drug precipitation kinetics rather than attempting to make absolute predictions for *in vivo* drug absorption.

We introduced a biopharmaceutically relevant dimensionless parameter: the Precipitation number ( $P_{nc}$ ). It is the ratio of the drug residence time in GIT ( $t_{res}$ ) to the induction time of crystalline precipitation ( $\tau_{ind}$ ). The induction time is a parameter characteristic to chemical engineering and the comparison with a physiologically relevant time was meaningful. All dispersed drug-loaded PEG-32 S formulations resulted in supersaturated solutions ( $SR^M > 1$ ). However, not all of them precipitated within a relevant intestinal transit time, which was reflected by different  $P_{nc}$  values. Therefore, the Precipitation number ( $P_{nc}$ ) provides a simple tool for fast screening of different formulations and/or drug loadings in formulations with respect to a relevant physiological time frame. It is important to compare crystalline precipitates, whereas the amorphous precipitates obtained from the OA-containing formulations were not directly comparable using  $P_{nc}$ .

The importance of applied hydrodynamics in the precipitation evaluation should be mentioned. As presented earlier, already unsaturated drug-loaded systems (anhydrous formulations without OA) were precipitating upon aqueous dispersion, when rigorous mixing of 500 rpm during FBRM testing was employed. In case of the drug release testing (USP 3 apparatus, 20 dpm), the precipitation occurred only for supersaturated systems ( $S = 1.5$ ). The release rate of loratadine was strongly influenced by the presence of OA and marked precipitation was noted in absence of the excipient. This excipient effect was also observed in case of carvedilol, but it was less pronounced. Such drug comparison on the same supersaturation level is meaningful to standardize the driving force of nucleation, but it is accompanied by different drug loads. Moreover, drug solubilities were different, *i.e.* carvedilol exhibited much higher solubility as compared to

loratadine. This certainly affected drug release under non-sink conditions, so the extent of the excipient effect for different drugs should be interpreted carefully.

Tables 5.3 and 5.4 allow comparing formulations at similar doses in view of the resulting maximal supersaturation. OA had always a clear effect and this would be also expected in a release experiment with comparing formulations at constant dose level. For absolute values, some care is needed when different *in vitro* tests are compared. Recently, Carlert *et al.* (161) also explored two different hydrodynamics for the *in vitro* precipitation studies of a basic BCS class II drug (AZD0865). They observed that precipitation rates were remarkably slower in the shaking model (85 cycles/min, amplitude 2 cm) compared to the stirring model (USP 2 mini-vessel set up, paddle speed of 150 rpm). The various shears were likely to be the main difference also in our FBRM experiments compared to the release analysis in the USP 3 apparatus. The effects of the capsule shell may have been less critical given the rather fast immediate drug release profiles.

## 5.5. Conclusions

The aim of the current study was to better understand the effects of basic drug-OA interactions in a solid lipid-based system on different biopharmaceutical levels, *i.e.* in the anhydrous formulation and upon aqueous dispersion. A particular interest was the influence on drug precipitation kinetics and on the solid-state properties of obtained precipitates following dispersion.

On the level of the anhydrous formulation, it was likely that the drug-OA molecular complexes were formed, which led to a substantial increase of solubilized drugs in the formulations. Once the formulations were dispersed, a clear complex formation was no longer apparent. This may have been due to the analytical sensitivity of the methods, but most likely the interactions were indeed partially lost. However, some interactions were still present upon dispersion on the level of evolving micelles, and probably also within

the bulk solution. OA clearly influenced supersaturation and the extent of drug precipitation as well as its kinetics. Most importantly, OA acted as a precipitation modifier, since it induced an amorphous precipitate that was otherwise crystalline without this excipient. Such an *in situ* forming amorphous system can be viewed as a novel formulation strategy to deliver poorly soluble basic drugs.

It was further concluded that relevant drug-excipient interactions must be studied separately on the different levels of biopharmaceutical testing. This appears to be critical for an improved biopharmaceutical understanding and also with respect to a more rational selection of systems in pharmaceutical formulation development. For such a development purpose, the introduced Precipitation number appears to be highly attractive to screen lipid-based candidate formulations. Future studies should address other drug-excipient systems on different biopharmaceutical levels that may also include an absorption step. An improved understanding of drug-excipient interactions would also advance the field of biopharmaceutical drug absorption modeling.

---

## Chapter 6

# Final remarks and outlook

For decades, gelatin has been used worldwide for the production of soft capsules due to its unique physicochemical properties. However, soft gelatin capsules (SGCs) are very dynamic systems and they present a challenge with respect to commonly observed drug-excipient-shell interactions. This motivates the need for novel inert shell-forming materials. This thesis presents an innovation in soft capsule technology using the novel starch-based thermoplastic shell material. In particular, the mechanistic understanding of drug-excipient-shell interactions using SGCs and various starch-based thermoplastic capsules (VegaGels<sup>®</sup> and S-PVA-Cs) were explored.

In the present work we successful introduced the novel starch-based thermoplastic capsules (S-PVA-Cs). The water migration pattern of these capsules was markedly superior to that of SGCs. The novel shell material was found to be suitable for encapsulation of a hydrophilic lipid-based formulation without exhibiting any drug crystallization. Moreover, the high resistance to mechanical deformation of the novel shell material may shorten manufacturing times (*e.g.* allow shorter drying process) and enable storage of capsules in bulk containers. Other characteristics of the new material, such as surface roughness and thermal stability can be advantageous for a subsequent coating step. Although the hydrophilic lipid-based system in this study profited from the new capsule technology, encapsulation of other formulations might be less critical. In the future work more formulations containing different drugs at varying dose strengths



should be examined. Moreover, to completely evaluate the inertness of the novel shell material, studies on co-solvent migration from the fill into the shell are needed. In addition, the investigation of possible drug migration into the shell is of major interest, as it could cause variations in drug release profiles. In summary, S-PVA-C could be a promising capsule technology for encapsulation of hydrophilic lipid-based formulations, but more studies are needed to finally assess the potential of these capsules in pharmaceuticals.

The study on biorelevant drug release from the novel thermoplastic capsules demonstrated that capsule shell material is freely selectable for a given formulation. Commonly, optimizing the biopharmaceutical formulation performance is the main objective during formulation development. However, our results suggested that some care is needed while choosing adequate capsule technology. Disintegration testing of various capsule types revealed different opening mechanisms. This influenced the drug release profile of a given formulation, but only in case of S-PVA-Cs. The interaction of the opening mechanism of capsules with formulation hydration should be considered during early formulation development. It would also be worthwhile to elucidate the structures of hydrated colloids formed during dilution, as it would help to better understand the biopharmaceutical formulation behaviour.

The quality of drug-excipient interactions may be different at the level of the anhydrous formulation and upon aqueous dispersion. Since such interactions are likely to impact on drug formulation loading in the anhydrous formulation and the drug behaviour upon formulation dispersion, it is of major importance to study them on these different levels. In our study, the addition of oleic acid to basic drugs resulted in different qualities of molecular interactions. On the level of the anhydrous formulation, molecular complexes were observed that caused marked drug solubility increase. Later upon formulation dispersion, drug-excipient interactions influenced the extent of drug precipitation and its kinetics. The most remarkable finding was the role of OA as a precipitation modifier, since the precipitated model drugs were amorphous. This *in situ* formation of amorphous

precipitates could be a novel formulation strategy for weak bases. In the future work, studies of other drug-excipient systems on different biopharmaceutical levels could also include an absorption step. In addition, advances in the field of biopharmaceutical drug absorption modeling may be expected with an improved understanding of drug-excipient interactions.

The present thesis introduced the novel starch-based thermoplastic capsules (S-PVA-Cs) and showed their advantage over SGCs with respect to hydrophilic lipid-based formulations. Drug-excipient-shell interactions observed in various capsule types (SGCs, S-PVA-Cs, and VegaGels<sup>®</sup>) were explored on different biopharmaceutical levels. In general, this thesis offers a better mechanistic understanding of such interactions, which should help in the future development of soft capsule products.

## Bibliography

1. B.E. Jones. The history of the medicinal capsule. In F. Podczeck and B.E. Jones (eds.), *Pharmaceutical capsules*, Pharmaceutical Press, London, UK, 2004, pp. 1-22.
2. R.P. Gullapalli. Soft gelatin capsules (Softgels). *Journal of Pharmaceutical Sciences*. 99:4107-4148 (2010).
3. J.P. Stanley. Soft gelatin capsules. In L. Lachman, H.A. Lieberman, and J.L. Kanig (eds.), *The theory and practice of industrial pharmacy*, Lea & Febiger, Philadelphia, USA, 1986, pp. 398-412.
4. L.L. Augsburger. Hard and soft capsules. In G.S. Banker and C.T. Rhodes (eds.), *Modern pharmaceuticals*, M. Dekker, New York, USA, 2002, pp. 548-565.
5. R. Schrieber and H. Gareis. From collagen to gelatine. *Gelatine handbook: theory and industrial practice*, Wiley-VCH, Weinheim, Germany, 2007, pp. 45-117.
6. N.A. Armstrong, K.C. James, and W.K.L. Pugh. Drug migration into soft gelatin capsule shells and its effect on in vitro availability. *Journal of Pharmacy and Pharmacology*. 36:361-365 (1984).
7. N.A. Armstrong, T. Gebre-Mariam, and K.C. James. An apparatus for investigating drug migration into gelatin capsule shells. *International Journal of Pharmaceutics*. 34:125-129 (1986).
8. T. Gebre-Mariam, N.A. Armstrong, K.R. Bran, and K.C. James. The effect of gelatin grade and concentration on the migration of solutes into and through glycerogelatin gels. *Journal of Pharmacy and Pharmacology*. 41:524-527 (1989).
9. N.A. Armstrong, T. Gebre-Mariam, K.C. James, and P. Kearney. The influence of viscosity on the migration of chloramphenicol and 4-hydroxybenzoic acid through glycerogelatin gels. *Journal of Pharmacy and Pharmacology*. 39:583-586 (1987).

10. N. Cao, X. Yang, and Y. Fu. Effects of various plasticizers on mechanical and water vapor barrier properties of gelatin films. *Food Hydrocolloids*. 23:729-735 (2009).
11. A.M. Tralhao, A.C. Watkinson, K.R. Brain, J. Hadgraft, and N.A. Armstrong. Use of ATR-FTIR spectroscopy to study the diffusion of ethanol through glycerogelatin films. *Pharmaceutical Research*. 12:572-575 (1995).
12. R.C. Moreton and N.A. Armstrong. The effect of film composition on the diffusion of ethanol through soft gelatin films. *International Journal of Pharmaceutics*. 161:123-131 (1998).
13. A.T.M. Serajuddin, P.C. Sheen, and M.A. Augustine. Water migration from soft gelatin capsule shell to fill material and its effect on drug solubility. *Journal of Pharmaceutical Sciences*. 75:62-64 (1986).
14. E. Brocker, I. Tomka, D. Engel, R. Ménard, and P. Greither. Method for manufacturing a shape body containing a starch, a homogenised mass containing a starch and a device for manufacturing a soft capsule, Swiss Caps AG, a member of AENOVA group, US 6,790,495, 2004.
15. K.E. Tanner, P.B. Drapper, J.J. Getz, S.W. Burnett, and E. Youngblood. Film forming compositions comprising modified starches and iota-carrageenan and methods for manufacturing soft capsules using same, R.P. Scherer Technologies, US 6,340,473, 2002.
16. M.D. Brown. Method of encapsulation, Morgan & Finnegan, US 2002/0026771, 2002.
17. K. Tanner, S. Burnett, D. Walker, P. Beke, N. Stroud, and M. Sundararajan. Apparatus for manufacturing encapsulated products, R.P. Scherer Technologies, US 6,884,060 B2, 2005.
18. J.J. Modliszewski, A.D. Ballard, C.J. SeWall, W.R. Blakemore, and P.J. Riley. Homogeneous, thermoreversible gel film containing kappa-2 carrageenan and soft capsules made therefrom, FMC Corporation, US 7,807,194 B2, 2010.
19. D.A. Archibald, Q. Fang, L.G. Fonkwe, G.L. Dietel, and C.S. Casault. Non-gelatin film and method and apparatus for producing same, Banner Pharmacaps, US 7,887,838, 2011.

20. E. Jantratid, N. Janssen, H. Chokshi, K. Tang, and J.B. Dressman. Designing biorelevant dissolution tests for lipid formulations: Case example-Lipid suspension of RZ-50. *European Journal of Pharmaceutics and Biopharmaceutics*. 69:776-785 (2008).
21. J. Dressman, K. Schamp, K. Beltz, and J. Alsenz. Characterizing release from lipid-based formulations. In D.J. Hauss (ed.), *Oral lipid-based formulations: enhancing the bioavailability of poorly water-soluble drugs*, Informa Helathcare USA, New York, 2007, pp. 241-256.
22. R.T. Jones. Gelatin: manufacture and physicochemical properties. In F. Podczek and B.E. Jones (eds.), *Pharmaceutical capsules*, Pharmaceutical Press, London, UK, 2004, pp. 23-60.
23. I.J. Haug and K.I. Draget. Gelatin. In G.O. Phillips and P.A. Williams (eds.), *Handbook of hydrocolloids*, CRC Press, Boca Raton, FL, USA, 2009, pp. 142-163.
24. The United States Pharmacopeia & The National Formulary. Monograph: Gelatin, USP 36-NF31. US Pharmacopoeial Convention Inc.2013.
25. G. Reich. Formulation and physical properties of soft capsule. In F. Podczek and B.E. Jones (eds.), *Pharmaceutical capsules*, Pharmaceutical Press, London, UK, 2004, pp. 201-212.
26. C.J.H. Porter, N.L. Trevaskis, and W.N. Charman. Lipids and lipid-based formulations: optimizing the oral delivery of lipophilic drugs. *Nature Reviews Drug Discovery*. 6:231-248 (2007).
27. D.L. Pole. Physical and biological considerations for the use of nonaqueous solvents in oral bioavailability enhancement. *Journal of Pharmaceutical Sciences*. 97:1071-1088 (2008).
28. G. Cornaire, J. Woodley, P. Hermann, A. Cloarec, U. Arellano, and G. Houin. Impact of excipients on the absorption of P-glycoprotein substrates in vitro and in vivo. *International Journal of Pharmaceutics*. 278:119-131 (2004).
29. M.J. Gumkowski, L.A. Fournier, N.K. Tierney, and W.J. Curatolo. Improved bioavailability through use of soft gelatin capsule formulations of terlakiren, a tripeptide rennin inhibitor. *Pharmaceutical Research*. 11:S-286 (1994).

30. International Organization for Standardization (ISO) 9001:2008, Quality management systems, Technical Committee ISO/TC 176, Geneva, Switzerland, 2008.
31. Note for guidance on minimising the risk of transmitting animal spongiform encephalopathy agents via human and veterinary medicinal products (EMA/410/01 rev.3), Official Journal of the European Union, London, UK, 2011, p. 18.
32. US Food and Drug Administration (FDA), "Guidance for industry-The sourcing and processing of gelatin to reduce the potential risk posed by bovine spongiform encephalopathy (BSE) in FDA-regulated products for human use", Rockville, USA, 1997.
33. The United States Pharmacopeia & The National Formulary. Dissolution <711>, USP 36-NF31. US Pharmacopoeial Convention Inc.2013.
34. D.S. Bindra, T.D. Williams, and V.J. Stella. Degradation of o-6-benzylguanine in aqueous polyethylene glycol 400 (PEG-400) solutions-concerns with formaldehyde in PEG-400. *Pharmaceutical Research*. 11:1060-1064 (1994).
35. R.P. Gullapalli. Ibuprofen-containing softgels, Banner Pharmacaps, US 6,251,426, 2001.
36. W. Brox. Soft gelatin capsules and methods for their production, R.P. Scherer, US 4,744,988, 1998.
37. A. Gennadios. Gum acacia substituted soft gelatin capsules, Banner Pharmacaps, US 6,193,999 B1, 2001.
38. G. Zoppetti and M. Marchiorri. Soft gelatin capsules containing cyclodextrin in the capsule shell, Altergon S.A., CA 2600969, 2013.
39. L.G. Fonkwe, D.A. Archibald, and A. Gennadios. Non-gelatin capsule shell formulation, Banner Pharmacaps, US 6,949,256, 2005.
40. C. Popescu, A. Francois, D. Damour, L. Zhou, P. Lefevre, X. Parrisiaux, and Q. Fang. Evaluation of a novel modified starch polymer as a gelatin replacement in soft capsule shells, [www.roquette-pharma.com](http://www.roquette-pharma.com).
41. S. Pohl and G. Reich. Evaluation of Kollicoat Protect<sup>®</sup> formulations for gelatin-free soft capsules, AAPS, Los Angeles, USA, 2009.

42. K. Meyer-Böhm. Influence of modified starch on gelatin-free soft capsule films, APV World meeting, Barcelona, Spain, 2008.
43. J.C. Wunderlich, U. Schick, J. Freidenreich, and J. Werry. Soft gelatin capsules, Alfatec Pharma GmbH, US 5,254,294, 1993.
44. F. Podczeck. Technology to manufacture soft capsule. In F. Podczeck and B.E. Jones (eds.), *Pharmaceutical capsules*, Pharmaceutical Press, London, UK, 2004, pp. 195-201.
45. G.L. Amidon, H. Lennernäs, V.P. Shah, and J.R. Crison. A theoretical basis for a biopharmaceutic drug classification: The correlation of in vitro drug product dissolution and in vivo bioavailability. *Pharmaceutical Research*. 12:413-420 (1995).
46. J.M. Butler and J.B. Dressman. The developability classification system: Application of biopharmaceutics concepts to formulation development. *Journal of Pharmaceutical Sciences*. 99:4940-4954 (2010).
47. C.M. O'Driscoll. Lipid-based formulations for intestinal lymphatic delivery. *European Journal of Pharmaceutical Sciences*. 15:405-415 (2002).
48. R.G. Strickley. Currently marketed oral lipid-based dosage forms: Drug products and excipients. In D.J. Hauss (ed.), *Oral lipid-based formulations: enhancing the bioavailability of poorly water-soluble drugs*, Informa Healthcare, New York, USA, 2007, pp. 1-33.
49. C.W. Pouton. Lipid formulations for oral administration of drugs: non-emulsifying, self-emulsifying and 'self-microemulsifying' drug delivery systems. *European Journal of Pharmaceutical Sciences*. 11:S93-S98 (2000).
50. C.W. Pouton. Formulation of poorly water-soluble drugs for oral administration: Physicochemical and physiological issues and the lipid formulation classification system. *European Journal of Pharmaceutical Sciences*. 29:278-287 (2006).
51. B.K. Kang, J.S. Lee, S.K. Chon, S.Y. Jeong, S.H. Yuk, G. Khang, H.B. Lee, and S.H. Cho. Development of self-microemulsifying drug delivery systems (SMEDDS) for oral bioavailability enhancement of simvastatin in beagle dogs. *International Journal of Pharmaceutics*. 274:65-73 (2004).

52. R.N. Gursoy and S. Benita. Self-emulsifying drug delivery systems (SEDDS) for improved oral delivery of lipophilic drugs. *Biomedicine & Pharmacotherapy*. 58:173-182 (2004).
53. N.H. Shah, M.T. Carvajal, C.I. Patel, M.H. Infeld, and A.W. Malick. Self-emulsifying drug-delivery systems (SEDDS) with polyglycolized glycerides for improving in-vitro dissolution and oral absorption of lipophilic drugs. *International Journal of Pharmaceutics*. 106:15-23 (1994).
54. N. Anton and T.F. Vandamme. Nano-emulsions and micro-emulsions: Clarifications of the critical differences. *Pharmaceutical Research*. 28:978-985 (2011).
55. I. Danielsson and B. Lindman. The definition of micro-emulsion. *Colloids and Surfaces*. 3:391-392 (1981).
56. A. Niederquell and M. Kuentz. Proposal of stability categories for nano-dispersions obtained from pharmaceutical self-emulsifying formulations. *International Journal of Pharmaceutics*. 446:70-80 (2013).
57. M. Kuentz. Lipid-based formulations for oral delivery of lipophilic drugs. *Drug Discovery Today: Technologies*. 9:e97-e104 (2012).
58. US Food and Drug Administration (FDA), Generally Recognized As Safe (GRAS), sections 201(s) and 409 of the Federal Food, Drug, and Cosmetic Act (the Act) , Rockville, USA, 2013.
59. US Food and Drug Administration (FDA), Inactive Ingredients Database (IID), 21 CFR 210.3, Rockville, USA, 2013.
60. C. Ditner, R. Bravo, G. Imanidis, and M. Kuentz. A systematic dilution study of self-microemulsifying drug delivery systems in artificial intestinal fluid using dynamic laser light backscattering. *Drug Development and Industrial Pharmacy*. 35:199-208 (2009).
61. R.L. Oberle, T.J. Moore, and D.A.P. Krummel. Evaluation of mucosal damage of surfactants in rat jejunum and colon. *Journal of Pharmacological and Toxicological Methods*. 33:75-81 (1995).
62. C.W. Pouton and C.J.H. Porter. Formulation of lipid-based delivery systems for oral administration: Materials, methods and strategies. *Advanced Drug Delivery Reviews*. 60:625-637 (2008).



63. M. Grove, A. Mullertz, J.L. Nielsen, and G.P. Pedersen. Bioavailability of seocalcitol II: Development and characterisation of self-microemulsifying drug delivery systems (SMEDDS) for oral administration containing medium and long chain triglycerides. *European Journal of Pharmaceutical Sciences*. 28:233-242 (2006).
64. S. Agatonovic-Kustrin and R. Beresford. Basic concepts of artificial neural network (ANN) modeling and its application in pharmaceutical research. *Journal of Pharmaceutical and Biomedical Analysis*. 22:717-727 (2000).
65. S. Agatonovic-Kustrin, B.D. Glass, M.H. Wisch, and R.G. Alany. Prediction of a stable microemulsion formulation for the oral delivery of a combination of antitubercular drugs using ANN methodology. *Pharmaceutical Research*. 20:1760-1765 (2003).
66. L. Djekic, S. Ibric, and M. Primorac. The application of artificial neural networks in the prediction of microemulsion phase boundaries in PEG-8 caprylic/capric glycerides based systems. *International Journal of Pharmaceutics*. 361:41-46 (2008).
67. C.J. Richardson, A. Mbanefo, R. Aboofazeli, M.J. Lawrence, and D.J. Barlow. Prediction of phase behavior in microemulsion systems using artificial neural networks. *Journal of Colloid and Interface Science*. 187:296-303 (1997).
68. E.S. Kostewicz, B. Abrahamsson, M. Brewster, J. Brouwers, J. Butler, S. Carlert, P.A. Dickinson, J. Dressman, R. Holm, S. Klein, J. Mann, M. McAllister, M. Minekus, U. Muenster, A. Müllertz, M. Verwei, M. Vertzoni, W. Weitschies, and P. Augustijns. In vitro models for the prediction of in vivo performance of oral dosage forms. *European Journal of Pharmaceutical Sciences*. In press. (2013).
69. B.T. Griffin, M. Kuentz, M. Vertzoni, E.S. Kostewicz, Y. Fei, W. Faisal, C. Stillhart, C. O'Driscoll, C. Reppas, and J.B. Dressman. Comparison of in vitro tests at various levels of complexity for the prediction of in vivo performance of lipid-based formulations: Case studies with fenofibrate. *European Journal of Pharmaceutics and Biopharmaceutics*. In press. (2013).
70. S.M. Khoo, A.J. Humberstone, C.J.H. Porter, G.A. Edwards, and W.N. Charman. Formulation design and bioavailability assessment of lipidic self-emulsifying formulations of halofantrine. *International Journal of Pharmaceutics*. 167:155-164 (1998).

71. F.S. Nielsen, K.B. Petersen, and A. Mullertz. Bioavailability of probucol from lipid and surfactant based formulations in minipigs: Influence of droplet size and dietary state. *European Journal of Pharmaceutics and Biopharmaceutics*. 69:553-562 (2008).
72. A.T. Larsen, A.G. Ohlsson, B. Polentarutti, R.A. Barker, A.R. Phillips, R. Abu-Rmaileh, P.A. Dickinson, B. Abrahamsson, J. Ostergaard, and A. Mullertz. Oral bioavailability of cinnarizine in dogs: Relation to SNEDDS droplet size, drug solubility and in vitro precipitation. *European Journal of Pharmaceutical Sciences*. 48:339-350 (2013).
73. P.J. Sassene, M.M. Knopp, J.Z. Hesselkilde, V. Koradia, A. Larsen, T. Rades, and A. Mullertz. Precipitation of a poorly soluble model drug during in vitro lipolysis: Characterization and dissolution of the precipitate. *Journal of Pharmaceutical Sciences*. 99:4982-4991 (2010).
74. A.T. Larsen, P. Sassene, and A. Mullertz. In vitro lipolysis models as a tool for the characterization of oral lipid and surfactant based drug delivery systems. *International Journal of Pharmaceutics*. 417:245-255 (2011).
75. E.S. Kostewicz, M. Wunderlich, U. Brauns, R. Becker, T. Bock, and J.B. Dressman. Predicting the precipitation of poorly soluble weak bases upon entry in the small intestine. *Journal of Pharmacy and Pharmacology*. 56:43-51 (2004).
76. Y.E. Arnold, G. Imanidis, and M.T. Kuentz. Advancing in-vitro drug precipitation testing: new process monitoring tools and a kinetic nucleation and growth model. *Journal of Pharmacy and Pharmacology*. 63:333-341 (2011).
77. J.W. Mullin. *Crystallization*, Butterworth & Heinemann, Oxford, UK, 2001.
78. D. Kashchiev and G.M. van Rosmalen. Review: Nucleation in solutions revisited. *Crystal Research and Technology*. 38:555-574 (2003).
79. J. Brouwers, M.E. Brewster, and P. Augustijns. Supersaturating drug delivery systems: The answer to solubility-limited oral bioavailability? *Journal of Pharmaceutical Sciences*. 98:2549-2572 (2009).
80. P. Gao, A. Akrami, F. Alvarez, J. Hu, L. Li, C. Ma, and S. Surapaneni. Characterization and optimization of AMG 517 supersaturatable self-emulsifying drug delivery system (S-SEDDS) for improved oral absorption. *Journal of Pharmaceutical Sciences*. 98:516-528 (2009).

81. A. Ruf, J. Worlitschek, and M. Mazzotti. Modeling and experimental analysis of PSD measurements through FBRM. *Particle & Particle Systems Characterization*. 17:167-179 (2000).
82. J. Scholl, L. Vicum, M. Muller, and M. Mazzotti. Precipitation of L-glutamic acid: Determination of nucleation kinetics. *Chemical Engineering & Technology*. 29:257-264 (2006).
83. Y. Arnold. Evaluation of lipid-based formulations of poorly water-soluble drugs in the gastro-intestinal tract using in vitro tests. PhD thesis. University of Basel. 2011.
84. H.D. Williams, N.L. Trevaskis, Y.Y. Yeap, M.U. Anby, C.W. Pouton, and C.J. Porter. Lipid-based formulations and drug supersaturation: Harnessing the unique benefits of the lipid digestion/absorption pathway. *Pharmaceutical Research*. 30:2926-2992 (2013).
85. K. Mohsin, M.A. Long, and C.W. Pouton. Design of lipid-based formulations for oral administration of poorly water-soluble drugs: Precipitation of drug after dispersion of formulations in aqueous solution. *Journal of Pharmaceutical Sciences*. 98:3582-3595 (2009).
86. M.U. Anby, H.D. Williams, M. McIntosh, H. Benameur, G.A. Edwards, C.W. Pouton, and C.J.H. Porter. Lipid digestion as a trigger for supersaturation: Evaluation of the impact of supersaturation stabilization on the in vitro and in vivo performance of self-emulsifying drug delivery systems. *Molecular Pharmaceutics*. 9:2063-2079 (2012).
87. Y.Y. Yeap, N.L. Trevaskis, T. Quach, P. Tso, W.N. Charman, and C.J.H. Porter. Intestinal bile secretion promotes drug absorption from lipid colloidal phases via induction of supersaturation. *Molecular Pharmaceutics*. 10:1874-1889 (2013).
88. Y.Y. Yeap, N.L. Trevaskis, and C.J.H. Porter. The potential for drug supersaturation during intestinal processing of lipid-based formulations may be enhanced for basic drugs. *Molecular Pharmaceutics*. 10:2601-2615 (2013).
89. Y.Y. Yeap, N.L. Trevaskis, and C.J. Porter. Lipid absorption triggers drug supersaturation at the intestinal unstirred water layer and promotes drug absorption from mixed micelles. *Pharmaceutical Research*. 30:3045-3058 (2013).

90. Z. Misic, D. Šišak-Jung, G. Sydow, and M. Kuentz. Understanding interactions of oleic acid with basic drugs in solid lipids on different biopharmaceutical levels. Submitted. (2013).
91. H.D. Williams, P. Sassene, K. Kleberg, M. Calderone, A. Igonin, E. Jule, J. Vertommen, R. Blundell, H. Benameur, A. Mullertz, C.W. Pouton, and C.J.H. Porter. Toward the establishment of standardized in vitro tests for lipid-based formulations, part 3: Understanding supersaturation versus precipitation potential during the in vitro digestion of type I, II, IIIa, IIIb and IV lipid-based formulations. *Pharmaceutical Research*. 30:3059-3076 (2013).
92. J. Bevernage, J. Brouwers, P. Annaert, and P. Augustijns. Drug precipitation-permeation interplay: Supersaturation in an absorptive environment. *European Journal of Pharmaceutics and Biopharmaceutics*. 82:424-428 (2012).
93. H.R. Guzman, M. Tawa, Z. Zhang, P. Ratanabanangkoon, P. Shaw, C.R. Gardner, H. Chen, J-P. Moreau, O. Almarsson, and J.F. Remenar. Combined use of crystalline salt forms and precipitation inhibitors to improve oral absorption of celecoxib from solid oral formulations. *Journal of Pharmaceutical Sciences*. 96:2686-2702 (2007).
94. K.A. Overhoff, J.T. McConville, W. Yang, K.P. Johnston, J.I. Peters, and R.O. Williams III. Effect of stabilizer on the maximum degree and extent of supersaturation and oral absorption of tacrolimus made by ultra-rapid freezing. *Pharmaceutical Research*. 25:167-175 (2008).
95. P. Gao and W. Morozowich. Development of supersaturatable self-emulsifying drug delivery system formulations for improving the oral absorption of poorly soluble drugs. *Expert Opinion on Drug Delivery*. 3:97-110 (2006).
96. J. Bevernage, T. Forier, J. Brouwers, J. Tack, P. Annaert, and P. Augustijns. Excipient-mediated supersaturation stabilization in human intestinal fluids. *Molecular Pharmaceutics*. 8:564-570 (2011).
97. D.B. Warren, H. Benameur, C.J.H. Porter, and C.W. Pouton. Using polymeric precipitation inhibitors to improve the absorption of poorly water-soluble drugs: A mechanistic basis for utility. *Journal of Drug Targeting*. 18:704-731 (2010).
98. S.L. Raghavan, A. Trividic, A.F. Davis, and J. Hadgraft. Crystallization of hydrocortisone acetate: influence of polymers. *International Journal of Pharmaceutics*. 212:213-221 (2001).

99. W-G. Dai, L.C. Dong, S. Li, and Z. Deng. Combination of Pluronic/Vitamin E TPGS as a potential inhibitor of drug precipitation. *International Journal of Pharmaceutics*. 355:31-37 (2008).
100. M.E. Brewster, R. Vandecruys, J. Peeters, P. Neeskens, G. Verreck, and T. Loftsson. Comparative interaction of 2-hydroxypropyl-beta-cyclodextrin and sulfobutylether-beta-cyclodextrin with itraconazole: Phase-solubility behavior and stabilization of supersaturated drug solutions. *European Journal of Pharmaceutical Sciences*. 34:94-103 (2008).
101. P. Gao, M.E. Guyton, T. Huang, J.M. Bauer, K.J. Stefanski, and Q. Lu. Enhanced oral bioavailability of a poorly water soluble drug PNU-91325 by supersaturatable formulations. *Drug Development and Industrial Pharmacy*. 30:221-229 (2004).
102. N. Thomas, R. Holm, A. Mullertz, and T. Rades. In vitro and in vivo performance of novel supersaturated self-nanoemulsifying drug delivery systems (super-SNEDDS). *Journal of Controlled Release*. 160:25-32 (2012).
103. N. Thomas, R. Holm, M. Garmer, J.J. Karlsson, A. Mullertz, and T. Rades. Supersaturated self-nanoemulsifying drug delivery systems (super-SNEDDS) enhance the bioavailability of the poorly water-soluble drug simvastatin in dogs. *AAPS Journal*. 15:219-227 (2013).
104. M.C. Meyer, A.B. Straughn, R.M. Mhatre, A. Hussain, V.P. Shah, C.B. Bottom, E.T. Cole, L.L. Lesko, H. Mallinowski, and R.L. Williams. The effect of gelatin cross-linking on the bioequivalence of hard and soft gelatin acetaminophen capsules. *Pharmaceutical Research*. 17:962-966 (2000).
105. M.J. Kontny and C.A. Mulski. Gelatin capsule brittleness as a function of relative-humidity at room-temperature. *International Journal of Pharmaceutics*. 54:79-85 (1989).
106. Lonza DHA and VegaGels<sup>®</sup>. The entirely vegetarian solution. *Innovations in Food Technology*. (2006).
107. DIN EN ISO 4287. Geometrical product specification (GPS). Surface texture: Profile method-terms, definitions and surface texture parameters. (1997).
108. S.B. Roy, B. Ramaraj, S.C. Shit, and S.K. Nayak. Polypropylene and potato starch biocomposites: Physicomechanical and thermal properties. *Journal of Applied Polymer Science*. 120:3078-3086 (2011).

109. B. Wunderlich. Thermal analysis, Academic Press, Boston, USA, 1990.
110. The United States Pharmacopeia & The National Formulary. The Official Compendia of Standards, USP 34-NF29. US Pharmacopoeial Convention Inc. (2011).
111. T. Do Thi, M. Van Speybroeck, V. Barillaro, J. Martens, P. Annaert, P. Augustijns, J. Van Humbeeck, J. Vermant, and G. Van den Mooter. Formulate-ability of ten compounds with different physicochemical profiles in SMEDDS. *European Journal of Pharmaceutical Sciences*. 38:479-488 (2009).
112. M. Kuentz, B. Rothenhuesler, and D. Roethlisberg. Time domain H-1 NMR as a new method to monitor softening of gelatin and HPMC capsule shells. *Drug Development and Industrial Pharmacy*. 32:1165-1173 (2006).
113. K. Pal, A.K. Banthia, and D.K. Majumdar. Preparation and characterization of polyvinyl alcohol-gelatin hydrogel membranes for biomedical applications. *AAPS PharmSciTech*. 8:(2007).
114. J.J.G. van Soest, S.H.D. Hulleman, D. de Wit, and J.F.G. Vliegthart. Crystallinity in starch bioplastics. *Industrial Crops and Products*:11-22 (1996).
115. S. Zhao, C.-Y. Wang, M.-M. Chen, and J-H. Sun. Mechanism for the preparation of carbon spheres from potato starch treated by NH<sub>4</sub>Cl. *Carbon*. 47:331-333 (2009).
116. A.R. Patel and P.R. Vavia. Preparation and in vivo evaluation of SMEDDS (Self-Microemulsifying Drug Delivery System) containing fenofibrate. *AAPS Journal*. 9:E344-E352 (2007).
117. D.J. McClements. Crystals and crystallization in oil-in-water emulsions: Implications for emulsion-based delivery systems. *Advances in Colloid and Interface Science*. 174:1-30 (2012).
118. S. Missaghi and R. Fassihi. Evaluation and comparison of physicomechanical characteristics of gelatin and hypromellose capsules. *Drug Development and Industrial Pharmacy*. 32:829-838 (2006).
119. Z. Misic, K. Muffler, G. Sydow, and M. Kuentz. Novel starch-based PVA thermoplastic capsules for hydrophilic lipid-based formulations. *Journal of Pharmaceutical Sciences*. 101:4516-4528 (2012).

120. B-M. Lue, F.S. Nielsen, T. Magnussen, H.M. Schou, K. Kristensen, L.O. Jacobsen, and A. Mullertz. Using biorelevant dissolution to obtain IVIVC of solid dosage forms containing a poorly-soluble model compound. *European Journal of Pharmaceutics and Biopharmaceutics*. 69:648-657 (2008).
121. I. Borst, S. Ugwu, and A.H. Beckett. New and extended applications for USP drug release apparatus 3. *Dissolution Technologies*. 4:11-18 (1997).
122. E. Jantratid, V. De Maio, E. Ronda, V. Mattavelli, M. Vertzoni, and J.B. Dressman. Application of biorelevant dissolution tests to the prediction of in vivo performance of diclofenac sodium from an oral modified-release pellet dosage form. *European Journal of Pharmaceutical Sciences*. 37:434-441 (2009).
123. A. Mullertz, A. Ogbonna, S. Ren, and T. Rades. New perspectives on lipid and surfactant based drug delivery systems for oral delivery of poorly soluble drugs. *Journal of Pharmacy and Pharmacology*. 62:1622-1636 (2010).
124. J.C. Lopez-Montilla, P.E. Herrera-Morales, S. Pandey, and D.O. Shah. Spontaneous emulsification: Mechanisms, physicochemical aspects, modeling, and applications. *Journal of Dispersion Science and Technology*. 23:219-268 (2002).
125. M.G. Wakerly, C.W. Pouton, and B.J. Meakin. Evaluation of the selfemulsifying performance of a non-ionic surfactant-vegetable oil mixture. *Journal of Pharmacy and Pharmacology*. 39:6P (1987).
126. M.G. Wakerly, C.W. Pouton, B.J. Meakin, and F.S. Morton. The effect of surfactant HLB on the self-emulsifying efficiency of non-ionic surfactant vegetable oil mixtures. *Journal of Pharmacy and Pharmacology*. 38(S12):2P (1987).
127. C.W. Pouton. Formulation of self-emulsifying drug delivery systems. *Advanced Drug Delivery Reviews*. 25:47-58 (1997).
128. O. Regev, S. Ezrahi, A. Aserin, N. Garti, E. Wachtel, E.W. Kaler, A. Khan, and Y. Talmon. A study of the microstructure of a four-component nonionic microemulsion by cryo-TEM, NMR, SAXS, and SANS. *Langmuir*. 12:668-674 (1996).
129. S.V. Biradar, R.S. Dhumal, and A. Paradkar. Rheological investigation of self-emulsification process: Effect of co-surfactant. *Journal of Pharmacy and Pharmaceutical Sciences*. 12:164-174 (2009).

130. S.S. Patil, E. Venugopal, S. Bhat, K.R. Mahadik, and A.R. Paradkar. Probing influence of mesophasic transformation on performance of self-emulsifying system: Effect of ion. *Molecular Pharmaceutics*. 9:318-324 (2012).
131. S.S. Patil, E. Venugopal, S. Bhat, K.R. Mahadik, and A.R. Paradkar. Microstructural elucidation of self-emulsifying system: Effect of chemical structure. *Pharmaceutical Research*. 29:2180-2188 (2012).
132. M. Fanun. Oil type effect on diclofenac solubilization in mixed nonionic surfactants microemulsions. *Colloids and Surfaces A: Physicochemical and Engineering Aspects*. 343:75-82 (2009).
133. M. Teubner and R. Strey. Origin of the scattering peak in microemulsions. *Journal of Chemical Physics*. 87:3195-3200 (1987).
134. L.X. Yu, J.T. Wang, and A.S. Hussain. Evaluation of USP apparatus 3 for dissolution testing of immediate-release products. *AAPS PharmSci*. 4:E1-E1 (2002).
135. S. Klein. Dissolution test methods for modified release dosage forms. PhD thesis. University of Frankfurt am Main. (2005).
136. E. Jantravid, N. Janssen, C. Reppas, and J.B. Dressman. Dissolution media simulating conditions in the proximal human gastrointestinal tract: An update. *Pharmaceutical Research*. 25:1663-1676 (2008).
137. M.J. Groves and D.A. Degalindez. Rheological characterization of self-emulsifying oil-surfactant systems. *Acta Pharmaceutica Suecica*. 13:353-360 (1976).
138. C.W. Pouton. Self-emulsifying drug delivery systems-assessment of the efficiency of emulsification. *International Journal of Pharmaceutics*. 27:335-348 (1985).
139. B.R. Rohrs, D.L. Burchelark, M.J. Witt, and D.J. Stelzer. USP dissolution apparatus 3 (reciprocating cylinder): Instrument parameter effects on drug release from sustained-release formulations. *Journal of Pharmaceutical Sciences*. 84:922-926 (1995).
140. The United States Pharmacopeia & The National Formulary. The Official Compendia of Standards, USP 35-NF30. US Pharmacopoeial Convention Inc.2012.



141. N. Fotaki, A. Aivaliotis, J. Butler, J. Dressman, M. Fischbach, J. Hempenstall, S. Klein, and C. Reppas. A comparative study of different release apparatus in generating in vitro-in vivo correlations for extended release formulations. *European Journal of Pharmaceutics and Biopharmaceutics*. 73:115-120 (2009).
142. M. Fanun. Properties of microemulsions based on mixed nonionic surfactants and mixed oils. *Journal of Molecular Liquids*. 150:25-32 (2009).
143. C. Cabos, P. Delord, and J. Marignan. Local lamellar structure in dense microemulsions. *Physical Review B*. 37:9796-9799 (1988).
144. A. Kogan, D.E. Shalev, U. Raviv, A. Aserin, and N. Garti. Formation and characterization of ordered bicontinuous microemulsions. *Journal of Physical Chemistry B*. 113:10669-10678 (2009).
145. J. Bevernage, J. Brouwers, M.E. Brewster, and P. Augustijns. Evaluation of gastrointestinal drug supersaturation and precipitation: Strategies and issues. *International Journal of Pharmaceutics*. 453:25-35 (2013).
146. V. Jannin, M. Di Cuia, S. Chevrier, A. Faure, Y. Chavant, C. Voutsinas, and F. Demarne. Characterization of a new self-emulsifying excipient to expand formulation options for poorly soluble drugs: Gelucire<sup>®</sup> 48/16, Poster presentation at the 2012 AAPS Annual Meeting and Exposition, 2012, San Diego, USA, Poster R6258.
147. J. Baldyga and W. Orciuch. Some hydrodynamic aspects of precipitation. *Powder Technology*. 121:9-19 (2001).
148. <http://www.chemicalize.org/structure/#!/mol=loratadine&source=fp>. (2013).
149. <http://www.chemicalize.org/structure/#!/mol=carvedilol&source=calculate>. (2013).
150. H.D. Williams, M.U. Anby, P. Sassene, K. Kleberg, J-C. Bakala-N'Goma, M. Calderone, V. Jannin, A. Igonin, A. Partheil, D. Marchaud, E. Jule, J. Vertommen, M. Maio, R. Blundell, H. Benameur, F. Carriere, A. Muellertz, C.W. Pouton, and C.J.H. Porter. Toward the establishment of standardized in vitro tests for lipid-based formulations: 2. The effect of bile salt concentration and drug loading on the performance of type I, II, IIIa, IIIb, and IV formulations during in vitro digestion. *Molecular Pharmaceutics*. 9:3286-3300 (2012).

151. N. Patel, D.M. Dalrymple, and A.T.M. Serajuddin. Development of solid SEDDS, III: application of Acconon<sup>®</sup> C-50 and Gelucire<sup>®</sup> 50/13 as both solidifying and emulsifying agents for medium-chain triglycerides. *Journal of Excipients and Food Chemicals*. 3:83-92 (2012).
152. G. Pavalache, V. Dorneanu, and A. Popescu. Determination of loratadine by UV molecular absorption spectrometry. *Ovidius University Annals of Chemistry*. 21:83-86 (2010).
153. H.W. Dibbern, R.M. Müller, and E. Wirbitzki. UV and IR Spectra of pharmaceutical substances and IR spectra of pharmaceutical and cosmetic excipients, ECV Editio Cantor, USA, 2003.
154. S. Ku. Preformulation consideration for drugs in oral CR formulation. In H. Wen and K. Park (eds.), *Oral controlled release formulation design and drug delivery: theory to practice*, John Wiley & sons, Inc., New Jersey, USA, 2010, pp. 47-70.
155. J.R. Kanicky and D.O. Shah. Effect of degree, type, and position of unsaturation on the pK(a) of long-chain fatty acids. *Journal of Colloid and Interface Science*. 256:201-207 (2002).
156. D. Reger, S. Goode, and D. Ball. Liquids and solids. In L. Lockwood and J. Campbell (eds.), *Chemistry: principles and solids*, Mary Finch, Belmont, Canada, 2010, pp. 435-447.
157. A. Nacsa, R. Ambrus, O. Berkesi, P. Szabo-Revesz, and Z. Aigner. Water-soluble loratadine inclusion complex: Analytical control of the preparation by microwave irradiation. *Journal of Pharmaceutical and Biomedical Analysis*. 48:1020-1023 (2008).
158. K. Patel, V. Sarma, and P. Vavia. Design and evaluation of Lumefantrine-Oleic acid self nanoemulsifying ionic complex for enhanced dissolution. *Daru-Journal of Pharmaceutical Sciences*. 21:(2013).
159. N. Rodriguez-Hornedo and D. Murphy. Significance of controlling crystallization mechanisms and kinetics in pharmaceutical systems. *Journal of Pharmaceutical Sciences*. 88:651-660 (1999).

160. C. Stillhart. Toward an improved understanding of the precipitation behavior of weakly basic drugs from oral lipid-based formulations. Submitted. (2013).
161. S. Carlert, A. Palsson, G. Hanisch, C. von Corswant, C. Nilsson, L. Lindfors, H. Lennernas, and B. Abrahamsson. Predicting intestinal precipitation-A case example for a basic BCS class II drug. *Pharmaceutical Research*. 27:2119-2130 (2010).

## List of Abbreviations

<b>AB</b>	Acid bone
<b>ATR</b>	Attenuated total reflection
<b>BCS</b>	Biopharmaceutics classification system
<b>BSE</b>	Bovine spongiform encephalopathy
<b>CLSM</b>	Confocal laser scanning microscopy
<b>CrMTrans</b>	Formulation containing Cremophor <sup>®</sup> RH 40, Miglyol <sup>®</sup> 812, and Transcutol HP
<b>D</b>	Drug
<b>D<sup>-</sup></b>	Ionized drug
<b>DHA</b>	Docosahexaenoic acid
<b>DMSO</b>	Dimethyl sulfoxide
<b>DSC</b>	Differential scanning calorimetry
<b>EMA</b>	European Medicinal Agency
<b>EPA</b>	Eicosapentaenoic acid
<b>FAMG</b>	Fatty acid monoglyceride
<b>FASSGF</b>	Fasted state simulated gastric fluid
<b>FASSIF</b>	Fasted state simulated intestinal fluid
<b>FBRM</b>	Focused beam reflectance measurement
<b>FDA</b>	Food and Drug Administration

---

<b>FF prec.</b>	Fenofibrate precipitate
<b>FF-TTMI</b>	Fenofibrate in formulation containing Tween <sup>®</sup> 80, Transcutol <sup>®</sup> HP, Miglyol <sup>®</sup> 812, and Imwitor <sup>®</sup> 742
<b>F ref.</b>	Fenofibrate (reference)
<b>FTIR</b>	Fourier transform infrared
<b>GI</b>	Gastro-intestinal
<b>GIT</b>	Gastrointestinal tract
<b>GRAS</b>	Generally recognised as safe
<b>HLB</b>	Hydrophilic-lipophilic balance
<b>HP<math>\beta</math>CD</b>	Hydroxypropyl- $\beta$ -cyclodextrin
<b>HPMC</b>	Hydroxypropyl methylcellulose
<b>HPLC</b>	High-performance liquid chromatography
<b>IID</b>	Inactive ingredient database
<b>ISO</b>	International Organization for Standardization
<b>IU</b>	International units
<b>LB</b>	Limed bone
<b>LBF(s)</b>	Lipid-based formulation(s)
<b>LCFA</b>	Long-chain fatty acid
<b>LCT</b>	Long-chain triglycerides
<b>LFCS</b>	Lipid formulation classification system
<b>LH</b>	Limed hide
<b>MC</b>	Methylcellulose
<b>MCT</b>	Medium-chain triglycerides
<b>ME</b>	Microemulsion

---

<b>MEMS</b>	Microelectromechanical system
<b>MW</b>	Molecular weight
<b>OA</b>	Oleic acid
<b>OTC</b>	Over the counter
<b>PDI</b>	Polydispersity index
<b>PEG</b>	Polyethylene glycol
<b>PEG-32 S</b>	Polyethylene glycol 32 stearate
<b>PEG-32 S/OA</b>	Polyethylene glycol 32 stearate/oleic acid
<b>PLM</b>	Polarizing light microscopy
<b>Pro-CrMTrans</b>	Probucol in formulation containing Cremophor <sup>®</sup> RH 40, Miglyol <sup>®</sup> 812, and Transcutol HP
<b>PS</b>	Pigskin
<b>PSD</b>	Particle size distribution
<b>PVA</b>	Polyvinyl alcohol
<b>PWSD</b>	Poorly water-soluble drugs
<b>QC</b>	Quality control
<b>RH</b>	Relative humidity
<b>RT</b>	Room temperature
<b>SAXS</b>	Small angle x-ray scattering
<b>SBE<math>\beta</math>CD</b>	Sulfobutylether- $\beta$ -cyclodextrin
<b>SD</b>	Standard deviation
<b>SDDS</b>	Supersaturating drug delivery systems
<b>SEDDS</b>	Self-emulsifying drug delivery system
<b>SDS</b>	Sodium dodecyl sulfate

---

<b>SGC(s)</b>	Soft gelatin capsule(s)
<b>SMEDDS</b>	Self-microemulsifying drug delivery systems
<b>S-PVA</b>	Starch-based polyvinyl alcohol
<b>S-PVA-C(s)</b>	Starch-based polyvinyl alcohol capsule(s)
<b>S-SEDDS</b>	Supersaturatable self-emulsifying drug delivery systems
<b>super-SNEDDS</b>	Supersaturated self-nanoemulsifying drug delivery system
<b>TG</b>	Triglyceride
<b>TJ</b>	Tight junction
<b>USP</b>	United States Pharmacopeia
<b>TPGS</b>	d-alpha tocopheryl polyethylene glycol 1000 succinate
<b>TTMI</b>	Formulation containing Tween <sup>®</sup> 80, Transcutol <sup>®</sup> HP, Miglyol <sup>®</sup> 812, and Imwitor <sup>®</sup> 742
<b>UV</b>	Ultraviolet
<b>XRD</b>	X-ray diffraction

## List of Symbols

$a_w$	Water activity
$d$	Displacement of deformed capsules before the rupture point (Chapter 3)
$d$	Domain size (or periodicity) (Chapter 4)
$k$	Boltzmann constant
$n$	Number of samples
$p$	Probability in statistics
$r^*$	Critical radius for particle growth
$t$	Time
$t_{res}$	Relevant drug residence time in the gastrointestinal tract (GIT)
$w$	Weight fraction
$C$	Maximum concentration of solubilized drug
$C^*$	Drug solubility in the dispersion of formulation in phosphate buffer
$C_{eq}$	Equilibrium solubility
$C_{sol}$	Actual concentration of solubilized drug
$F$	Tensile force
$\Delta H_f$	Heat of fusion
$\Delta H_{f100}$	Heat of fusion of a PVA with 100% crystallinity



---

$P_{nc}$	Precipitation number
$R^2$	Coefficient of correlation
$S$	Supersaturation (Chapter 2)
$S$	Saturation level in the anhydrous formulation (Chapter 5)
$S_{eq}$	Equilibrium solubility at 37° C (Chapter 5)
$SR$	Supersaturation ratio
$SR_a$	Average roughness
$SR_p$	Maximum peak height
$SR_q$	Root mean square roughness
$SR_v$	Maximum valley depth
$SR^M$	Maximum supersaturation ratio
$T$	Temperature
$T_m$	Melting temperature
$W$	Work
$X_c$	Degree of crystallinity
$Z$	Average diameter of particles
$\mu$	Chemical potential
$\mu_{eq}$	Chemical potential at equilibrium
$\lambda$	Wavelength
$\xi$	Correlation length
$\tau_{ind}$	Induction time

## List of Figures

<b>2.1:</b> Fill/shell dynamics during drying process and storage. ....	11
<b>2.2:</b> Process outline of the Globex method.....	19
<b>2.3:</b> Illustration of the rotary die method. ....	21
<b>2.4:</b> Schematic outline of the manufacturing process of VegaGels <sup>®</sup> . ....	23
<b>2.5:</b> BCS drug classification. ....	26
<b>2.6:</b> Schematic diagram of intestinal drug transport from LBF via the portal and the mesenteric lymphatic routes.....	27
<b>2.7:</b> The ternary phase diagram of SMEDDS dispersed in water.....	32
<b>2.8:</b> Nucleation nomenclatures .....	35
<b>2.9:</b> The Gibbs free energy of dissolved molecules in supersaturated solution.....	36
<b>2.10:</b> FBRM probe .....	37
<b>2.11:</b> “Spring and parachute” approach of supersaturatable drug delivery systems.....	41
<b>3.1:</b> Three-dimensional surface profiles of SG and S-PVA films using CLSM.....	57
<b>3.2:</b> XRD patterns of PVA, potato starch and S-PVA film.....	59
<b>3.3:</b> DSC thermograms of PVA, potato starch and S-PVA film.....	60
<b>3.4:</b> Solubility of fenofibrate in placebo formulation-water mixtures .....	63
<b>3.5:</b> Measured $a_w$ during drying of (a) drug formulation with soft gelatin shell and (b) drug formulation with S-PVA shell. ....	64

---

<b>3.6:</b> $a_w$ of mixtures of drug-containing formulation and water.....	65
<b>3.7:</b> X-ray diffractogram patterns of fenofibrate precipitate upon mixing of the formulation with 32% w/w water .....	67
<b>3.8:</b> Comparison of the force-displacement profiles of SGCs and S-PVA-Cs.....	68
<b>3.9:</b> Drug release profiles from SGCs and S-PVA-Cs .....	69
<b>4.1:</b> Viscosity profiles of the self-emulsifying systems upon hydration.....	86
<b>4.2:</b> SAXS intensity profiles of hydrated formulations. ....	88
<b>4.3:</b> Plot of domain size ( $d$ ) versus hydration levels.....	89
<b>4.4:</b> Plot of correlation length ( $\zeta$ ) versus hydration levels.....	90
<b>4.5:</b> Disintegration profiles of SGCs, VegaGels <sup>®</sup> , and S-PVA-Cs using texture analyzer .....	91
<b>4.6:</b> Drug release profiles of fenofibrate formulation from S-PVA-Cs, SGCs, and VegaGels <sup>®</sup> .....	92
<b>4.7:</b> Drug release profiles of probucol formulation from S-PVA-Cs, SGCs, and VegaGels <sup>®</sup> .....	93
<b>4.8:</b> Effect of the mechanical force on release behaviour of probucol formulation .....	94
<b>5.1:</b> Different biopharmaceutical levels of formulation <i>in vitro</i> performance.....	104
<b>5.2:</b> XRD patterns of the solid systems containing different concentrations of OA in PEG-32 S/OA mixtures (w/w). ....	113
<b>5.3:</b> DSC thermograms of the solid systems containing different concentrations of OA in PEG-32 S/OA mixtures (w/w).....	114
<b>5.4:</b> Effect of PEG-32 S : OA ratio on particle size and polydispersity index (PDI). ....	115
<b>5.5:</b> UV spectra and viscosity profiles of loratadine-OA and carvedilol-OA molecular complexes.....	116

---

<b>5.6:</b> FTIR spectra of loratadine, carvedilol, OA and of their binary drug-OA mixtures.....	117
<b>5.7:</b> Plot of van't Hoff model of loratadine solubility in PEG-32 S and in PEG-32 S/OA (8:2 w/w).....	118
<b>5.8:</b> Plot of van't Hoff model of carvedilol solubility in PEG-32 S and in PEG-32 S/OA (8:2 w/w).....	119
<b>5.9:</b> DSC thermograms of the supersaturated solid lipid-based formulations.....	120
<b>5.10:</b> Effect of different saturation levels in the anhydrous formulations on the induction times upon dispersion.....	123
<b>5.11:</b> Mean PSD profiles observed at t = 3h upon dispersion of drug-loaded solid lipid-based formulations.....	124
<b>5.12:</b> Effect of the drug-OA interaction on the type of precipitation kinetics.....	125
<b>5.13:</b> XRD patterns of the pellets obtained from drug-loaded solid lipid-based systems upon dispersion.....	126
<b>5.14:</b> Drug release profiles of drug-loaded solid lipid-based systems encapsulated in VegaGels <sup>®</sup> .....	131

## List of Tables

<b>2.1:</b> Physicochemical properties of soft capsule gelatins .....	8
<b>2.2:</b> Overview of non-gelatin soft capsules .....	16
<b>2.3:</b> List of lipophilic oils encapsulated in non-gelatin soft capsules .....	17
<b>2. 4:</b> Soft gelatin capsules <i>versus</i> non-gelatin soft capsules .....	24
<b>2.5:</b> The LFCS .....	29
<b>3.1:</b> Surface roughness parameters of SG and S-PVA films calculated by CLSM.....	58
<b>3.2:</b> Solubility of fenofibrate in excipients and their mixture.....	62
<b>3.3:</b> Particle size and PDI of dispersed formulations.....	62
<b>3.4:</b> The concentration of dissolved drug in SGCs and S-PVA-Cs after 4 months.....	66
<b>4.1:</b> Characteristics of different capsule types.....	79
<b>4.2:</b> HPLC methods .....	85
<b>5.1:</b> Drug solubility in PEG-32 S, OA, and PEG-32 S/OA (8:2 w/w).....	120
<b>5.2:</b> Zeta potential of drug-free and drug-loaded PEG-32 S/OA (8:2 w/w), dispersed in phosphate buffer and 0.025 M HCl .....	122
<b>5.3:</b> Loratadine doses, $S$ , $SR^M$ , and $P_{nc}$ .....	128
<b>5.4:</b> Carvedilol doses, $S$ , $SR^M$ , and $P_{nc}$ .....	129

# Curriculum Vitae

## Zdravka Misic

Mattenstrasse 55  
4058 Basel  
tadic.zdravka@gmail.com

Born in Sisak, Croatia  
July 10<sup>th</sup>, 1980.

## Education

09/2010 – 04/2014	<b>Ph.D. studies in Pharmaceutical Sciences</b> University of Basel and University of Applied Sciences and Arts Northwestern Switzerland
09/1998 – 09/2003	<b>M.Sc. in Pharmacy</b> University of Zagreb, Croatia
09/1994 – 06/1998	<b>Gymnasium</b> Sisak, Croatia

## Work experience

09/2009 – 08/2010	<b>Guest student (ESKAS scholarship holder)</b> ETH Zürich, Switzerland
-------------------	--

---

03/2009 – 08/2009	<b>Regulatory Affairs Specialist</b> Teva Pharmaceutical Industries Ltd., Croatia
04/2005 – 02/2009	<b>Formulation Scientist</b> Teva Pharmaceutical Industries Ltd., Croatia
11/2004 – 03/2005	<b>Licensed pharmacist</b> Pharmacy “Bingula”, Jastrebarsko, Croatia
09/2003 – 10/2004	<b>Pharmacist -in-training</b> Pharmacy “Lukačin”, Zagreb, Croatia

## List of Publications

- Z. Misić, K. Muffler, G. Sydow, and M. Kuentz. Novel starch-based PVA thermoplastic capsules for hydrophilic lipid-based formulations. *Journal of Pharmaceutical Sciences*. 101:4516-4528 (2012).
- Z. Misić, R. Urbani, T. Pfohl, K. Muffler, G. Sydow, and M. Kuentz. Understanding biorelevant drug release from a novel thermoplastic capsule by considering microstructural formulation changes during hydration. *Pharmaceutical Research*. 31:194-203 (2013).
- Z. Misić, D. Šišak Jung, G. Sydow, M. Kuentz. Understanding interactions of oleic acid with basic drugs in solid lipids on different biopharmaceutical levels. *Journal of Excipients and Food Chemicals*. 5 (2): 113-134 (2014).

---

## List of Poster and Oral Presentations

- Z. Mistic, G. Sydow, and M. Kuentz. Oleic acid as dispersion promoter and precipitation inhibitor of a lipid-based delivery system for a poorly soluble model base (poster presentation).  
*Surface Dissolution Imaging symposium, Bath, United Kingdom, 2013.*
- Z. Mistic. New technological approaches to soft capsules (oral presentation).  
*Forschungsevent. School of Life Sciences, University of Applied Sciences and Arts Northwestern Switzerland, 2013.*
- Z. Mistic, K. Muffler, G. Sydow, and M. Kuentz. Novel thermoplastic capsules for robust encapsulation of hydrophilic SMEDDS (poster presentation).  
*8<sup>th</sup> World Meeting on Pharmaceutics, Biopharmaceutics and Pharmaceutical Technology, Istanbul, Turkey, 2012.*
- Z. Mistic. Introduction of a new soft capsule technology (oral presentation).  
*Forschungsevent. School of Life Sciences, University of Applied Sciences and Arts Northwestern Switzerland, 2012.*
- Z. Mistic, K. Muffler, G. Sydow, and M. Kuentz. Starch-based PVA thermoplastic capsules for encapsulation of hydrophilic SMEDDS (poster presentation).  
*Annual Research Meeting, Department of Pharmaceutical Sciences, University of Basel, Switzerland, 2012.*
- Z. Mistic, K. Muffler, G. Sydow, and M. Kuentz. Biorelevant drug release studies of novel thermoplastic soft capsules (poster presented by prof. dr. Martin Kuentz).  
*AAPS, Annual Meeting and Exhibition, Chicago, USA, 2012.*



## Awards

- Poster award for the best poster in Pharmaceutical Technology on Swiss Pharma Science Day, Bern, Switzerland, 2012.
- Swiss Government Scholarship holder (ESKAS) -research study at ETH Zürich, Switzerland, 2009/2010.
- Award for scientific presentation, Teva, Croatia, 2008.
- Annual award, For outstanding achievements in formulations and analytics of creams, gels and ointments, Teva, Croatia, 2008.
- Scholarship holder from PLIVA Croatia, 2002/2003.
- Rector's award, University of Zagreb, Croatia. Research on copper and hydroxamic acid complexes, 2001.

## Acknowledgements

Above all, I would like to express my deepest sense of gratitude to my supervisor Prof. Dr. Georgios Imanidis for providing me an opportunity to perform PhD studies in this interesting field on thermoplastic starch-based capsules. I especially appreciate his valuable suggestions and continuous support throughout my study.

I would like to thank to my co-examiner Prof. Dr. Martin Kuentz for many fruitful discussions and his help and support during my study. I am more than happy that I had the possibility to work with such friendly, optimistic and approachable person like him. It would have been tough without his support.

My special thanks goes to my co-examiner Prof. Dr. Bruno Gander, Drug Formulation and Delivery group at ETH Zurich, for his friendly and kind support throughout my study.

I am deeply grateful to Dubravka Šišak-Jung, Crystallography at ETH Zurich, for many fruitful discussions on XRD and drug-exciipient interactions. Her friendly attitude and very optimistic spirit kept me going forward during difficult phases of my study.

I greatly acknowledge Prof. Dr. Thomas Pfohl and Raphael Urbani, Department of Chemistry at University of Basel, for the kind support and great collaboration. SAXS measurements would not have been possible without their support.

I would like to acknowledge the financial support of Swiss caps AG, member of the Aenova group (Kirchberg, Switzerland). My sincerest thanks goes to Dr. Georg Sydow and Mrs Katherina Muffler from Swiss caps for the excellent collaboration and encouragement.

I would like to thank my lab mates (Jan, Dr. Cordula, Dr. Ursula, Dr. Michael, Katerina, Jonas, Myriam, Fabienne, Martin) for their friendship and support. My special thanks goes to Andreas for his priceless help and support.

I thank my friends Therese, Korana, Sara, Rajesh, Darko, Miriam, Ana, Tatjana, Victoria, Nataša, Vlatka, and Tihana for their friendship and support.

I would like to thank to my Mother (Ljuba Tadić), Father (Stevo Tadić), and my sister (Tatjana Tadić) for their love and continuous support.

I am especially grateful to my husband Miran for all his support during my study. Without him it would be very difficult, if not impossible.

Zdravka Misic